Nuclear molecules

1. Molecular configurations

A nuclear molecule consists of two (or more) touching nuclei which keep their individualty.

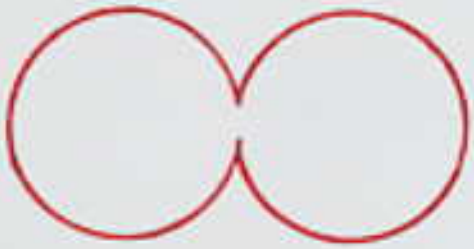

Other notations: dinuclear system,
bi-cluster system

Historically nuclear molecular physics started with measurements of resonances in the $^{12}C + ^{12}C$ reaction in 1960.
Importance for element synthesis in astrophysics.

D.A. Bromley, J.A. Kuehner and E. Almqvist, Phys. Rev. Lett. 4 (1960) 365

a) Microscopical picture

two-center shell model (TCSM)

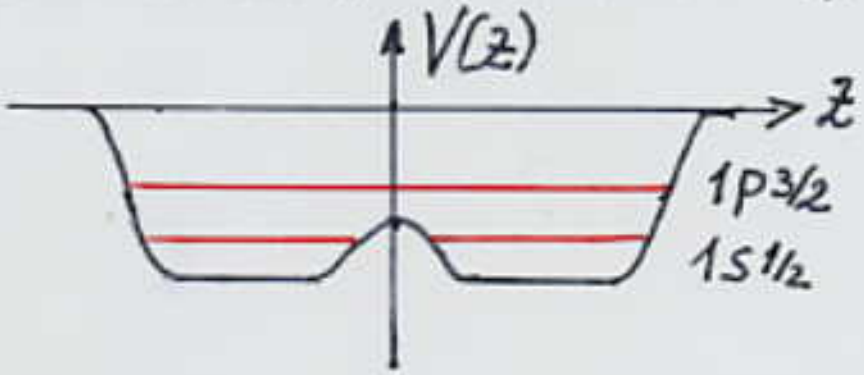

1. nucleons belonging to individual clusters,
2. nucleons constituting a bonding, homopolar or covalent bonding

b) Types of nuclear molecules

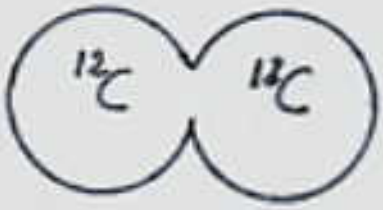

dinuclear configuration

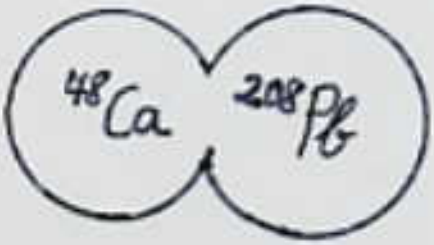

fusion configuration

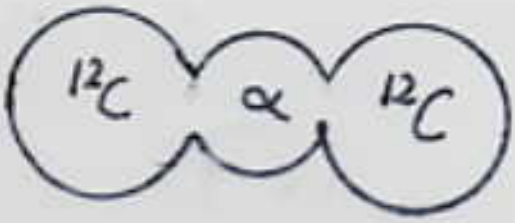

three-cluster config.

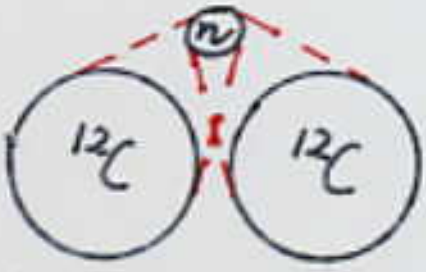

molec. single-particle conf.

c) Main degrees of freedom

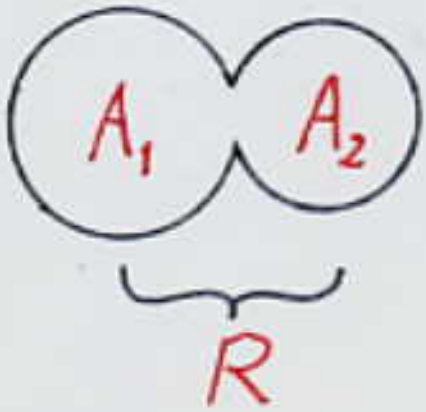

1. Relative motion described by R
2. Mass and charge asymmetry motion described by the coordinates

$$\eta = \frac{A_1 - A_2}{A_1 + A_2} \qquad \eta_Z = \frac{Z_1 - Z_2}{Z_1 + Z_2}$$

mass and charge numbers: A_1, A_2, Z_1, Z_2

Change of these numbers means
transfer of nucleons between nuclei.

$$-1 \leq \eta, \eta_Z \leq 1$$

$\eta, \eta_Z = 0$: Symmetric system
$|\eta| = 1$: fused system

These lectures are divided into two parts:

I. Molecular dynamics in relative motion

Molecular resonances,
nucleus-nucleus potential by solving the inverse scattering problem,
collective molecular states with deformed nuclei,
semimicroscopic algebraic cluster model,
hyperdeformed states in heavy ion collisions.

II. Molecular dynamics in mass (charge) asymmetry motion

Dinuclear system model,
normal- and superdeformed bands,
dinuclear dynamics in the fusion process,
quasifission as a signature for dinuclear systems.

2. Molecular resonances

In light systems, e.g. $^{12}C + ^{12}C$, nuclear molecules can be observed by resonances in cross sections.

2.1 Gross structure in cross sections

Symmetric systems: e.g. $^{12}C + ^{12}C$
Elastic differential cross section is symmetric about $\vartheta_{cm} = 90°$.
Only even angular momenta $\ell = 0, 2, 4 \ldots$

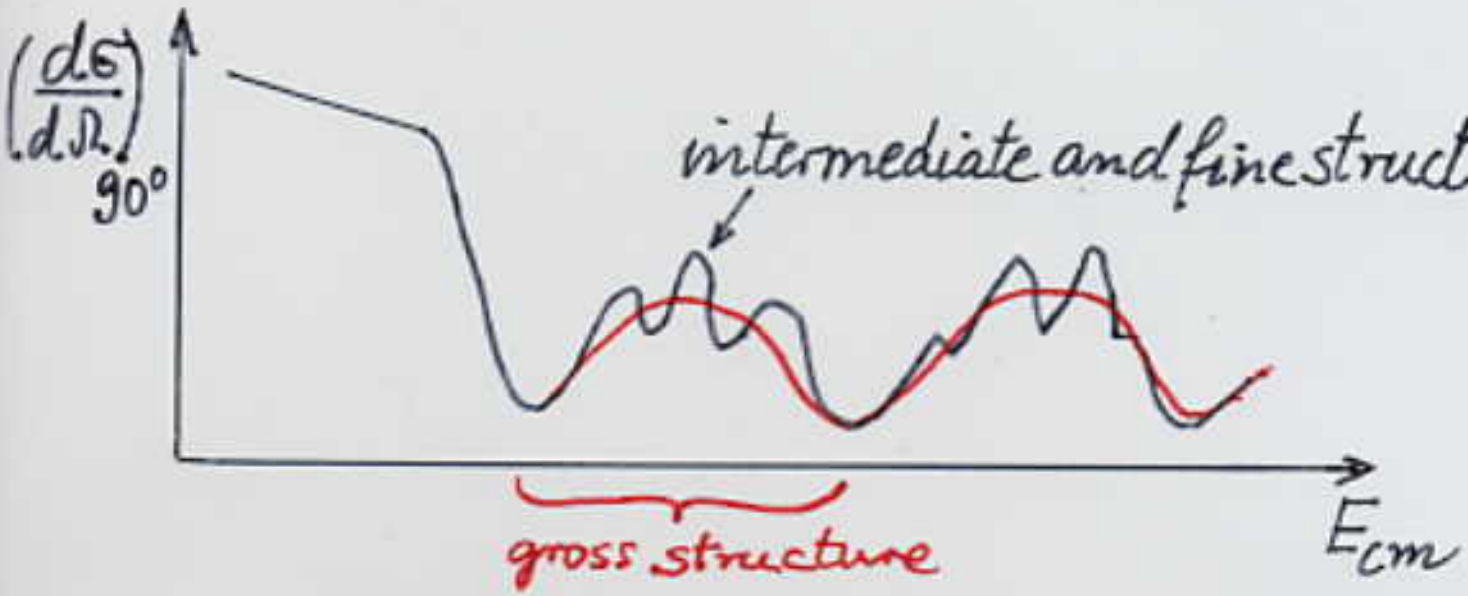

Gross structure $\Gamma \sim 2$ MeV in light systems.

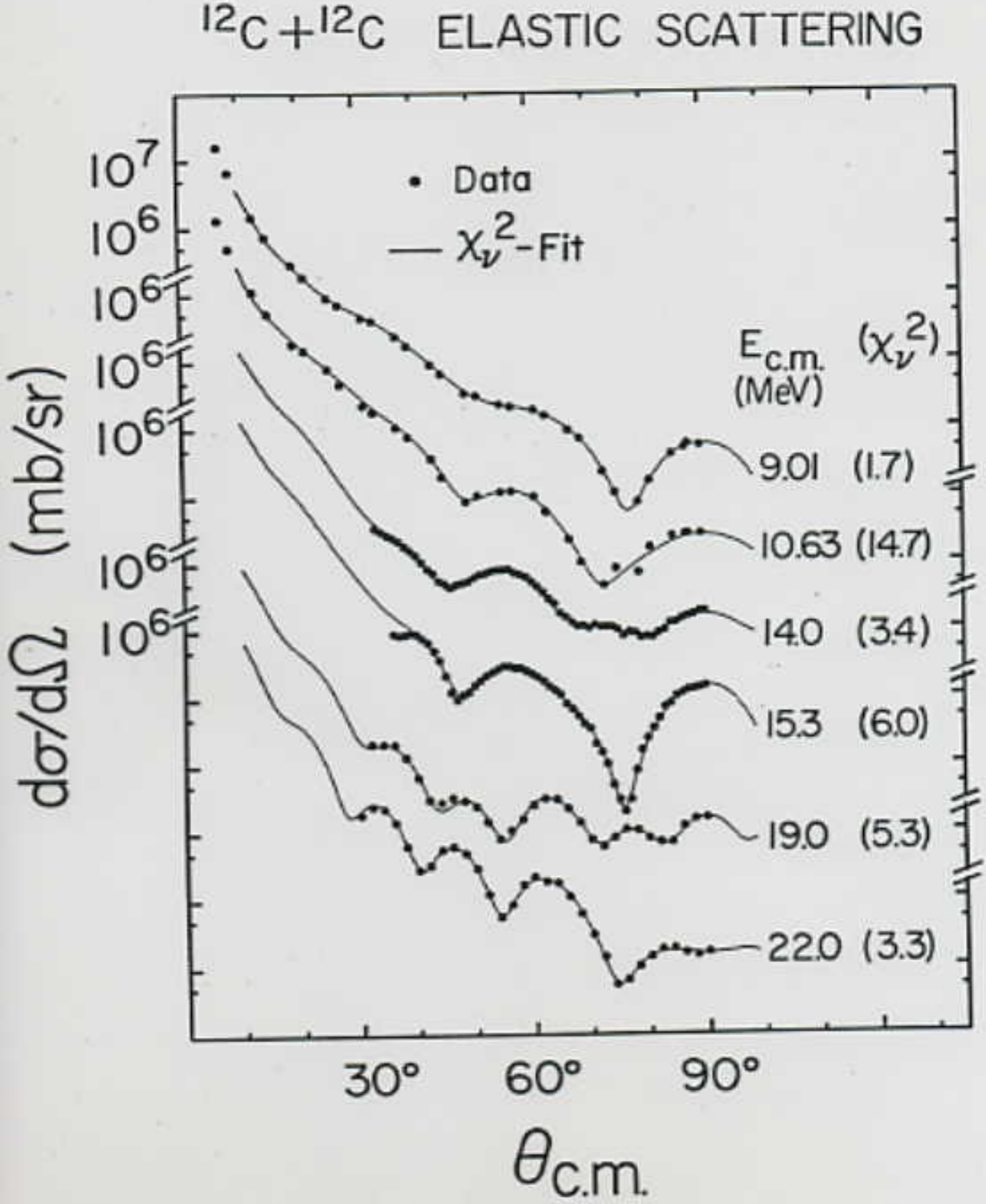
$^{12}C + ^{12}C$ ELASTIC SCATTERING
Data
χ_ν^2-Fit
$E_{c.m.}$ (MeV)
(χ_ν^2)
9.01 (1.7)
10.63 (14.7)
14.0 (3.4)
15.3 (6.0)
19.0 (5.3)
22.0 (3.3)
10^7
10^6
$d\sigma/d\Omega$ (mb/sr)
30°
60°
90°
$\theta_{c.m.}$

Fig. 2

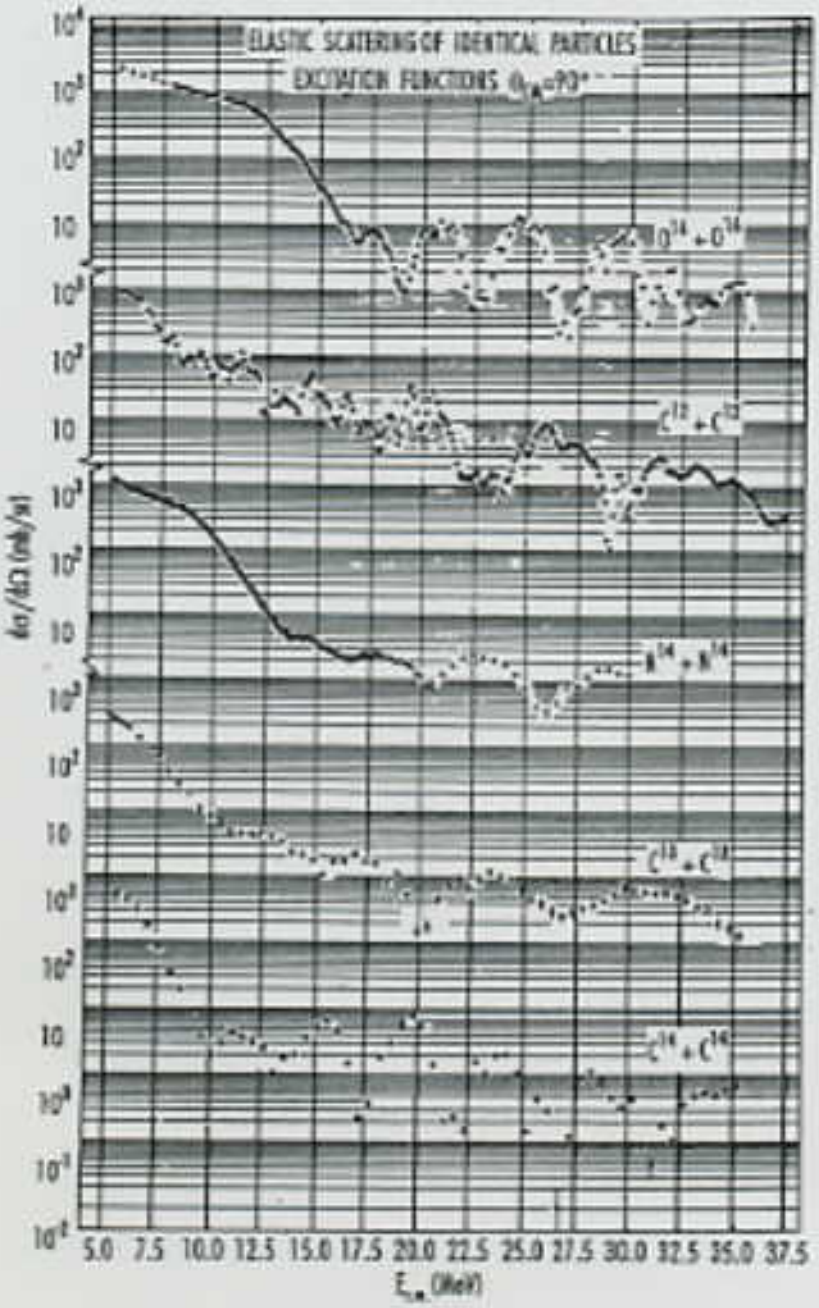
ELASTIC SCATTERING OF IDENTICAL PARTICLES
EXCITATION FUNCTIONS
dσ/dΩ (mb/sr)
5.0 7.5 10.0 12.5 15.0 17.5 20.0 22.5 25.0 27.5 30.0 32.5 35.0 37.5

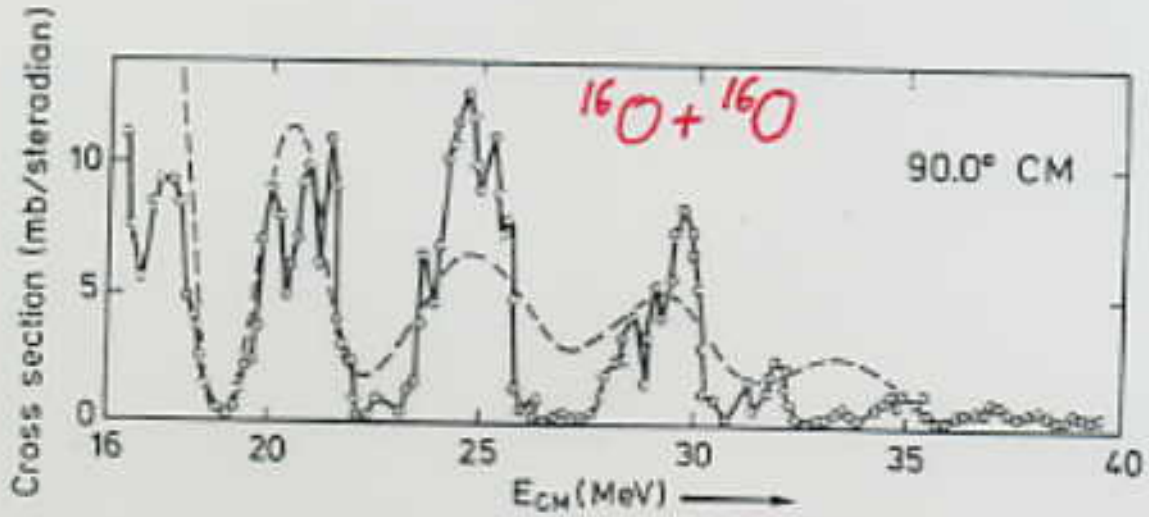
16O + 16O
90.0° CM
Cross section (mb/steradian)
10
5
0
16
20
25
30
35
40
ECM (MeV)

gross structure is caused by

virtual potential resonances

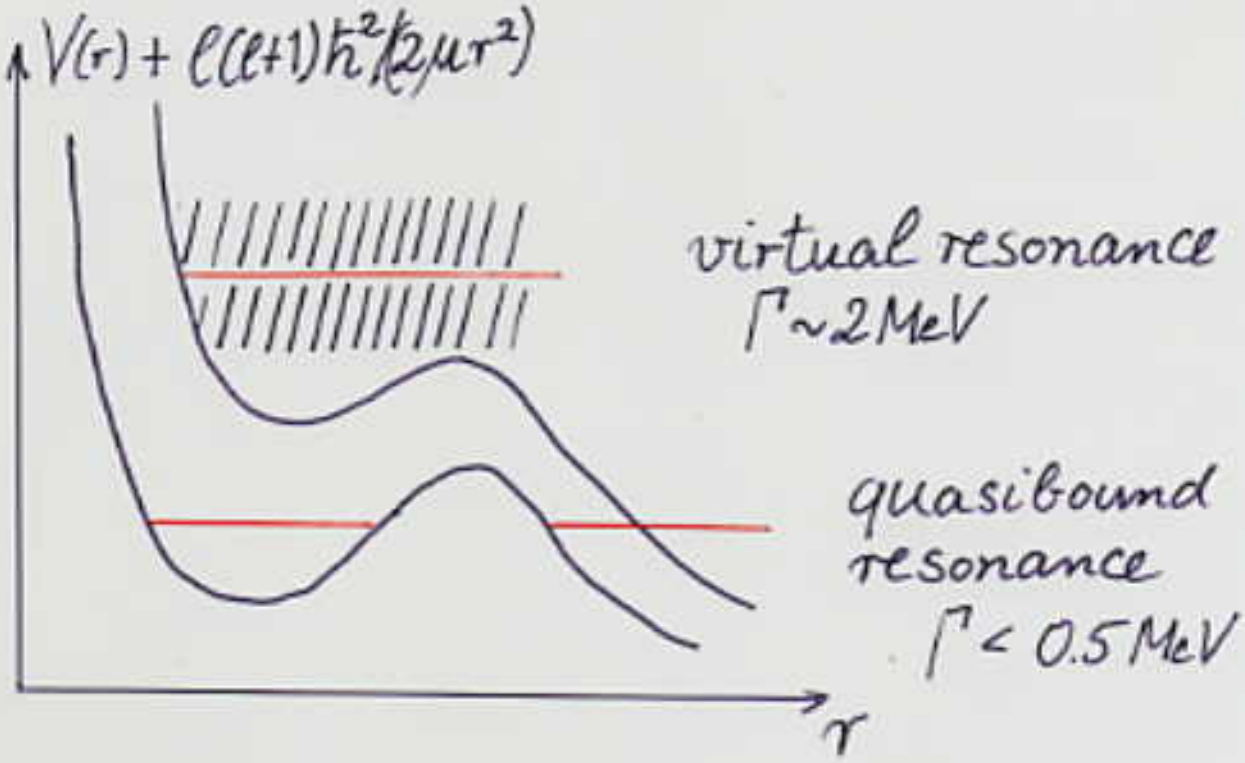

gross structure in elastic, inelastic, α-transfer, and fusion cross sections

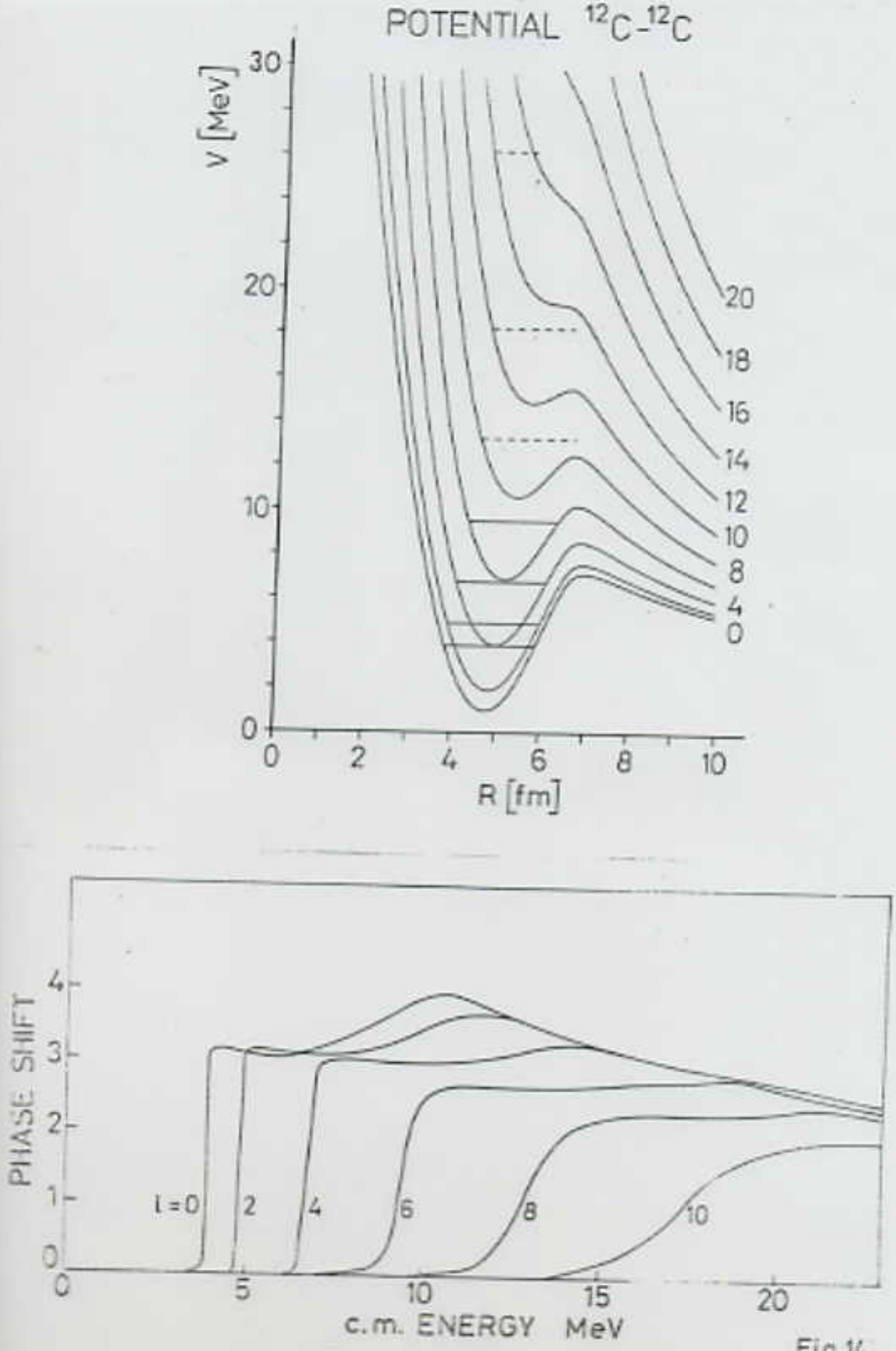
POTENTIAL ^{12}C-^{12}C
V [MeV]
30
20
10
0
0
2
4
6
8
10
R [fm]
20
18
16
14
12
10
8
4
0
PHASE SHIFT
4
3
2
1
0
l=0
2
4
6
8
10
0
5
10
15
20
c.m. ENERGY MeV

Fig.14

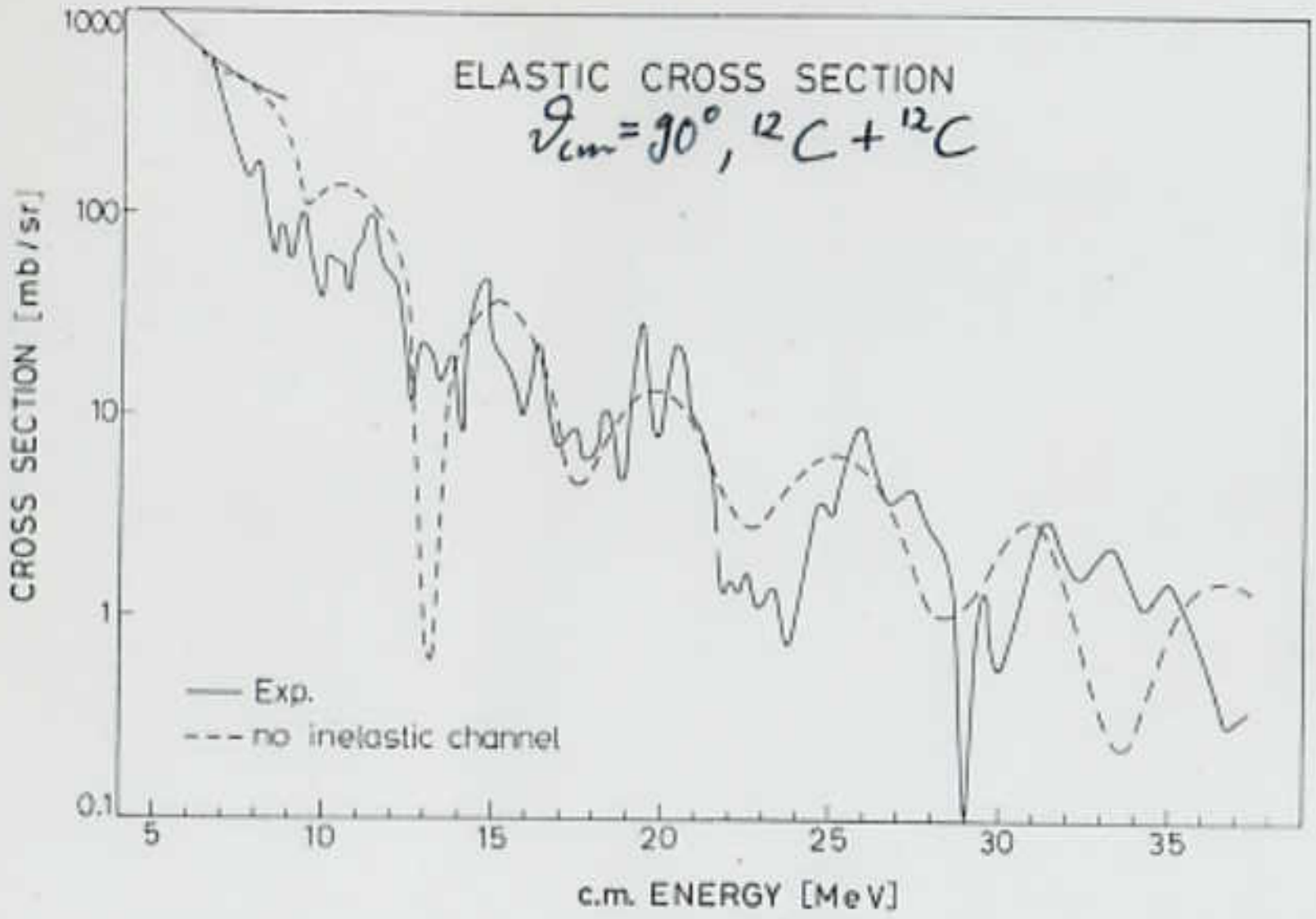
ELASTIC CROSS SECTION
$\vartheta_{cm} = 90°$, $^{12}C + ^{12}C$
CROSS SECTION [mb/sr]
1000
100
10
1
0.1
5
10
15
20
25
30
35
c.m. ENERGY [MeV]
Exp.
no inelastic channel

2.2 Molecular window

Molecular states with angular momentum of grazing partial wave have small spreading width to complex states.

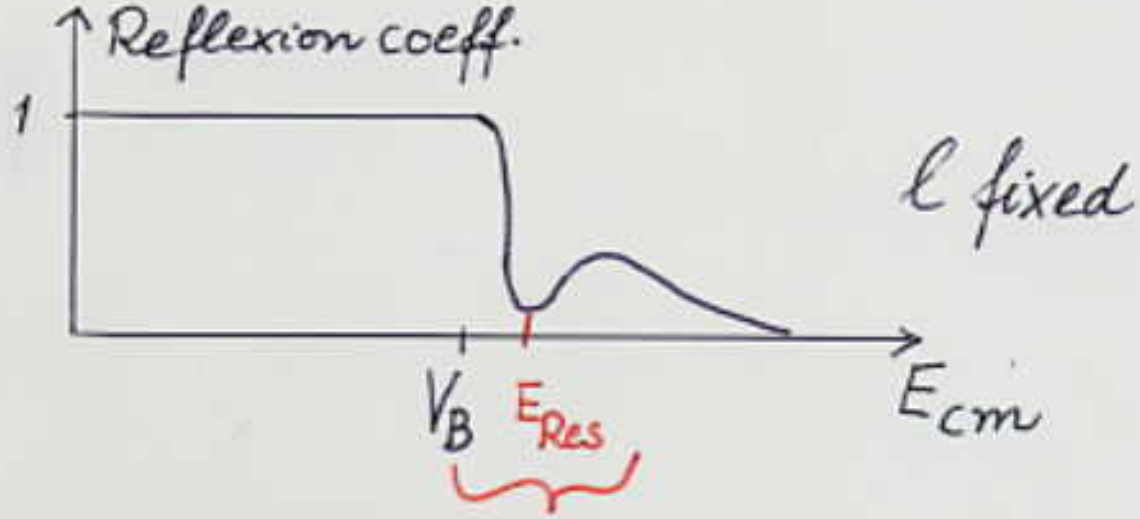

width of window $\approx \Gamma_{virtual\ res.}$

Spreading width:

$$\Gamma^{\downarrow} = 2\pi \rho(E^*, I) \left| \langle \Psi_{elast.} | V | \Psi_{compl.\ states} \rangle \right|^2$$

level density of complex states:

$$\rho(E^*, I) \sim (2I+1) \exp(-I(I+1)/2\sigma^2(E^*))$$

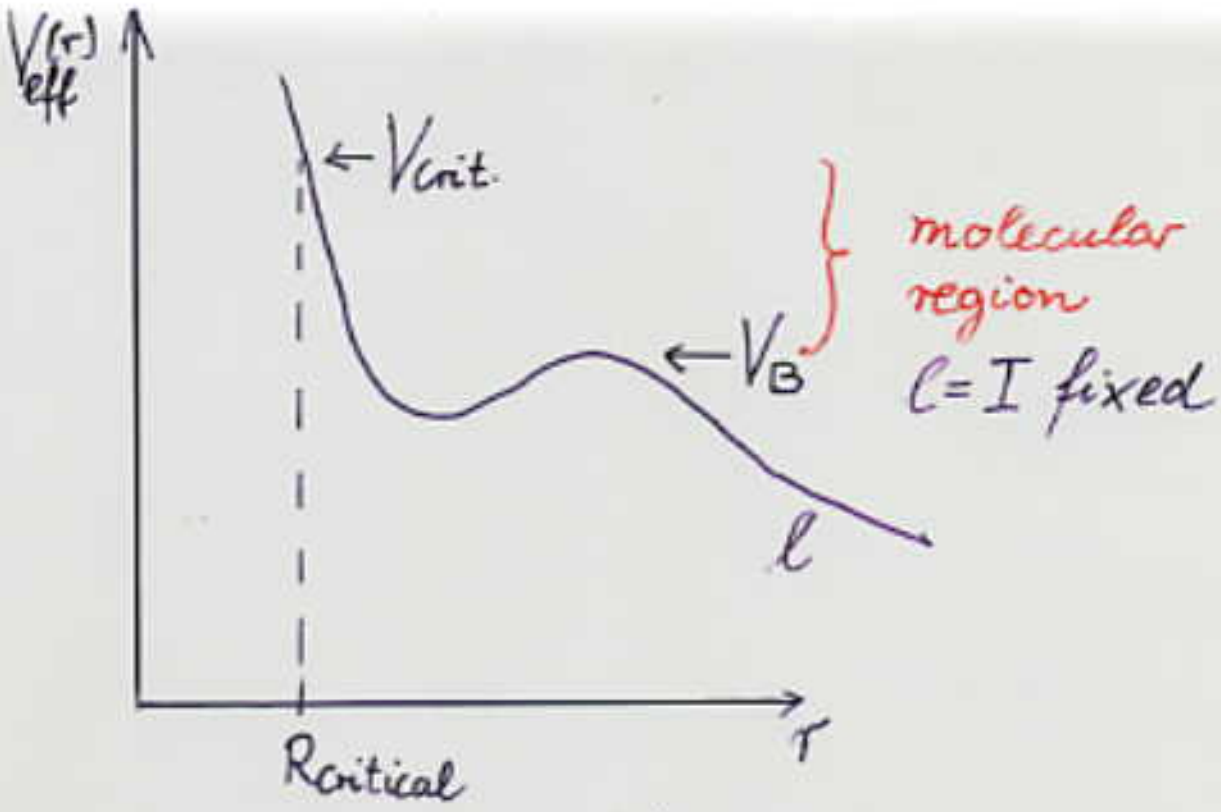

small decay width for states in molec. region,

grazing partial wave is not absorbed.

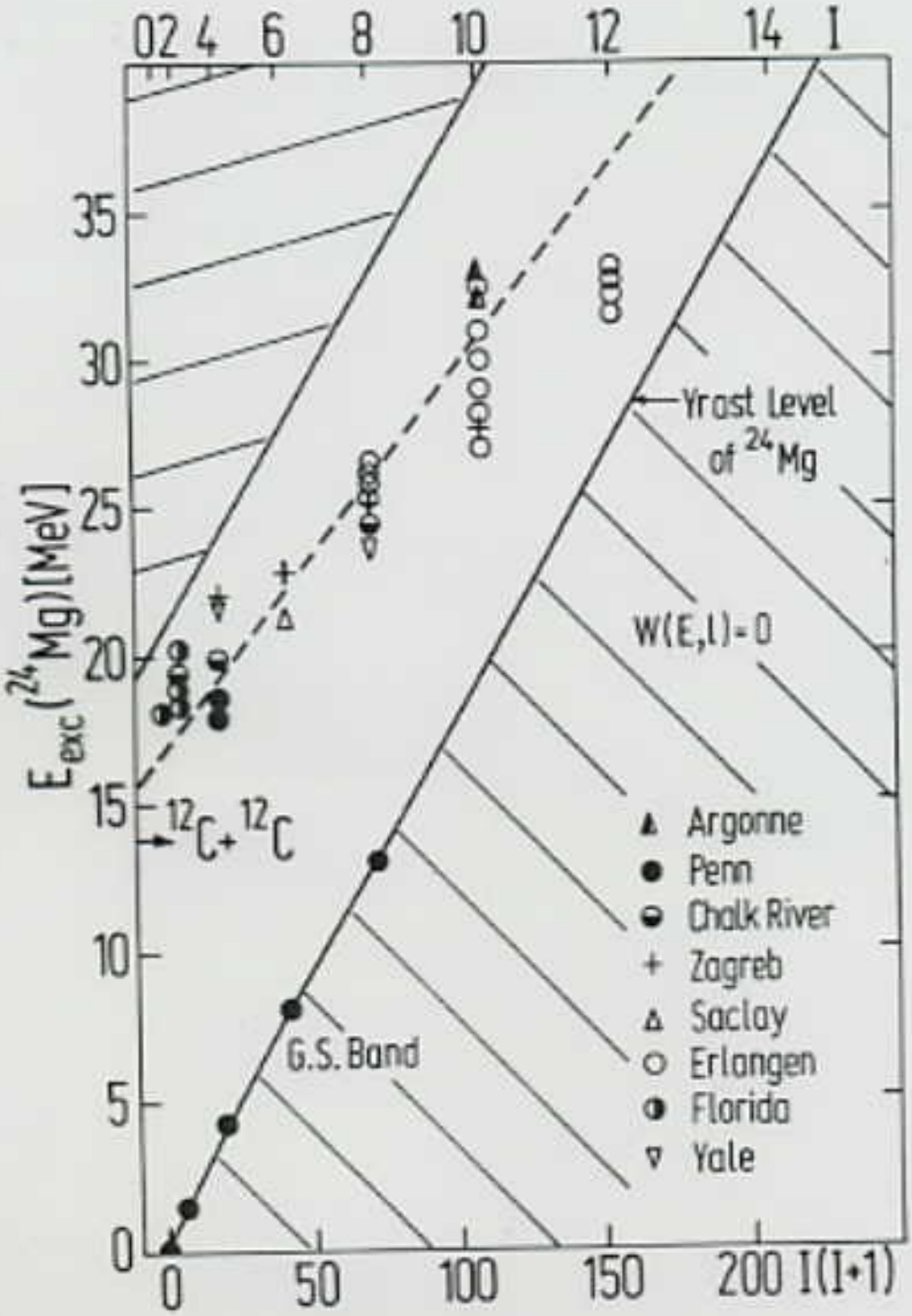
0 2 4 6 8 10 12 14 I
35
30
25
20
15
10
5
0
$E_{exc}(^{24}Mg)$[MeV]
Yrast Level of ^{24}Mg
W(E,I)=0
$^{12}C+^{12}C$
G.S. Band
Argonne
Penn
Chalk River
Zagreb
Saclay
Erlangen
Florida
Yale
0 50 100 150 200 I(I+1)

2.3 Excitation of quasibound states

Strongly excited inelastic channels

e.g. $^{12}C(gs) + {}^{12}C(gs) \longrightarrow {}^{12}C(2^+) + {}^{12}C(gs)$

$\longrightarrow {}^{12}C(2^+) + {}^{12}C(2^+)$

Enhanced excitation of quasibound states is possible.

a) Double resonance mechanism

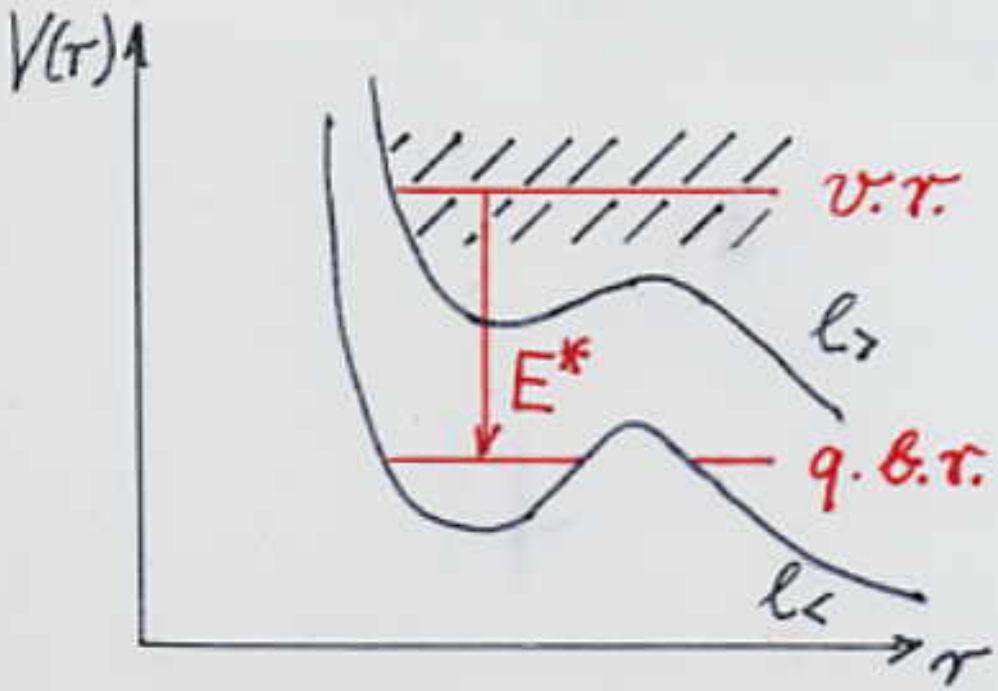

Simultaneous resonance excitation:

$$E_{cm} \approx E_{v.r.} \approx E_{q.b.r.} + E^*$$

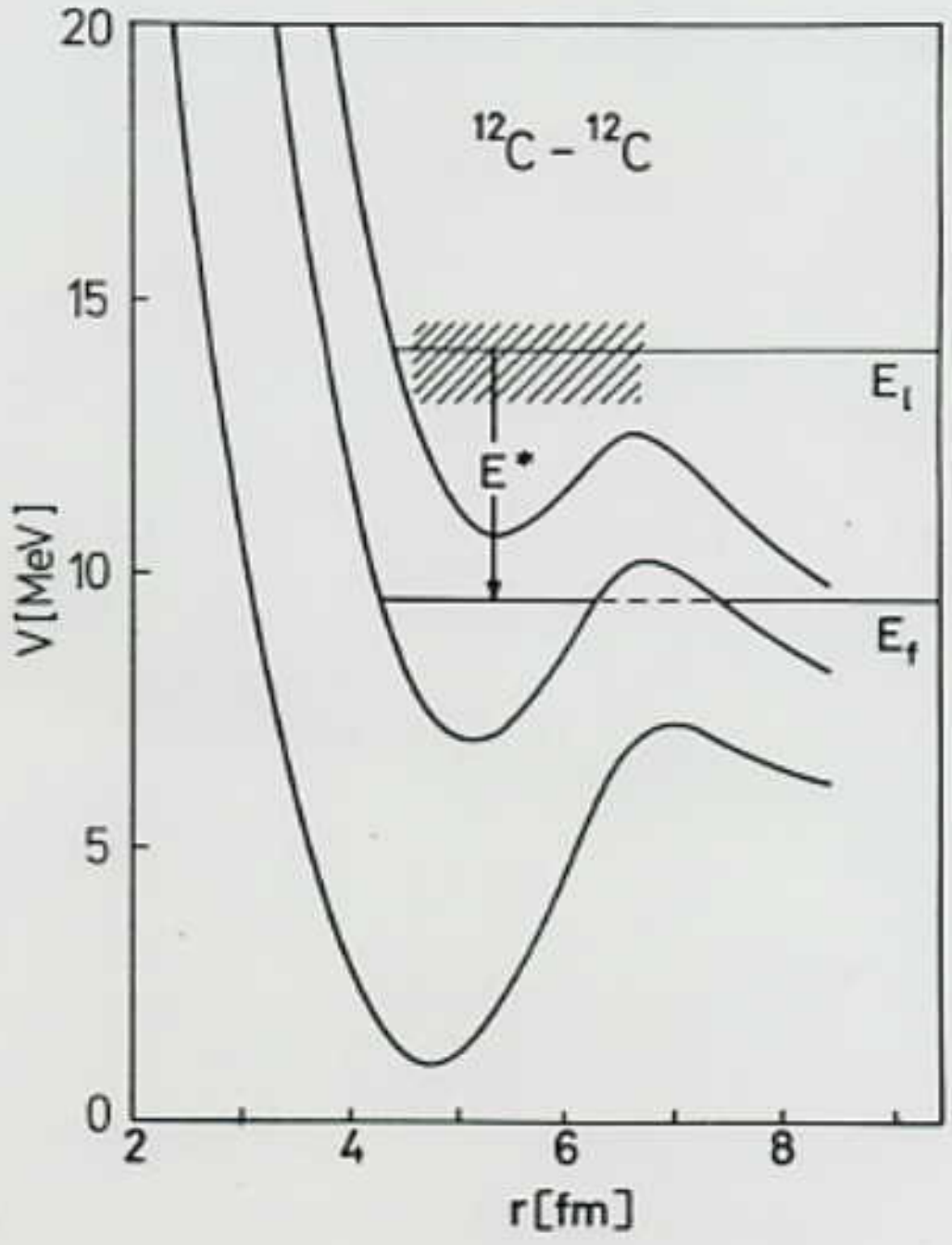
20
15
10
5
0
V[MeV]
$^{12}C - ^{12}C$
E_i
E^*
E_f
2
4
6
8
r[fm]

b) Band crossing model of Abe

Potential states form a rotational band.

$$E_{v.r.}, E_{q.b.r.} = E_0 + \frac{\ell(\ell+1)\hbar^2}{2\Theta}$$

$$\ell_{elast.} = I$$

aligned configuration: $\ell_{inelast.} + I_{exc.} = I$

elastic band:

$$E_{elast.}(I) = E_0 + I(I+1)\hbar^2/(2\Theta)$$

inelastic band:

$$E_{inelast.}(I) = E_0 + E^* + (I - I_{exc})(I - I_{exc}+1)/(2\Theta)$$

Crossing of bands : strong excitation

$\hat{=}$ double resonance mechanism

→ intermediate structures, $\Gamma \approx 100\text{-}500\,keV$

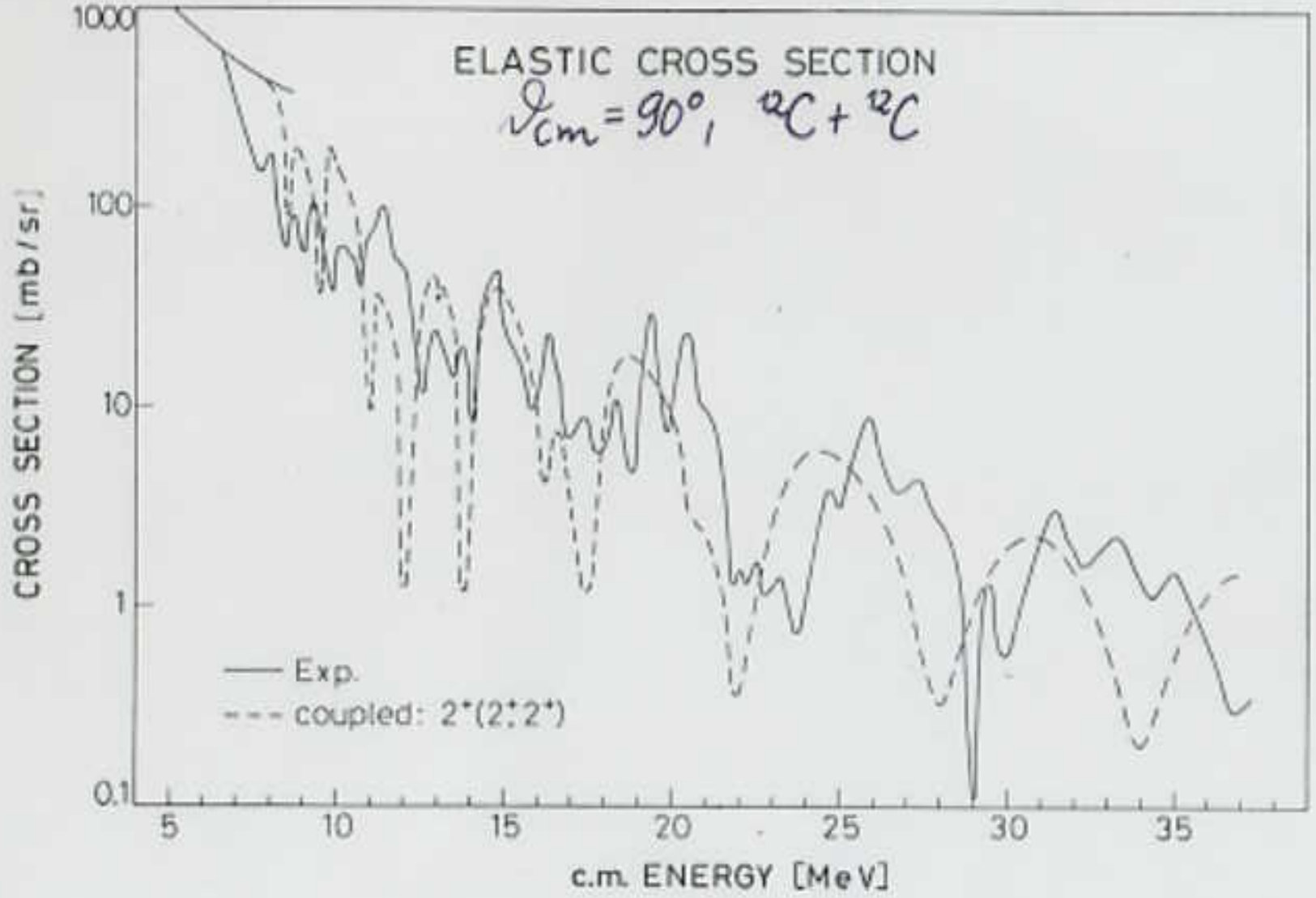
ELASTIC CROSS SECTION
$\vartheta_{cm} = 90°$, $^{12}C + ^{12}C$
CROSS SECTION [mb/sr]
1000
100
10
1
0.1
5
10
15
20
25
30
35
c.m. ENERGY [MeV]
Exp.
coupled: 2⁺(2⁺2⁺)

3. $^{12}C + ^{12}C$ potential by solving the inverse scattering problem

Determination of potentials from measured elastic differential cross sections at fixed energy.

$\frac{d\sigma_{ee}(\vartheta)}{d\Omega}$ → phase shift analysis

→ solution of inverse scattering problem
here: Newton-Sabatier method,

→ potential

example for quality of Newton-Sabatier method: $^{16}O + ^{12}C$

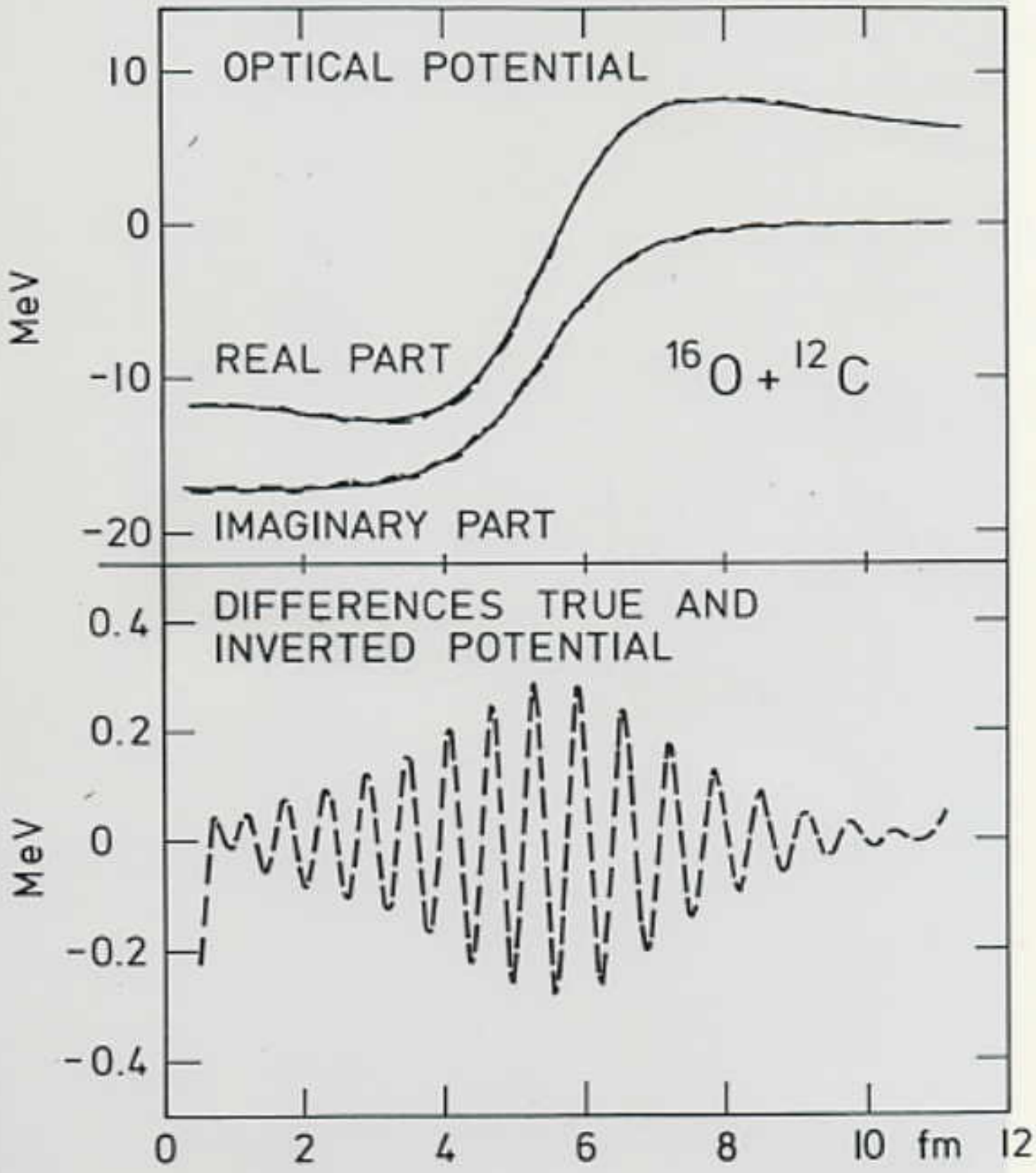
OPTICAL POTENTIAL
10
0
-10
-20
MeV
REAL PART
IMAGINARY PART
$^{16}O + ^{12}C$
DIFFERENCES TRUE AND
INVERTED POTENTIAL
0.4
0.2
0
-0.2
-0.4
MeV
0
2
4
6
8
10
fm
12

Fig. 2

a) Elastic differential cross section of $^{12}C + ^{12}C$

$\frac{d\sigma_{ee}}{d\Omega} = |f(\vartheta) + f(\pi - \vartheta)|^2$ in C.M. system

$$f(\vartheta) = f_{coul}(\vartheta) + \frac{1}{2ik}\sum_{\ell=0}^{\infty}(2\ell+1)e^{2i\sigma_\ell}(e^{2i\delta_\ell} - 1)P_\ell(\cos\vartheta)$$

Coulomb phase shifts : σ_ℓ

nuclear phase shifts : $\delta_\ell = Re(\delta_\ell) + i\,Im(\delta_\ell)$

Because of $d\sigma(\vartheta) = d\sigma(\pi - \vartheta)$ only nuclear phases for even ℓ-values ($\ell = 0, 2, 4, \ldots$) can be determined in a phase shift analysis.

The inversion procedure needs the phase shifts for odd ℓ-values too : $\delta_1, \delta_3, \delta_5 \ldots$

They are undetermined from experiment.

Assumption:

Potential should be a smooth function of r.

→ Interpolation between phases with even ℓ.

b) Analysis of a resonance in the potential

$^{12}C + ^{12}C$ scattering at $E_{cm} = 18.5\,MeV$

Phase shift analysis by Ordonez : $\delta_0, \delta_2 \ldots \delta_{16}$

Result: potential depends sensitively on the choice of $Re(\delta_{\ell=11})$.

→ Resonance in the $\ell = 11$ partial wave.

c) $^{12}C + ^{12}C$ potential as function of energy

used in the analysis:

$\frac{d\sigma_{ee}(\vartheta)}{d\Omega}$ of $^{12}C + ^{12}C$ for $E_{cm} = 5.3 - 14.3\,MeV$

measured by Treu, Ostrowski, Voit (Erlangen)

Extension of method: combination of phase shift analysis and solution of inverse scattering problem.

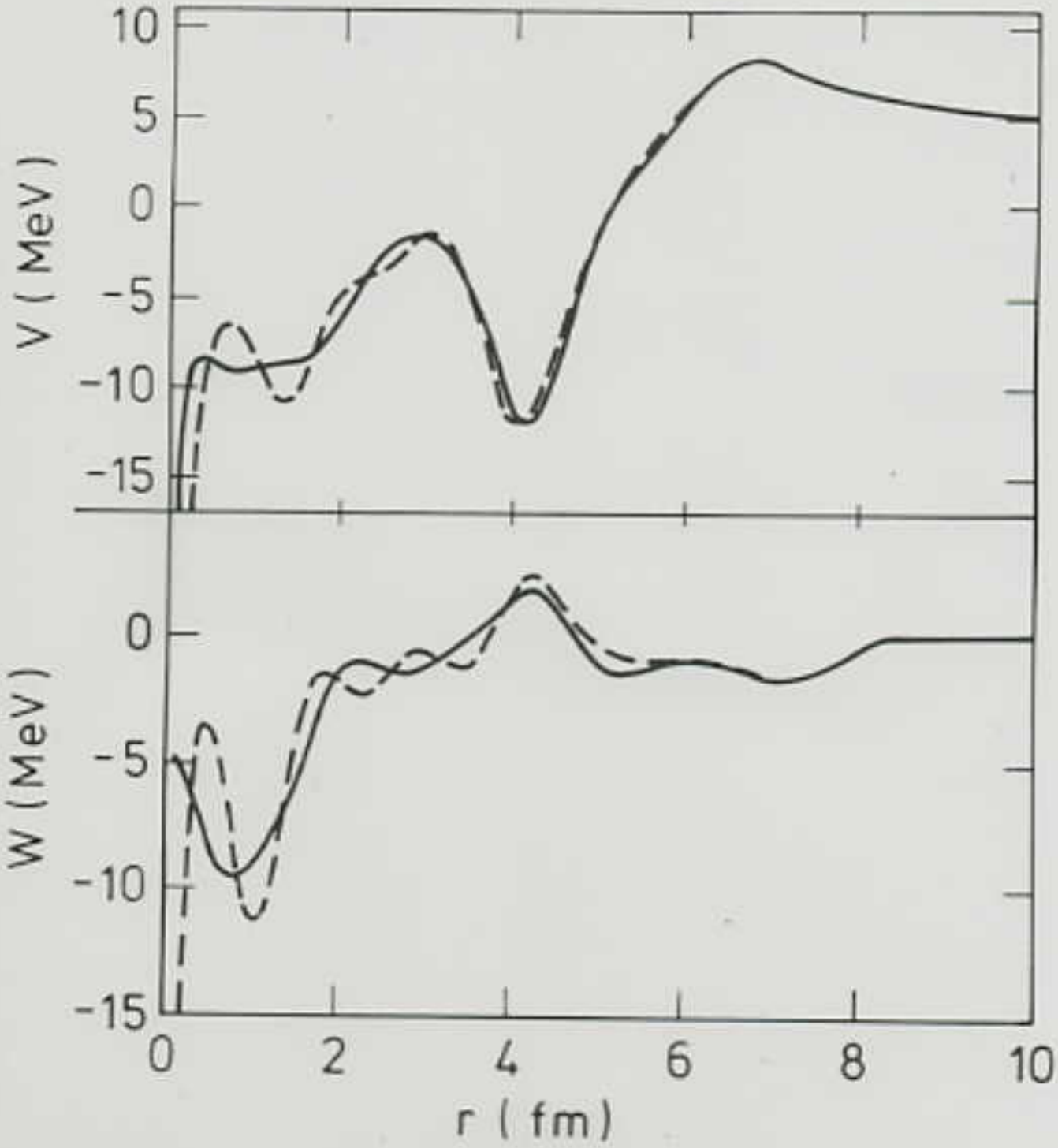

Fig. 2

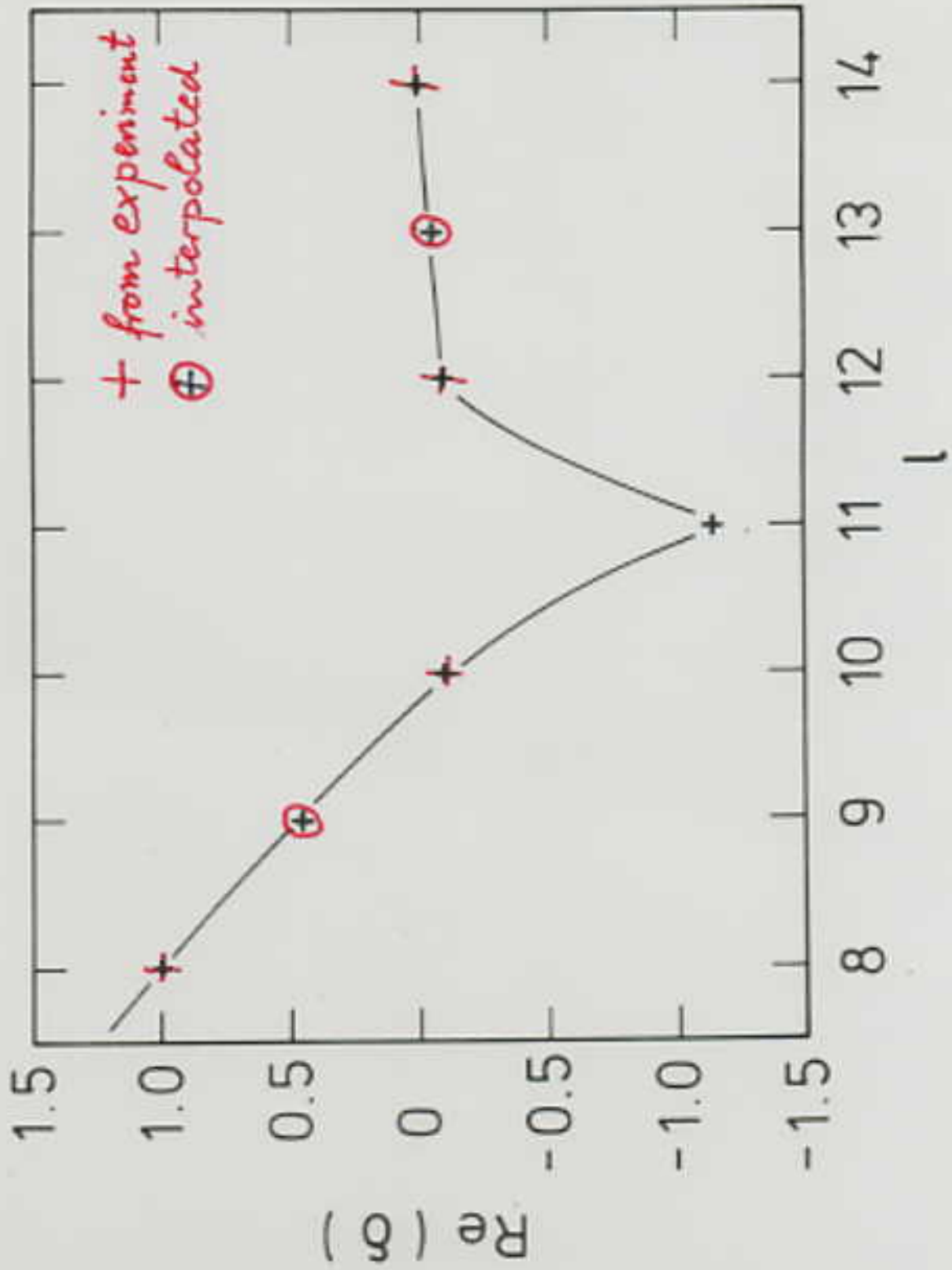
+ from experiment
⊕ interpolated
Re (δ)
1.5
1.0
0.5
0
-0.5
-1.0
-1.5
8
9
10
11
12
13
14
l

Fig. 4

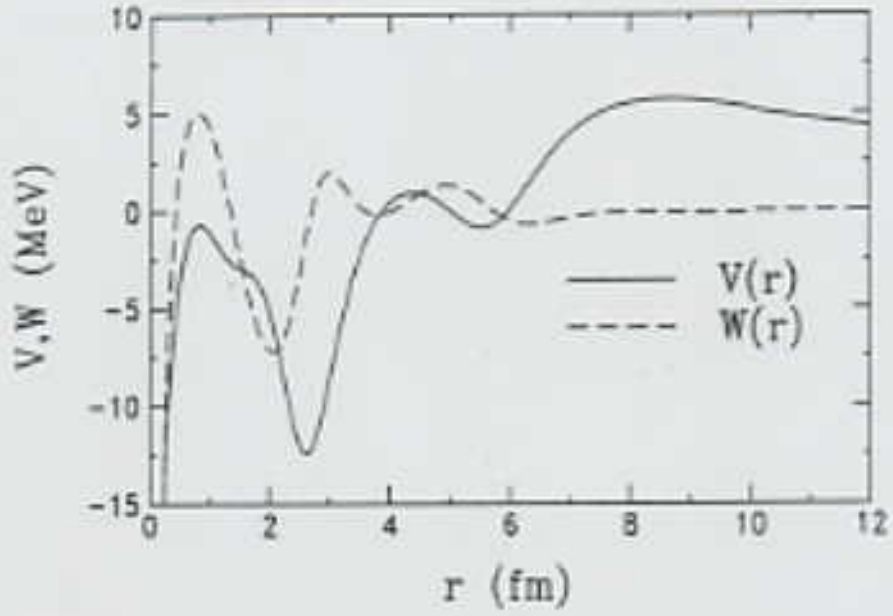

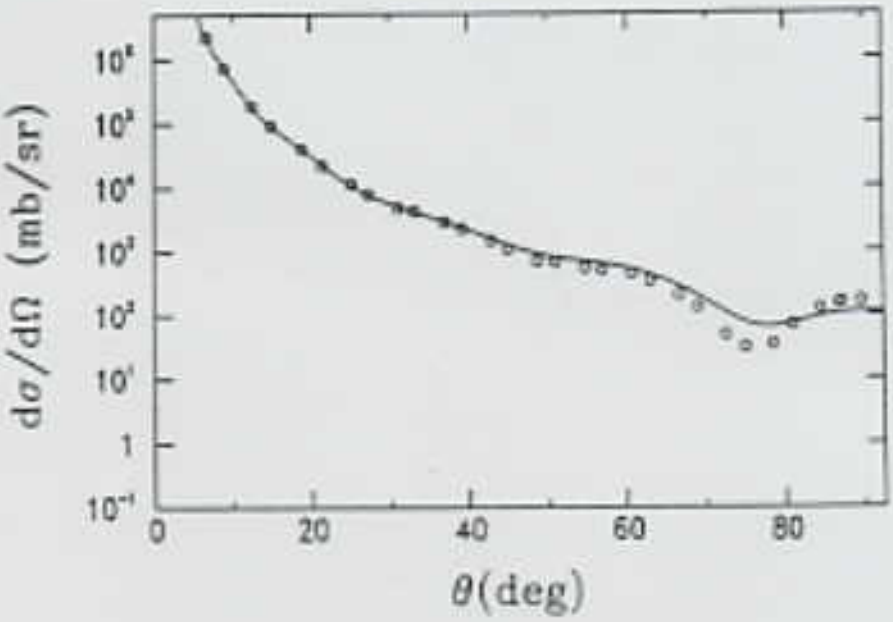

$^{12}C + ^{12}C$

$E_{cm} = 8\,MeV$

Voit et al.

Abbildung 5.1: *a) Invertiertes Potential für* $E_{c.m.} = 7.988 MeV$ *mit dem Phasensatz von Tabelle D.1 mit* $r_0 = 10 fm$ *und* $\rho_{g_i} = 11.5, 12.5, 13.5$
b) Vergleich des aus dem Potential errechneten Wirkungsquerschnitts mit den experimentellen Daten

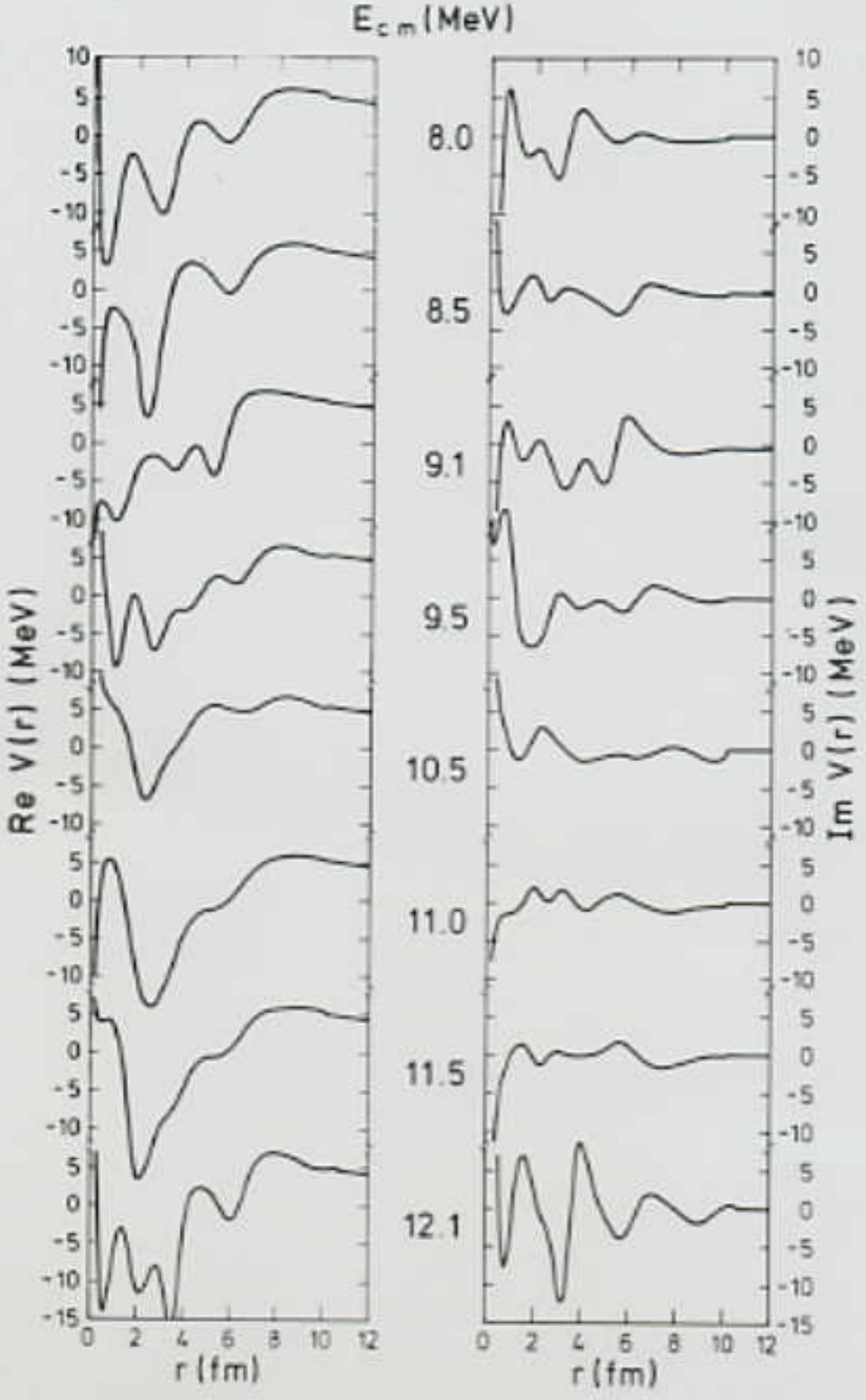
E c m (MeV)
8.0
8.5
9.1
9.5
10.5
11.0
11.5
12.1
Re V(r) (MeV)
Im V(r) (MeV)
r (fm)
r (fm)

$^{12}C + ^{12}C$ potential as function of energy

Real potential:

molecular minimum at $r = 5-6$ fm

additional minimum at $r = 2-3$ fm

Imaginary potential:

partially positive, e.g. at 5–6 fm

back feeding of flux from

inelastic channels

Method is tested by recalculating the differential cross sections with the inverted potentials.

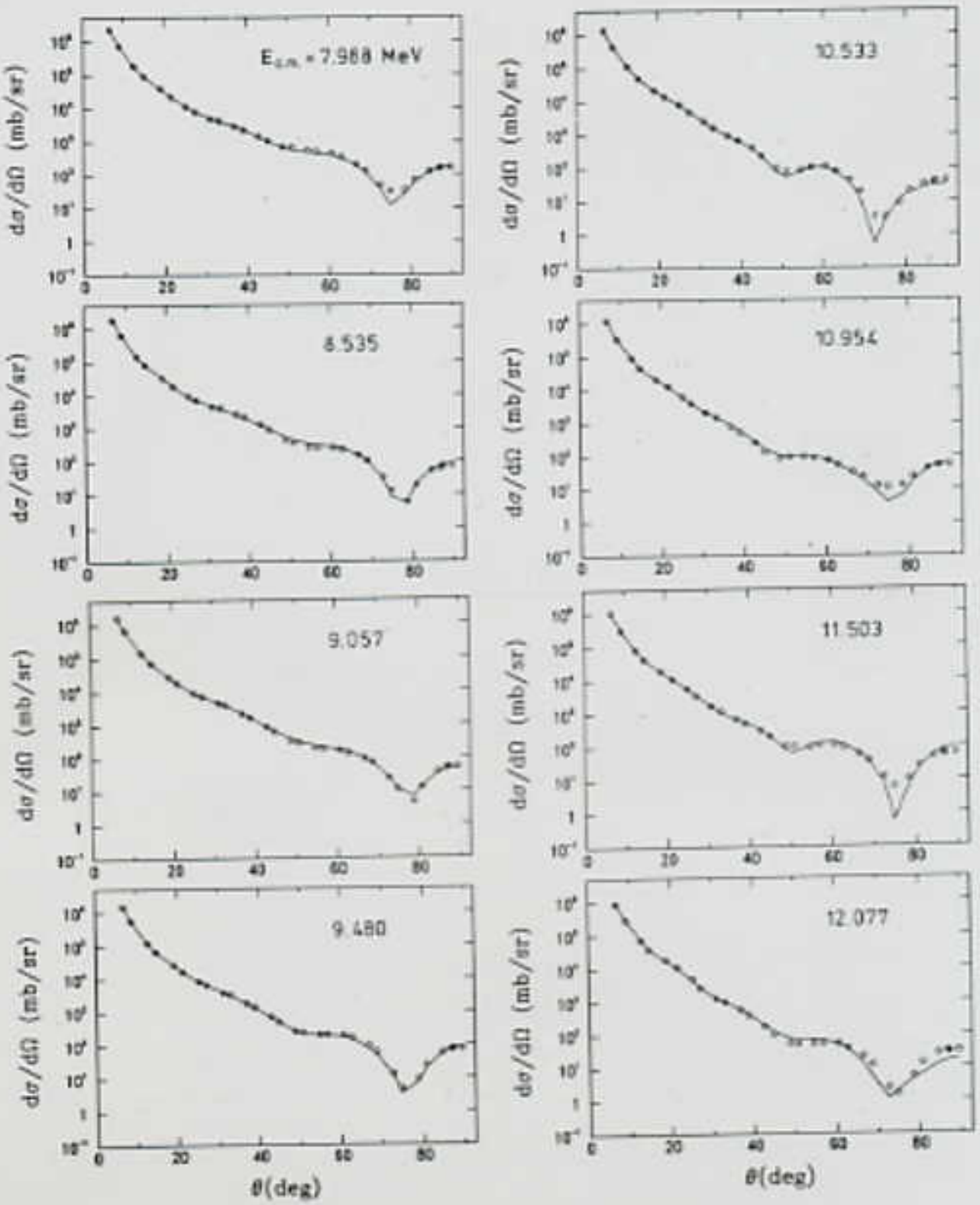
$E_{c.m.}$ = 7.988 MeV
10.533
8.535
10.954
9.057
11.503
9.480
12.077
dσ/dΩ (mb/sr)
θ(deg)

4. Collective molecular states with deformed nuclei: $^{12}C + ^{12}C$

Phenomenological model with oblately deformed ^{12}C nuclei.

Calculation of quasibound states with equator-equator-like configurations.

Similar treatment is possible for prolately deformed nuclei, e.g. $^{24}Mg + ^{24}Mg$.

a) Molecular configurations of $^{12}C + ^{12}C$

^{12}C : oblate deformation of $\beta_0 = -0.6$

configurations with minimal energies

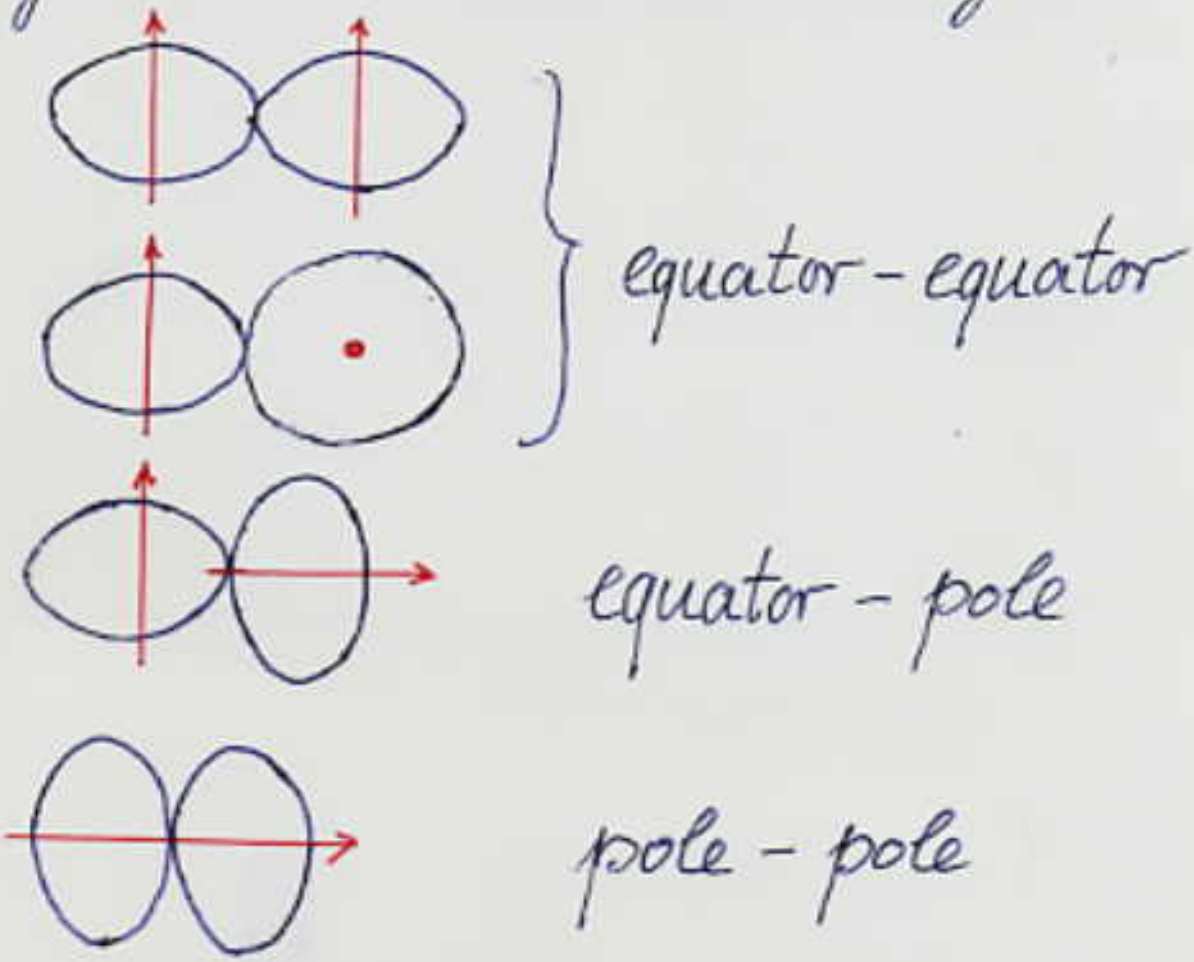

equator-equator-like configurations are energetically favoured, triaxial rotator, complex dynamics

b) Hamiltonian

Molecular coordinate system (MO-system):
z'-axis has direction of $\vec{r}$.

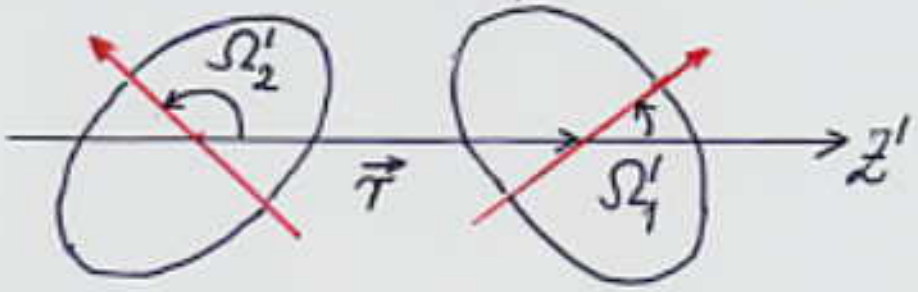

Ω_1', Ω_2' Euler angles with respect to MO-system.
$\beta_1, \beta_2, \gamma_1, \gamma_2$ intrinsic quadrupole deformation coord.,
γ_1 and γ_2 disregarded in the following.

$$H = \frac{P_r^2}{2\mu} + \frac{(I-J_1-J_2)_{x'}^2 + (I-J_1-J_2)_{y'}^2}{2\mu r^2} + \sum_{i=1}^{2} T_{RVM}(\vec{J}_i, \beta_i, \gamma_i)$$
$$+ U(r, \beta_1, \gamma_1, \Omega_1', \beta_2, \gamma_2, \Omega_2') + iW$$
$$+ \sum_{i=1}^{2} \left(\frac{C_\beta}{2}(\beta_i \cos\gamma_i - \beta_0)^2 + \frac{C_\gamma}{2}(\beta_i \sin\gamma_i)^2 \right)$$

This Hamiltonian describes elastic and inelastic scattering and contains quasibound molecular states, which generate resonances with small widths in cross sections.

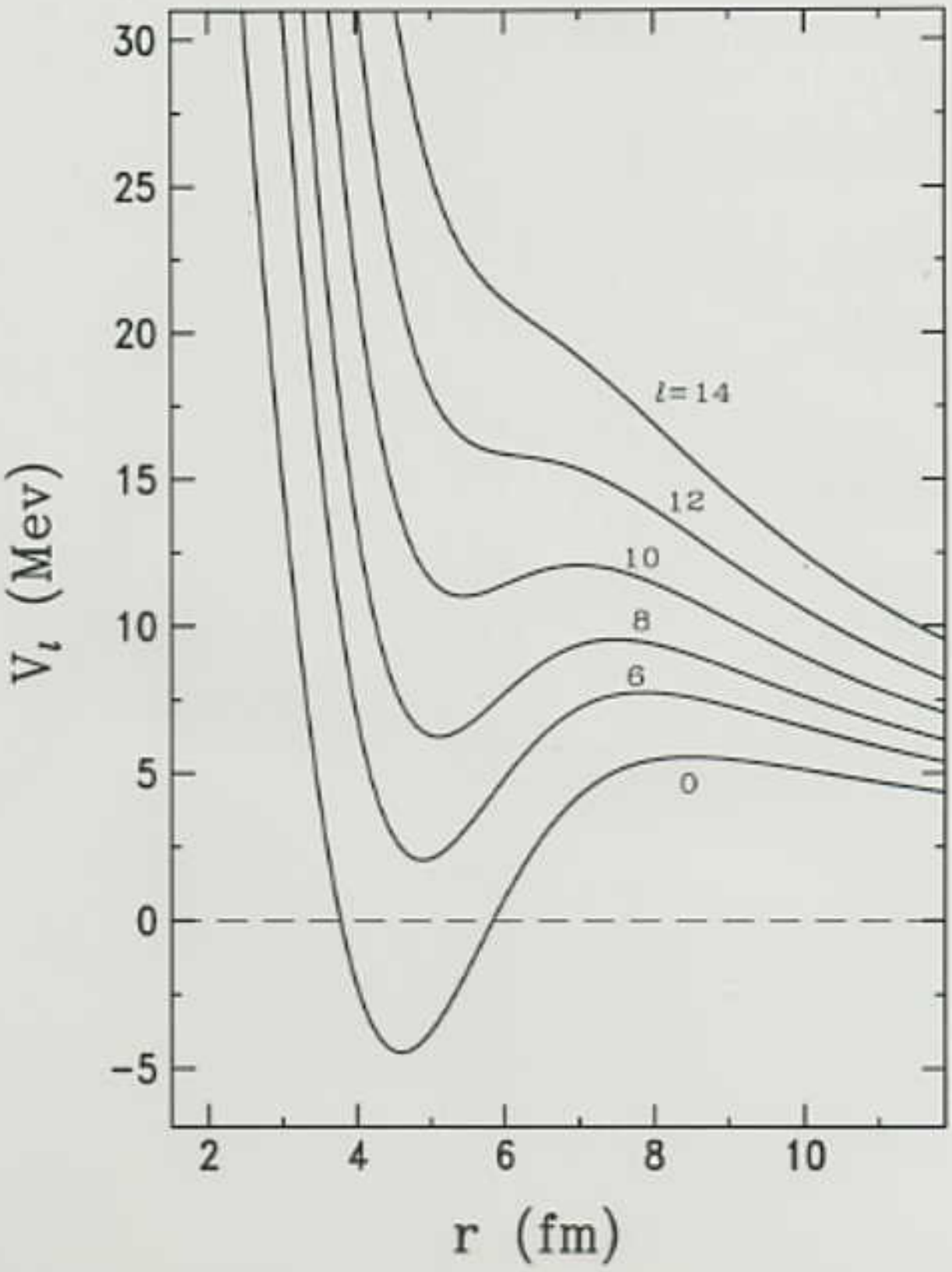
30
25
20
15
10
5
0
−5
2
4
6
8
10
V_l (Mev)
r (fm)
l=14
12
10
8
6
0

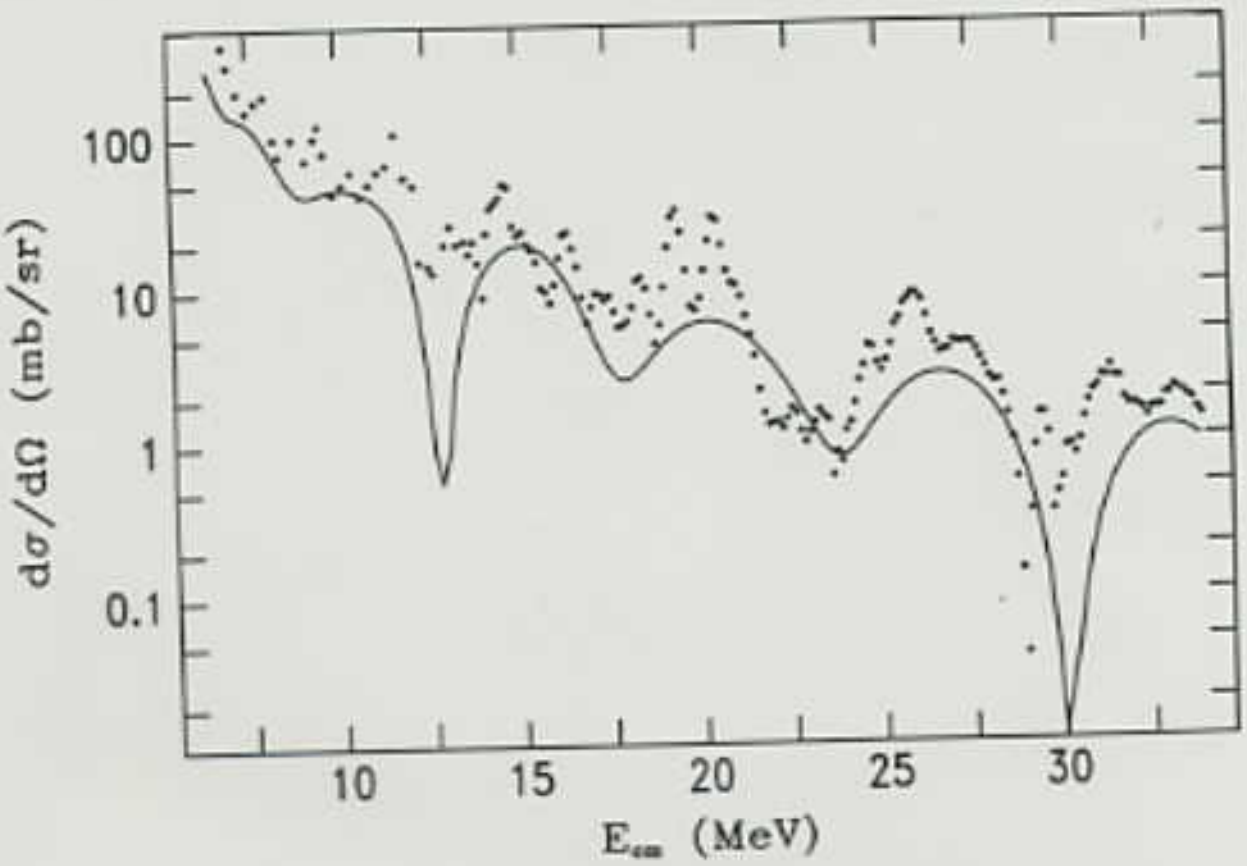
100
10
1
0.1
dσ/dΩ (mb/sr)
10
15
20
25
30
E_cm (MeV)

c) Potential energy surfaces around special orientations of intrinsic axes

PES for stiff rotation of the molecule with frozen intrinsic degrees of freedom

$$H^{I}_{PES} = \frac{1}{2}\vec{I}\,\Theta^{-1}\vec{I} + U(r, \beta_1, \varphi_1', \vartheta_1', \beta_2, \varphi_2', \vartheta_2') + \sum_{i=1}^{2} \frac{C_2}{2}(\beta_i - \beta_0)^2$$

Θ = tensor of moment of inertia

e.g. equator-equator orientation:

$$\varphi_1' = \varphi_2' = 0, \quad \vartheta_1' = \vartheta_2' = \pi/2$$

$$\Theta_{x'x'} = \mu r^2, \quad \Theta_{y'y'} = \mu r^2 + 2\Theta_0, \quad \Theta_{z'z'} = 2\Theta_0$$

$$\Theta_0 = 3B_0\beta_i^2, \quad \beta_0 = -0.60$$

Kinetic energy operator: triaxial rotator, energy by diagonalisation.

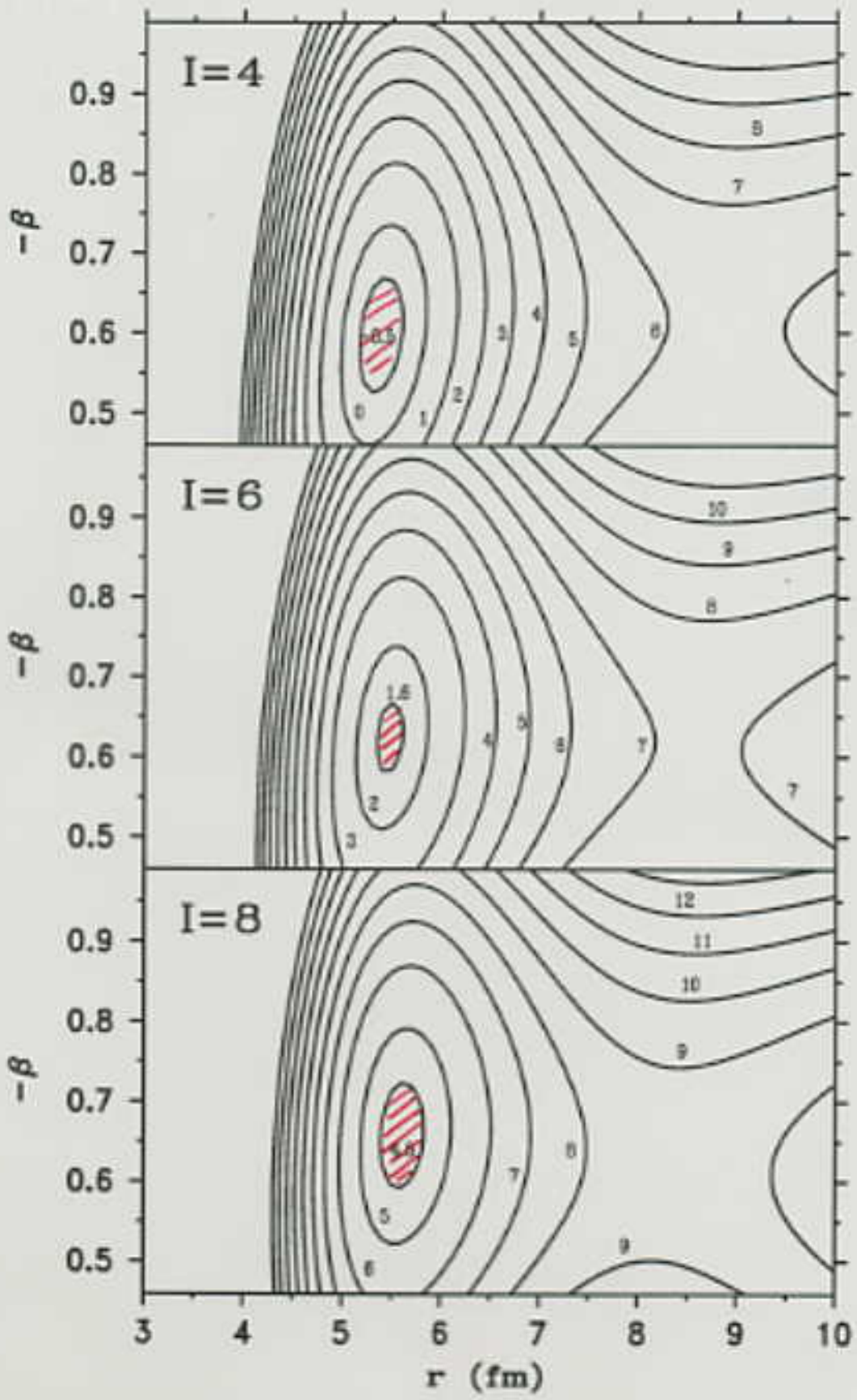
I=4
I=6
I=8
-β
0.9
0.8
0.7
0.6
0.5
3
4
5
6
7
8
9
10
r (fm)

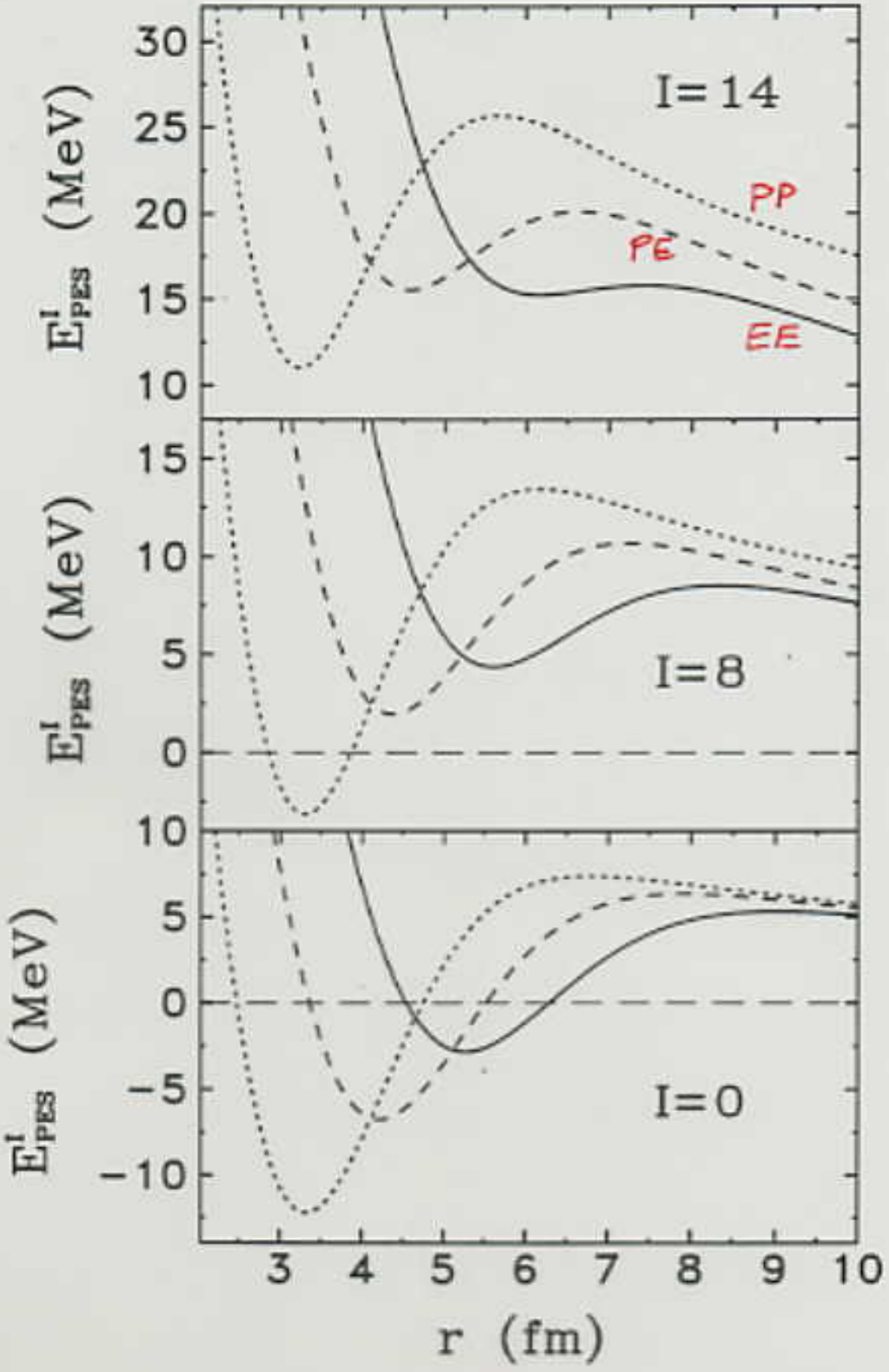
I=14
PP
PE
EE
I=8
I=0
E^I_{PES} (MeV)
r (fm)
30
25
20
15
10
5
0
−5
−10
3
4
5
6
7
8
9
10

d) States around equator - equator orientation

Important for appearence of molecular resonances.

Assumption: independent degrees of freedom around the energy minimum of the EE-orientation.

$$H_{EE}\,\psi_\nu = E_\nu\,\psi_\nu$$

$$E_\nu = E_0(I) + D_K K^2 + D_\kappa(\kappa^2-2) + \hbar\omega_r(n_r+\tfrac{1}{2})$$

$$+\hbar\omega_{\vartheta_1}(n_1+\tfrac{1}{2}) + \hbar\omega_{\vartheta_2}(n_2+\tfrac{1}{2}) + \hbar\omega_\beta(\mu_+ + \mu_-)$$

for $I = 8$:

$$D_K = 0.216\,\text{MeV},\quad D_\kappa = 0.306\,\text{MeV},$$
$$\hbar\omega_{\vartheta_i}(K=\kappa=0) = 2.115\,\text{MeV},$$
$$\hbar\omega_\beta = 7.66\,\text{MeV},\quad \hbar\omega_r = 6.82\,\text{MeV}.$$

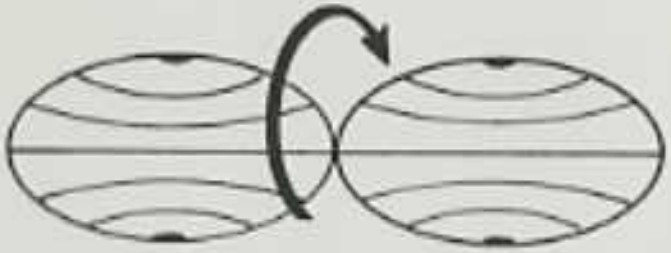

a) K-mode

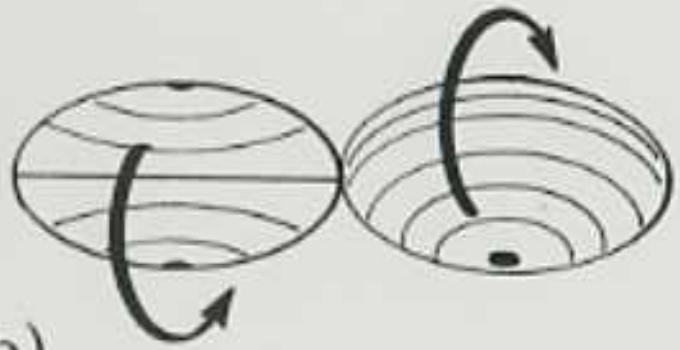

b) K-mode

c) butterfly osaillations

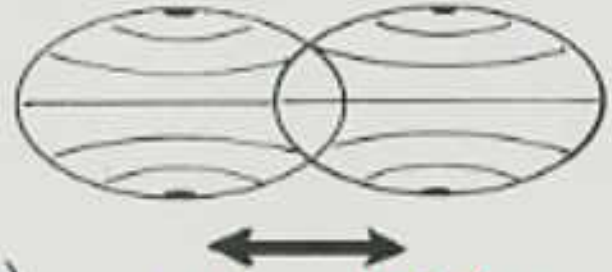

d) radial oscillation

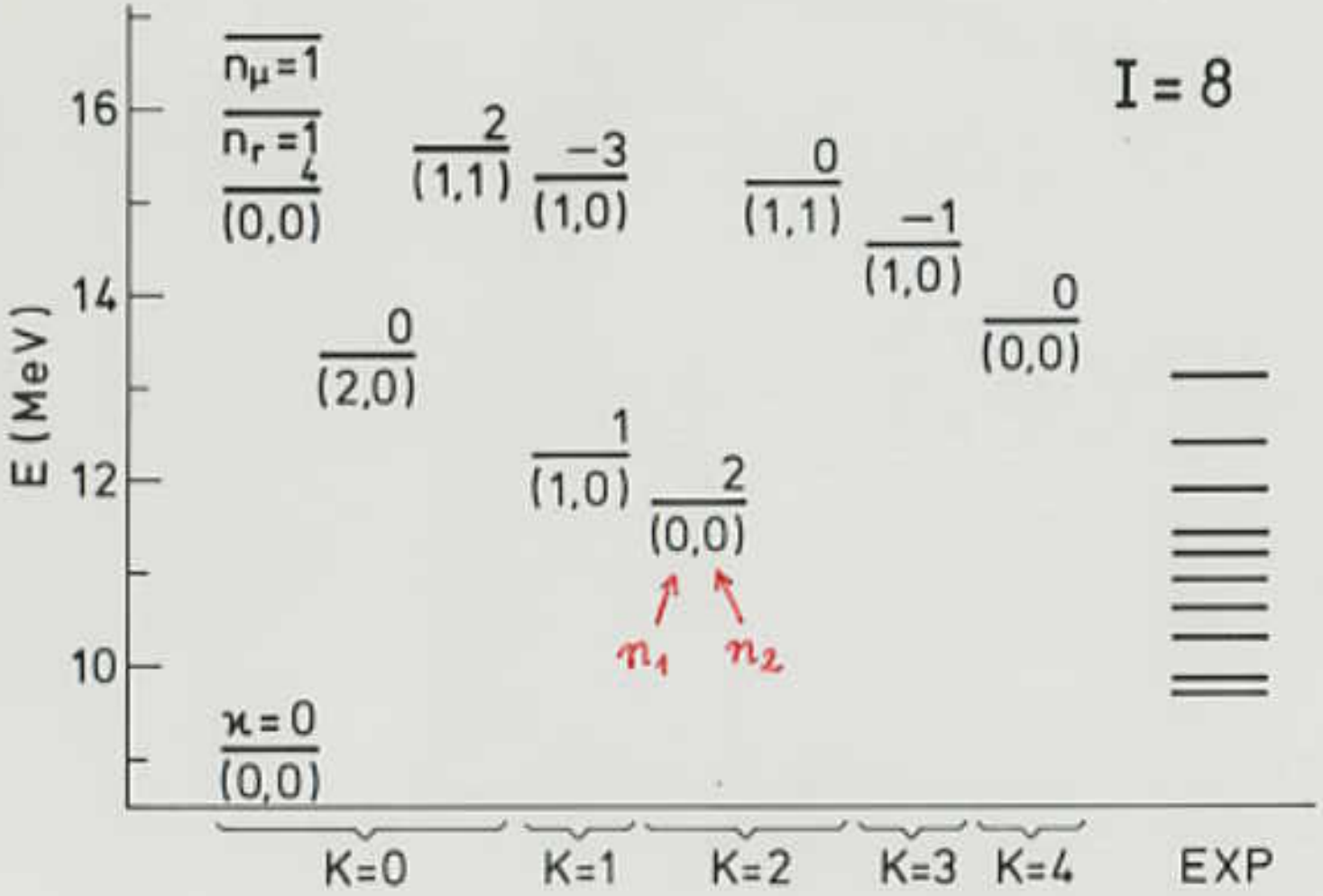
I = 8
E (MeV)
16
14
12
10
$n_\mu = 1$
$n_r = 1$
4
(0,0)
2
(1,1)
−3
(1,0)
0
(1,1)
−1
(1,0)
0
(0,0)
0
(2,0)
1
(1,0)
2
(0,0)
n_1
n_2
$\varkappa = 0$
(0,0)
K=0
K=1
K=2
K=3
K=4
EXP

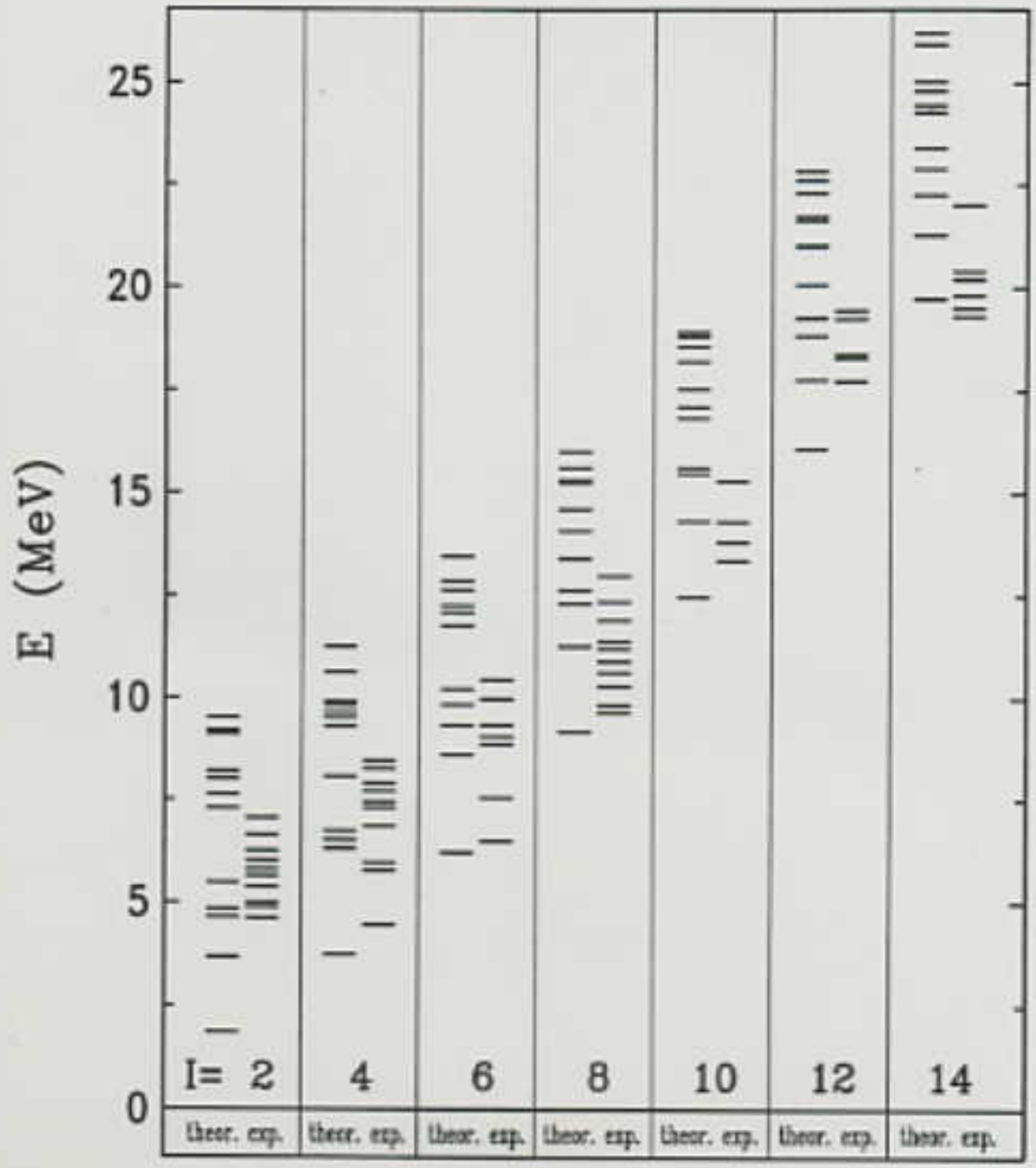
E (MeV)
25
20
15
10
5
0
I= 2
4
6
8
10
12
14
theor. exp.
theor. exp.
theor. exp.
theor. exp.
theor. exp.
theor. exp.
theor. exp.

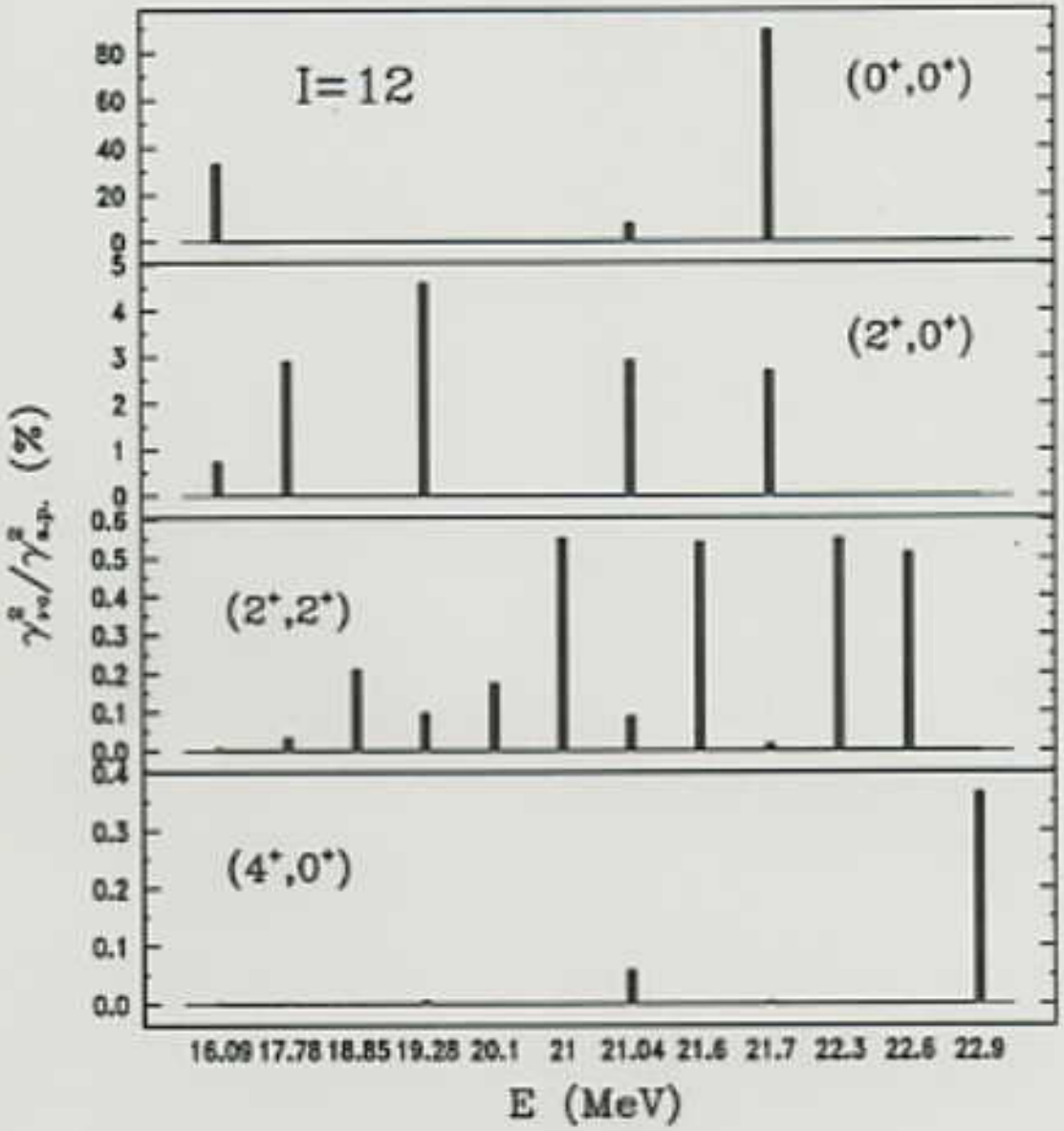
I=12
(0⁺,0⁺)
(2⁺,0⁺)
(2⁺,2⁺)
(4⁺,0⁺)
80
60
40
20
0
5
4
3
2
1
0
0.6
0.5
0.4
0.3
0.2
0.1
0.0
0.4
0.3
0.2
0.1
0.0
16.09 17.78 18.85 19.28 20.1 21 21.04 21.6 21.7 22.3 22.6 22.9
E (MeV)
$\gamma^2_{\gamma,\gamma'}/\gamma^2_{\alpha,\alpha'}$ (%)

e) Resonances in the $^{24}Mg + ^{24}Mg$ system

Origin of resonances:

nuclear molecular configurations

Coupled channel calculations with ^{24}Mg states:

gross structure +
broader intermediate structures

^{24}Mg nucleus is prolately deformed.

Resonances with total width ~200keV can be explained by quasibound states in a pole-to-pole-like configuration of ^{24}Mg nuclei.

^{24}Mg ^{24}Mg

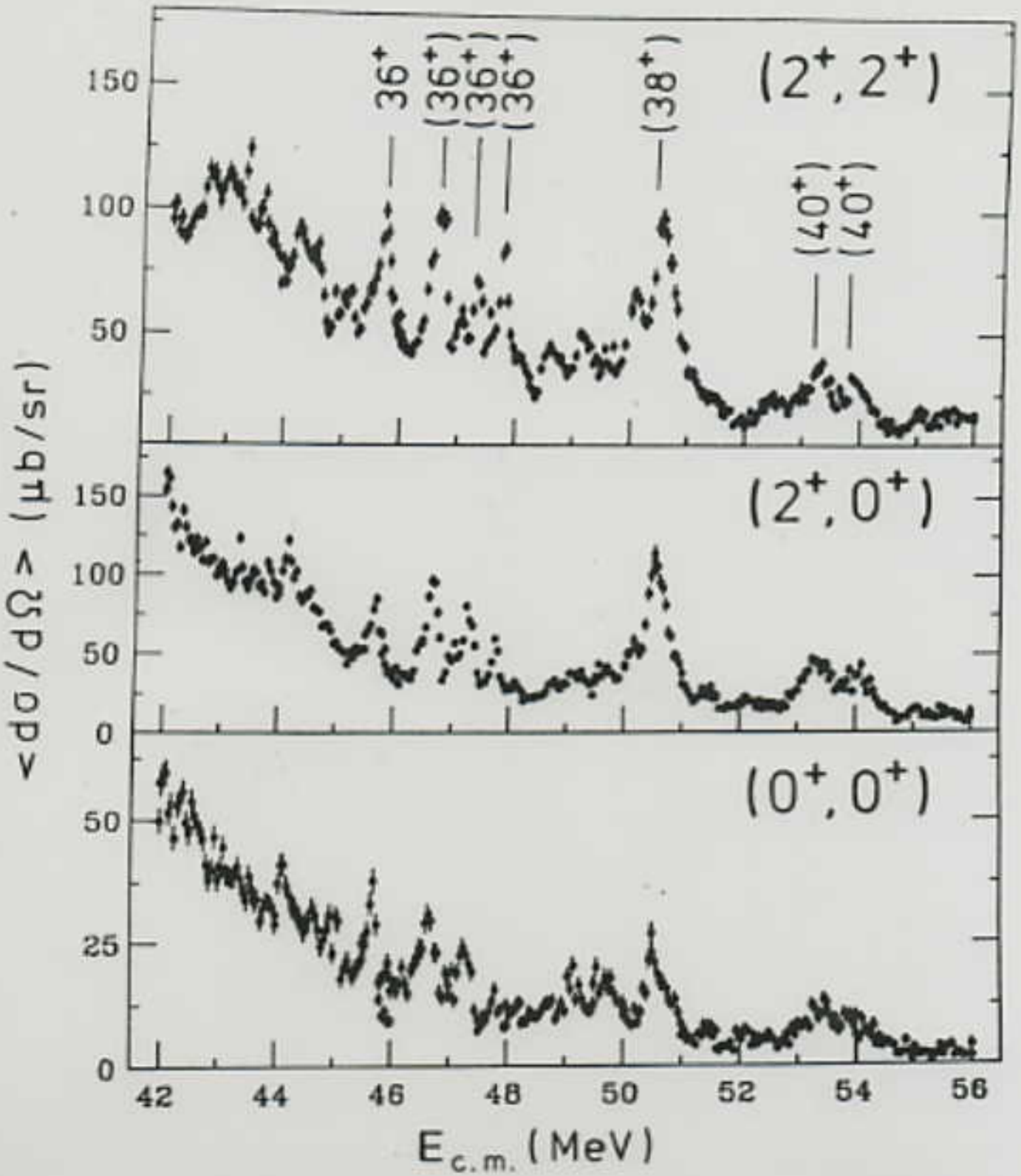
(2+, 2+)
(2+, 0+)
(0+, 0+)
36+
(36+)
(36+)
(36+)
(38+)
(40+)
(40+)
150
100
50
150
100
50
0
50
25
0
42
44
46
48
50
52
54
56
< dσ / dΩ > (μb/sr)
Ec.m. (MeV)

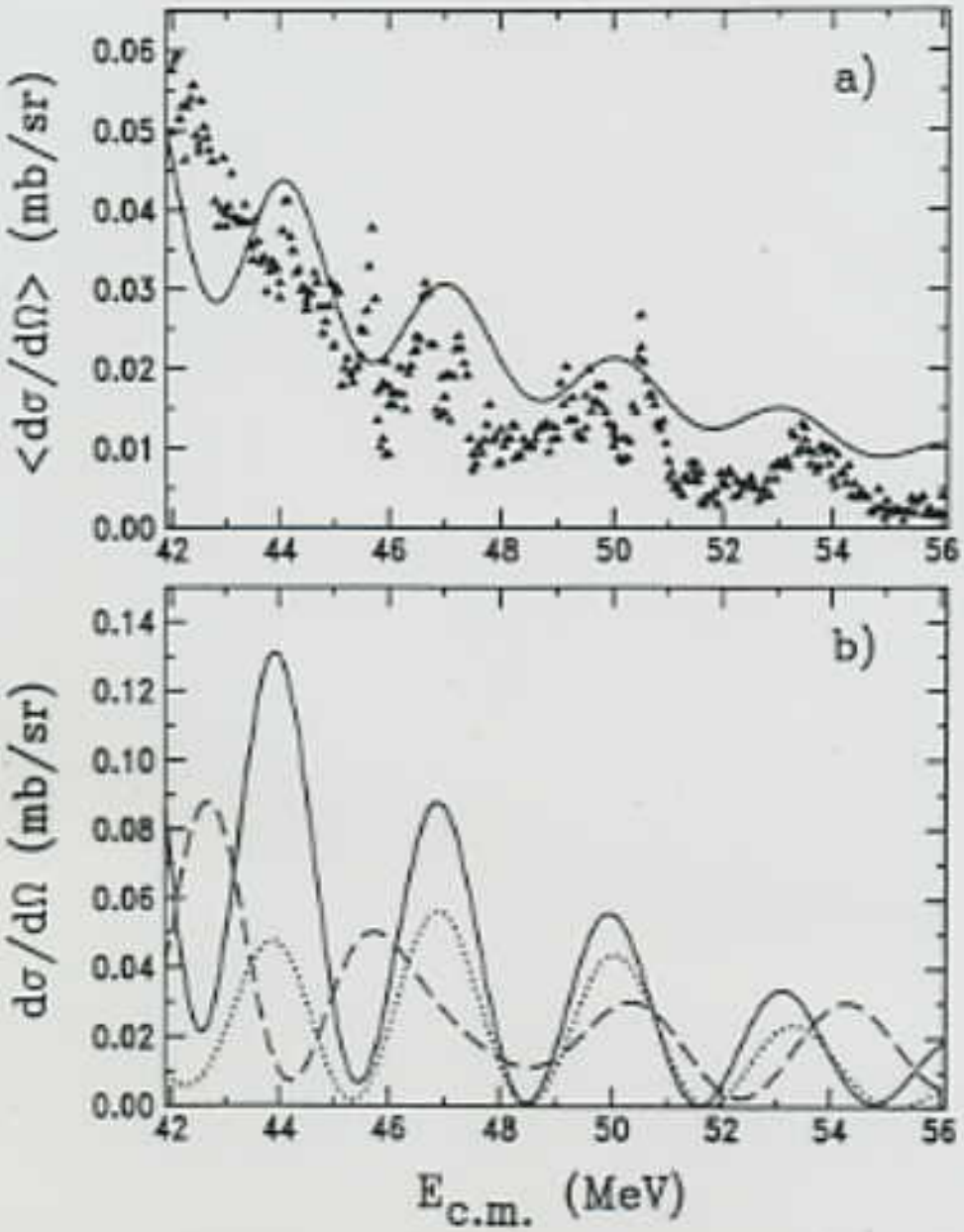

Figure 4. (*a*) Elastic excitation function from an uncoupled calculation with parameters as given in sections 3.1 and 3.3. The triangles represent the data of [1]. The cross section is averaged over an angular range $33.4° \leqslant \theta_{lab} \leqslant 46.9°$. (*b*) Excitation functions for individual angles. The full, dotted and broken curves represent $\theta_{CM} = 90°$, 80° and 70°, respectively.

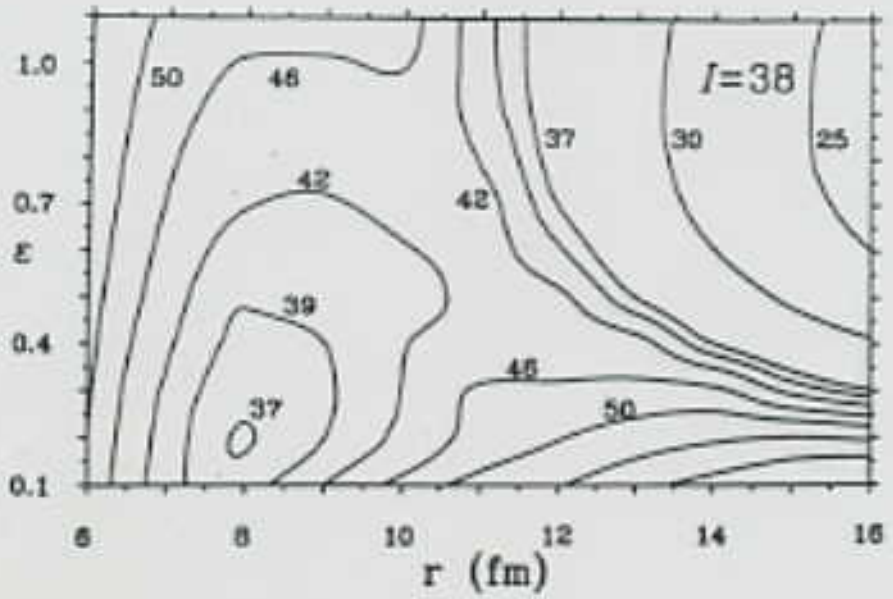

Fig. 2 Potential energy surface for the $^{24}Mg + ^{24}Mg$ system including the centrifugal potential for $I = 38$.

$^{24}Mg+^{24}Mg$ (r=8.1fm,ε=0.21)

Fig. 3 Nuclear shape of the $^{24}Mg + ^{24}Mg$ system at the minimum of the potential as shown in Fig. 2.

Rotation:

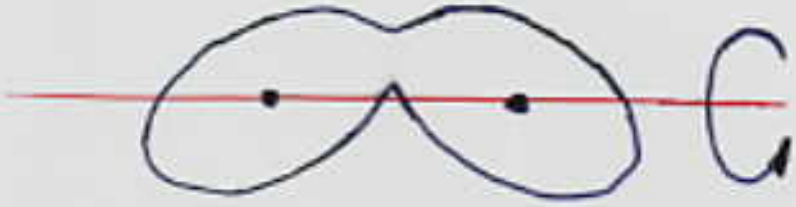

ϕ_+

Vibrations:

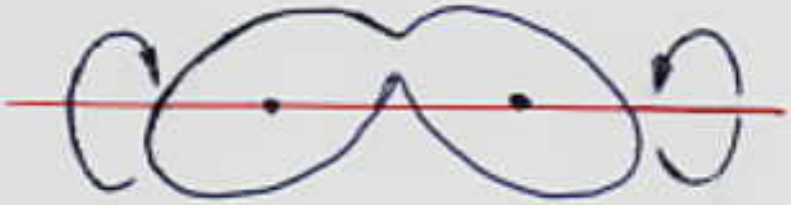

ϕ_-

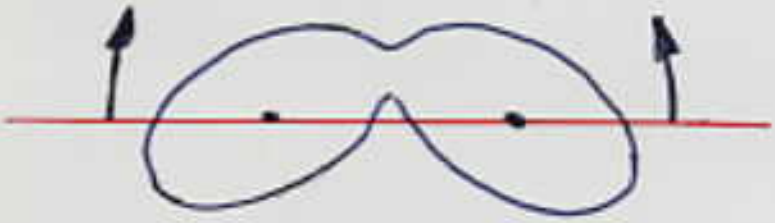

ϑ_+

ϑ_-

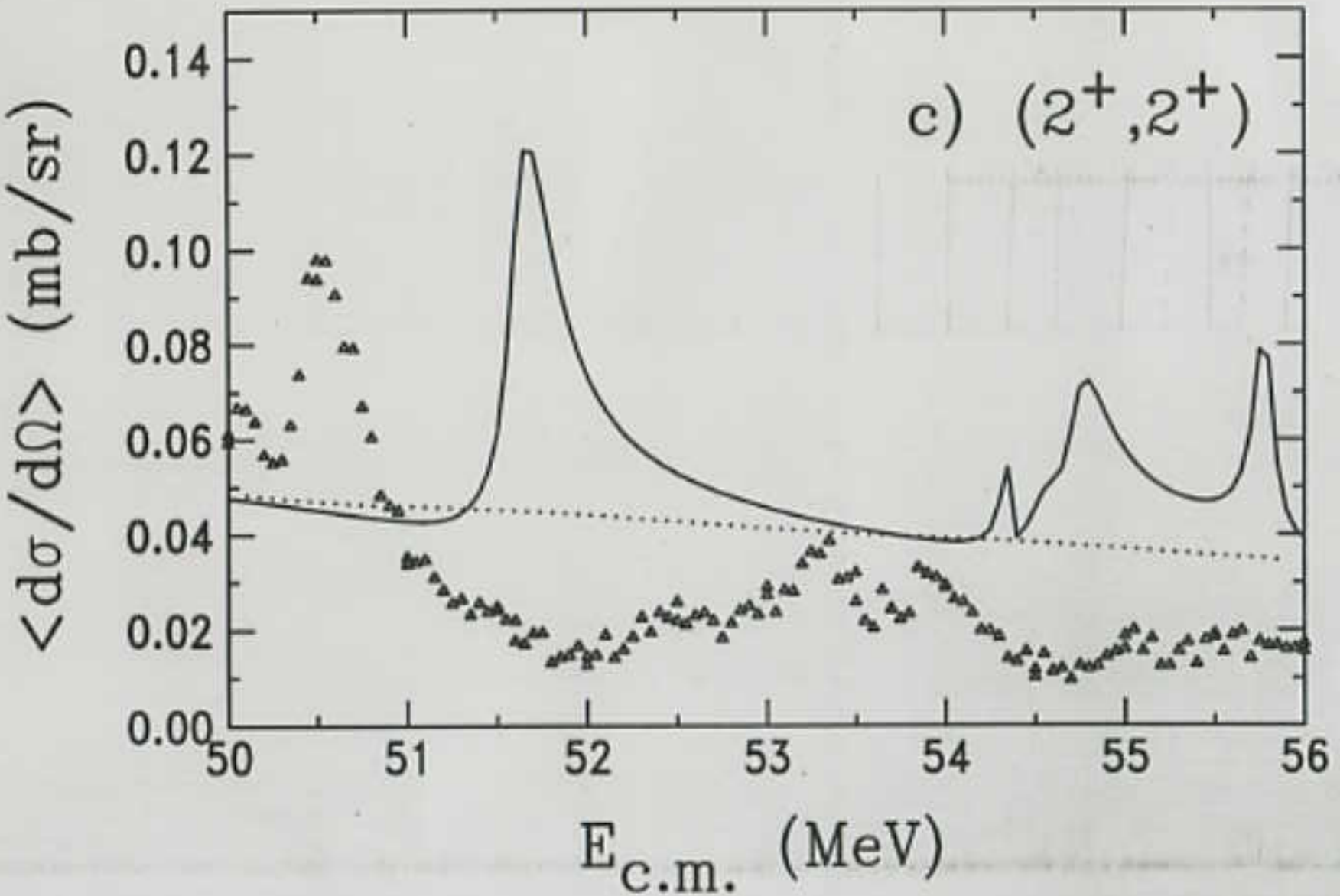
c) (2+,2+)
<dσ/dΩ> (mb/sr)
0.14
0.12
0.10
0.08
0.06
0.04
0.02
0.00
50
51
52
53
54
55
56
E c.m. (MeV)

5. Semimicroscopic algebraic cluster model for ^{24}Mg states

Description of low energy spectrum of ^{24}Mg and $^{12}C + ^{12}C$ resonance states

$^{12}C + ^{12}C$ - cluster model

Relative motion: vibron model with $U(4)$-group structure

Internal motion: $SU(3)$ shell model in terms of $U(3)$ group for the orbitals and $U^{ST}(4)$ for spin and isospin degrees of freedom

$$U_{C_1}(3) \otimes U^{ST}_{C_1}(4) \otimes U_{C_2}(3) \otimes U^{ST}_{C_2}(4) \otimes U_R(4)$$

C = cluster, R = relative motion

a) States

Basis states are characterized by irreducible representations of the group chain:

$$U_{C_1}(3) \otimes U_{C_2}(3) \otimes U_R(4) \supset U_C(3) \otimes U_R(3) \supset U(3) \supset SU(3) \supset O(3)$$

b) Hamiltonian

H is expressed in terms of invariants of groups (Casimir operators):

$$H = E_0 + \alpha_R n_\pi + \beta_R C_2(SU_R(3)) + \beta_C C_2(SU_C(3)) + (\beta + \tilde{\beta} n_\pi) C_2(SU(3)) + \gamma C_3(SU(3)) + (\delta + \tilde{\delta}(-1)^{n_\pi}) \chi^2 + \tilde{\omega}(-1)^{n_\pi + \chi^2} + (\epsilon + \tilde{\epsilon} n_\pi) C_2(O(3))$$

$\chi \hat{=}$ K-quantum number

$n_\pi \geq 12$, number of oscillator quanta of relative motion

parameters: $E_0, \alpha_R, \beta_R, \beta_C, \beta, \tilde{\beta}, \gamma, \delta, \tilde{\delta}, \tilde{\omega}, \epsilon, \tilde{\epsilon}$

Eigenvalues:

$$E = E_0 + \alpha_R n_\pi + \beta_R n_\pi(n_\pi+3) + \beta_C(\lambda_c^2+\mu_c^2+\lambda_c\mu_c + 3\lambda_c+3\mu_c) + (\beta+\tilde{\beta}n_\pi)(\lambda^2+\mu^2+\lambda\mu+3\lambda+3\mu) + \gamma(\lambda-\mu)(\lambda+2\mu+3)(2\lambda+\mu+3) + (\delta+\tilde{\delta}(-1)^{n_\pi})\chi^2 + \tilde{\omega}(-1)^{n_\pi+\chi^2} + (\epsilon+\tilde{\epsilon}n_\pi)J(J+1)$$

Parameters fitted in a two-step procedure:

1. $E_0, \beta_c, \beta, \gamma, \delta, \epsilon$ fitted to the positive and negative parity spectrum at low energies
2. n_π-dependent factors $\alpha_R, \beta_R, \tilde{\beta}, \tilde{\delta}, \tilde{\omega}, \tilde{\epsilon}$ determined by fitting the molecular resonances with $n_\pi = 14$

c) Resulting spectrum

Model describes all observed rotational bands and predicts some more around $E_x = 10\,MeV$.

Negative-parity states are somewhat less well reproduced. Reason: No negative-parity internal excitations of the ^{12}C-clusters were taken into account.

Also distribution of resonance states reasonably well reproduced.

In addition we calculated electromagnetic transition probabilities with these states.

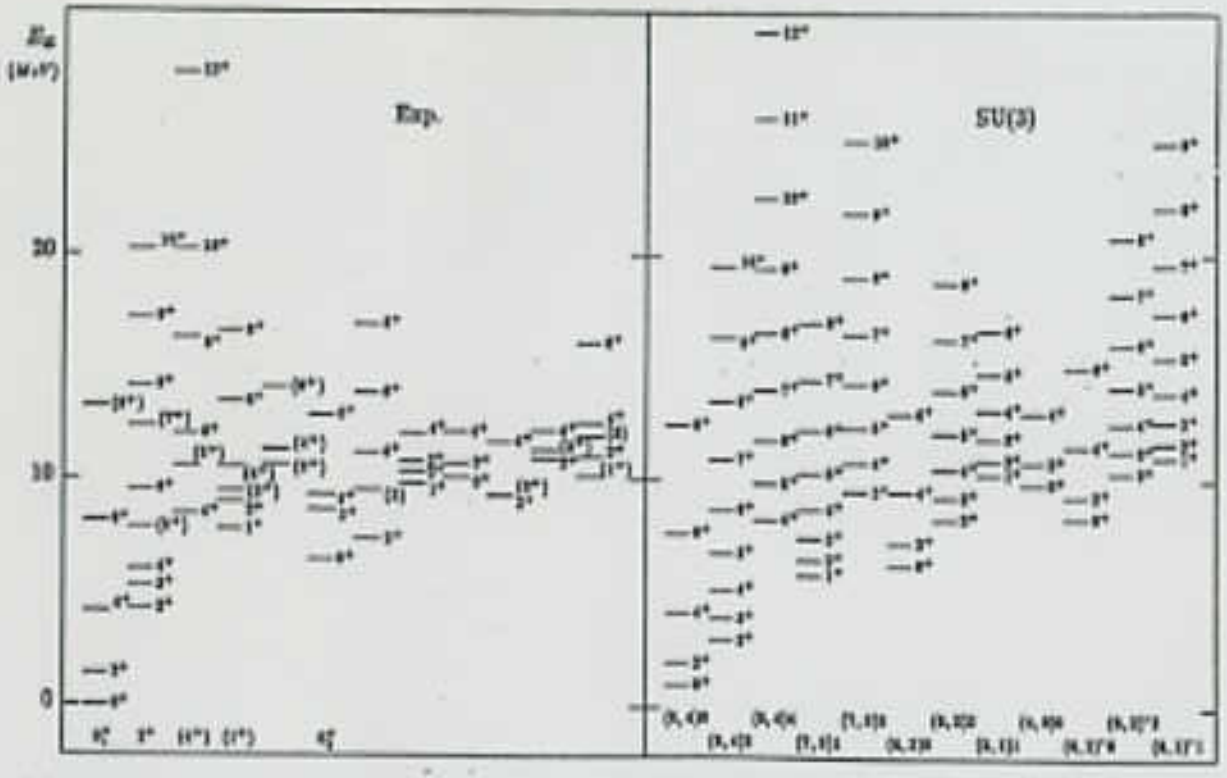

FIG. 1. The positive-parity energy spectrum of the ^{24}Mg nucleus: experimental level scheme (a), and its interpretation in terms of the semimicroscopic algebraic cluster model (b). The experimental data were taken from Ref. [29], except the $J^\pi = 9^-$, 10^+, and 12^+ levels. (See text for details.) K^π labels of known bands in the experimental spectrum are also displayed. The model bands are labeled by n_σ=12 (not shown) and by the $(\lambda,\mu)\chi$ quantum numbers.

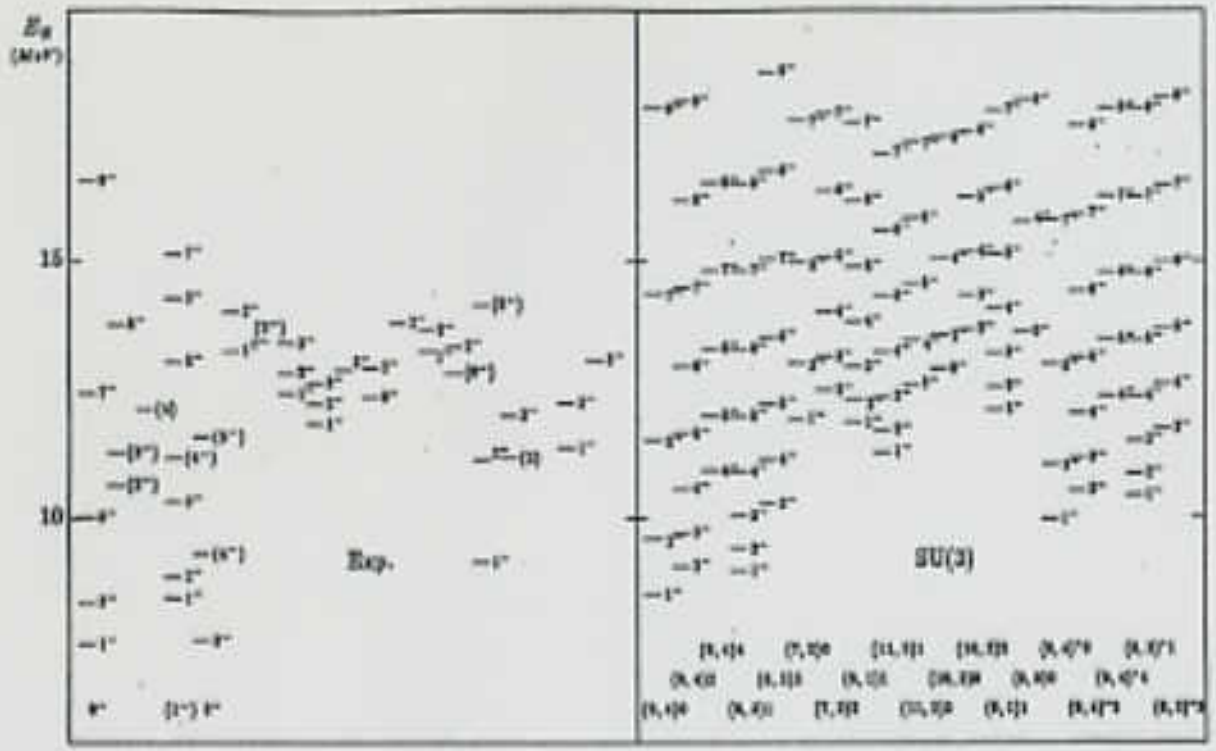

FIG. 2. The same as Fig. 1, for negative parity. The model bands are labeled by $n_s=13$ (not shown) and by the $(\lambda,\mu)\chi$ quantum numbers. Two model bands above $E_x=14$ MeV are not displayed.

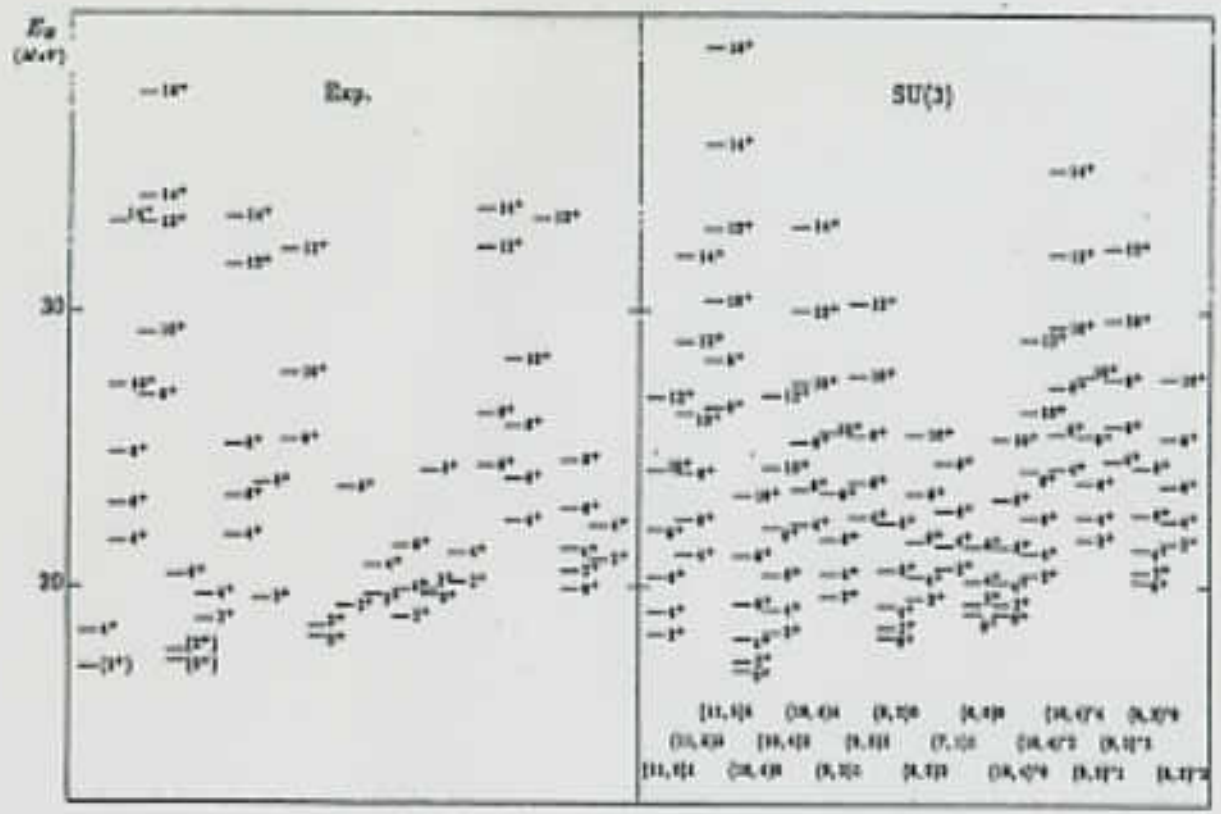

FIG. 3. The same as Fig. 1, in the $^{12}C+^{12}C$ molecular resonance region. The experimental data were taken from Ref. [31], except for the three low-lying levels with ambiguous spin assignment, which are from Ref. [9]. The model bands are labeled by $n_\omega=14$ (not shown) and by the $(\lambda,\mu)\chi$ quantum numbers. Model bands lying above $E_x=24$ MeV are not displayed.

6. Excitation of hyperdeformed states in heavy ion collisions

The question arises whether nuclear molecular states and hyperdeformed states are the same objects.

Shell model calculations of Gwiok et al. show that hyperdeformed (HD) states correspond to touching nuclei.

This opens the possibility to form HD states in heavy ion collisions.

Hyperdeformed states can be quasibound states of the dinuclear system.

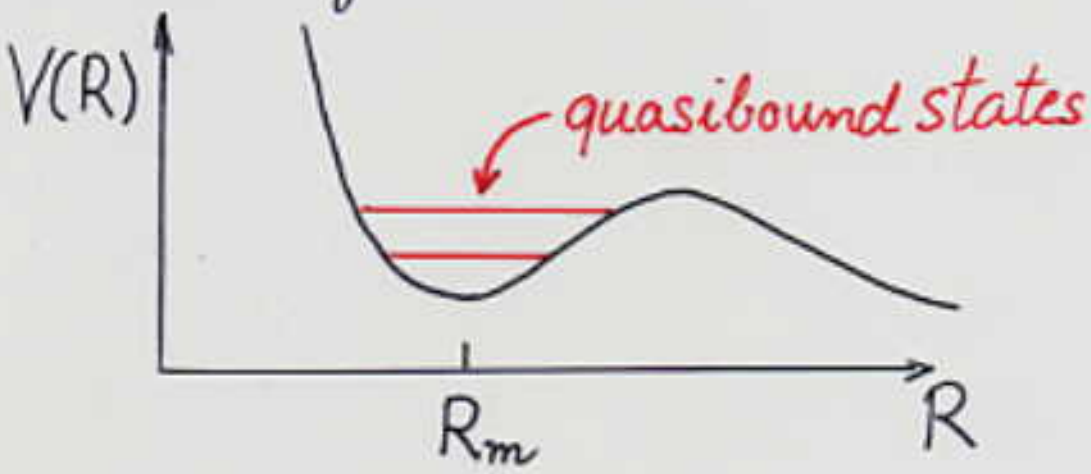

Investigation of the systems:

$^{48}Ca + {}^{140}Ce \longrightarrow {}^{188}Pt$, $\eta = 0.49$

$^{90}Zr + {}^{90}Zr \longrightarrow {}^{180}Hg$, $\eta = 0$

One to three quasibound states with $\hbar\omega \approx 2.2$ MeV for $L > 40\hbar$

Width for decay through barrier ~ 10 eV.

Energy values at $L=0$, quadrupole moments $(40-50)\cdot 10^2 e fm^2$ and moments of inertia $(160-190)\,\hbar^2/\text{MeV}$ of these configurations are close to those estimated for HD-states.

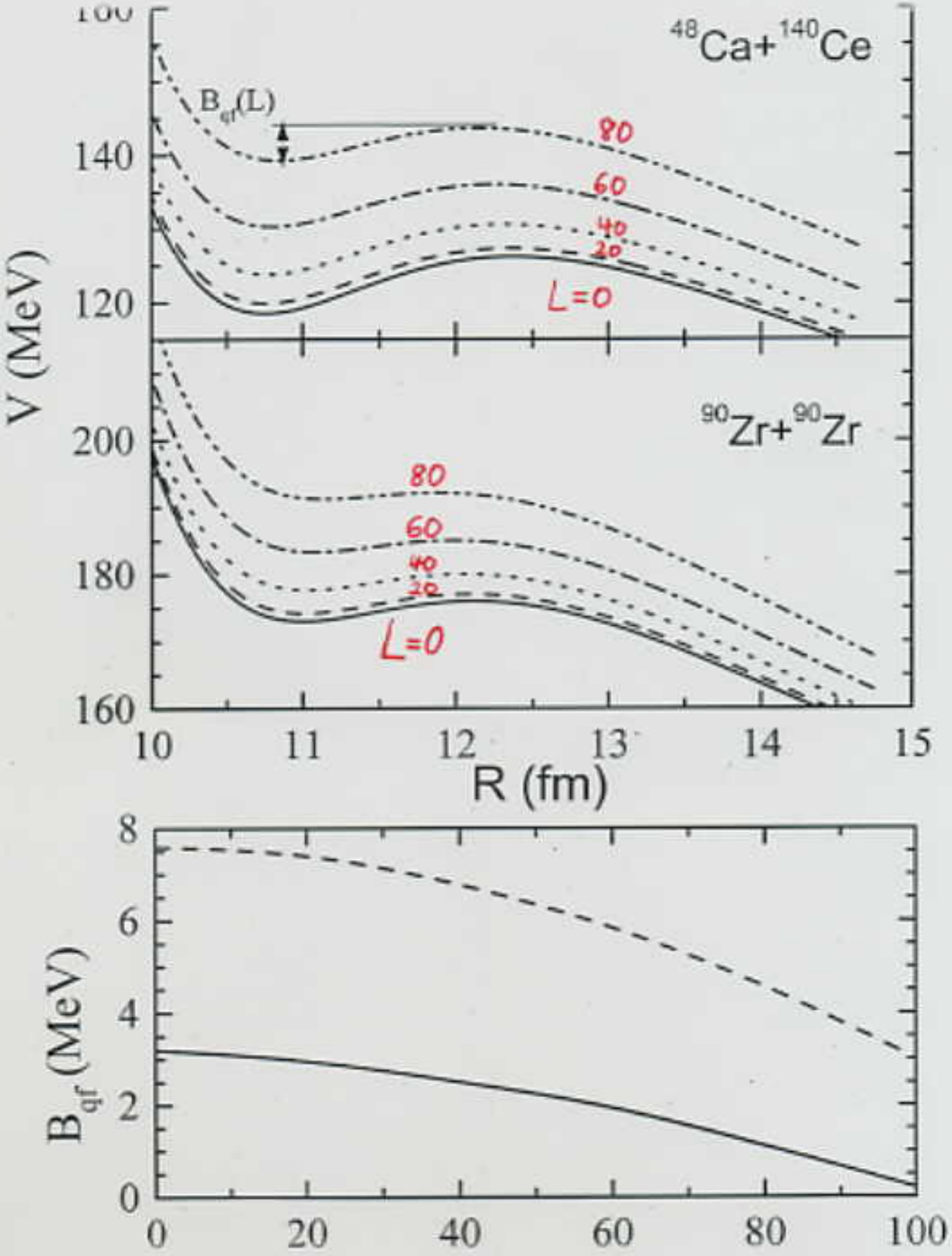
^{48}Ca+^{140}Ce
B_{qf}(L)
80
60
40
20
L=0
^{90}Zr+^{90}Zr
80
60
40
20
L=0
V (MeV)
R (fm)
160
180
200
120
140
10
11
12
13
14
15

B_{qf} (MeV)
0
2
4
6
8
0
20
40
60
80
100

Conditions for production of dinuclear states in heavy ion collisions

1. Formed DNS is nearly cold, states directly excited by tunneling through barrier
2. The initial DNS should stay stable against nucleon transfer, no change of mass asymmetry, minimum in $V(\eta)$ at $\eta = \eta_i$,
   spherical, stiff nuclei (magic or double magic)

Cross section for penetrating the barrier:

$$\sigma(E_{c.m.}) = \frac{\pi \hbar^2}{2\mu E_{c.m.}} \sum_{L=L_{min}}^{L_{max}} (2L+1)\, T_L(E_{c.m.})$$

$$T_L(E_{c.m.}) = 1/\left(1 + \exp\left(2\pi\left(V(R_b, \eta, L) - E_{c.m.}\right)/(\hbar\omega)\right)\right)$$

Molecular window $L_{min} \leq L \leq L_{max}$,
for smaller L-values fusion.

Decay of the dinuclear system by γ-transitions to lower L-values in coincidence with quasifission of dinuclear system (lifetime against quasifission $\sim 10^{-16}$ s).

Optimum conditions:

$^{48}Ca + ^{140}Ce$ $\quad E_{cm} = 147$ MeV, $90 < L < 100$

$^{90}Zr + ^{90}Zr$ $\quad E_{cm} = 180$ MeV, $40 < L < 50$

Estimated cross section for formation of HD-system about 1 μb.

Heavy ion experiments with coincidences of γ-rays and quasifission could verify whether the cluster interpretation is suitable for hyperdeformed states.
In principle, it means the search of nuclear molecular resonances in heavier systems.

7. Summary

Nuclear molecules have importance for the structure of exotic nuclei, e.g. $^{10}Be \leftrightarrow \alpha + \alpha + 2n$, and in astrophysics for the synthesis of elements.

Mainly nuclear systems with α-like structures show molecular properties.

Nucleus-nucleus potential has minimum in the touching region of nuclei. In this minimum there exist localized molecular states.
Molecular states survive in the molecular window because of the small spreading width to the compound system.

Nuclear molecular states can be observed as bound states or by resonances.

Gross structures in cross sections are produced by virtual states in the potential, intermediate structures by quasibound states.

Equator-to-equator-like and pole-to-pole-like configurations in the systems $^{12}C + ^{12}C$ and $^{24}Mg + ^{24}Mg$, respectively, are responsible for smaller resonances in the cross sections.

The semimicroscopic algebraic cluster model describes both the low-energy and molecular parts of the spectrum, e.g. of ^{24}Mg.

Hyperdeformed states are assumed as quasibound molecular states. They can be excited in heavy ion collisions.

The theory of nuclear molecules is interesting and a demanding task because it combines both the nuclear structure theory and a complex reaction theory.

———— • ————

The ideas presented in this part originated from Prof. W. Greiner (Frankfurt), Prof. Jae Park (Raleigh), Prof. Apagyi (Budapest), Prof. J. Cseh (Debrecen), Dr. G. Adamian (Dubna) and Dr. N. Antonenko (Giessen, Dubna).

Second Part

Molecular dynamics in mass (charge) asymmetry motion

1. Dinuclear system concept

This concept was introduced by V.V. Volkov for explanation of fusion.

The dinuclear system (other notation: nuclear molecule) is a configuration of two touching nuclei which keep their individuality.

In addition to the relative motion of the nuclei, the mass and charge asymmetry can change by transfer of nucleons.

Two main degrees of freedom:

1. transfer of nucleons between the nuclei, change of mass and charge asymmetry

$$\eta = \frac{A_1 - A_2}{A_1 + A_2} \quad , \quad \eta_Z = \frac{Z_1 - Z_2}{Z_1 + Z_2}$$

$\eta = 0$ for $A_1 = A_2$, $\eta = \pm 1$ for A_1 or $A_2 = 0$

2. Relative motion of nuclei, decay of dinuclear system: quasifission

Applications of dinuclear system model:

1. Nuclear structure phenomena: super- and hyperdeformed bands
2. Fusion to superheavy nuclei
3. Quasifission, no compound nucleus formed
4. Fission

2. The dinuclear configuration

Dinuclear configuration describes quadrupole- and octupole-like deformations and extreme deformations as super- and hyperdeformations.

a) Multipole moments

Mass (m) or charge (c) moments of a nucleus

$$Q_{\lambda\mu}^{(m\,or\,c)} = \sqrt{\frac{16\pi}{2\lambda+1}} \int \rho^{(m\,or\,c)}(\vec{r})\, r^{\lambda} Y_{\lambda\mu}(\Omega)\, d\tau$$

Dinuclear system :

density : $\rho(\vec{r}) = \rho_1(\vec{r}_1) + \rho_2(\vec{r}_2)$

parameters : mass and charge asymmetry η_1, η_2

Axially deformed nucleus:

shape expansion : $R = R_0\left(1 + \sum_{\lambda=0} \beta_\lambda Y_{\lambda 0}\right)$

parameters : $\beta_0, \beta_1, \beta_2, \beta_3 \ldots$

Comparison:

$$Q_{\lambda\mu}^{(m\,or\,c)}(\beta_\lambda) = Q_{\lambda\mu}^{(m\,or\,c)}(\eta \text{ or } \eta_z)$$

$$\longrightarrow \quad \beta_\lambda = \beta_\lambda(\eta \text{ or } \eta_z)$$

nearly independent of A for spherical clusters,
specific dependence on surface thickness,
radius parameter, deformation of clusters

DNS model can be applied:

$\eta = 0\text{-}0.3$: large quadrupole deformation,
hyperdeformed states

$\eta = 0.6\text{-}0.8$: quadrupole and octupole deformations
similar, superdeformed states

$\eta \approx 1$: linear increase of deformations,
parity splitting of bands

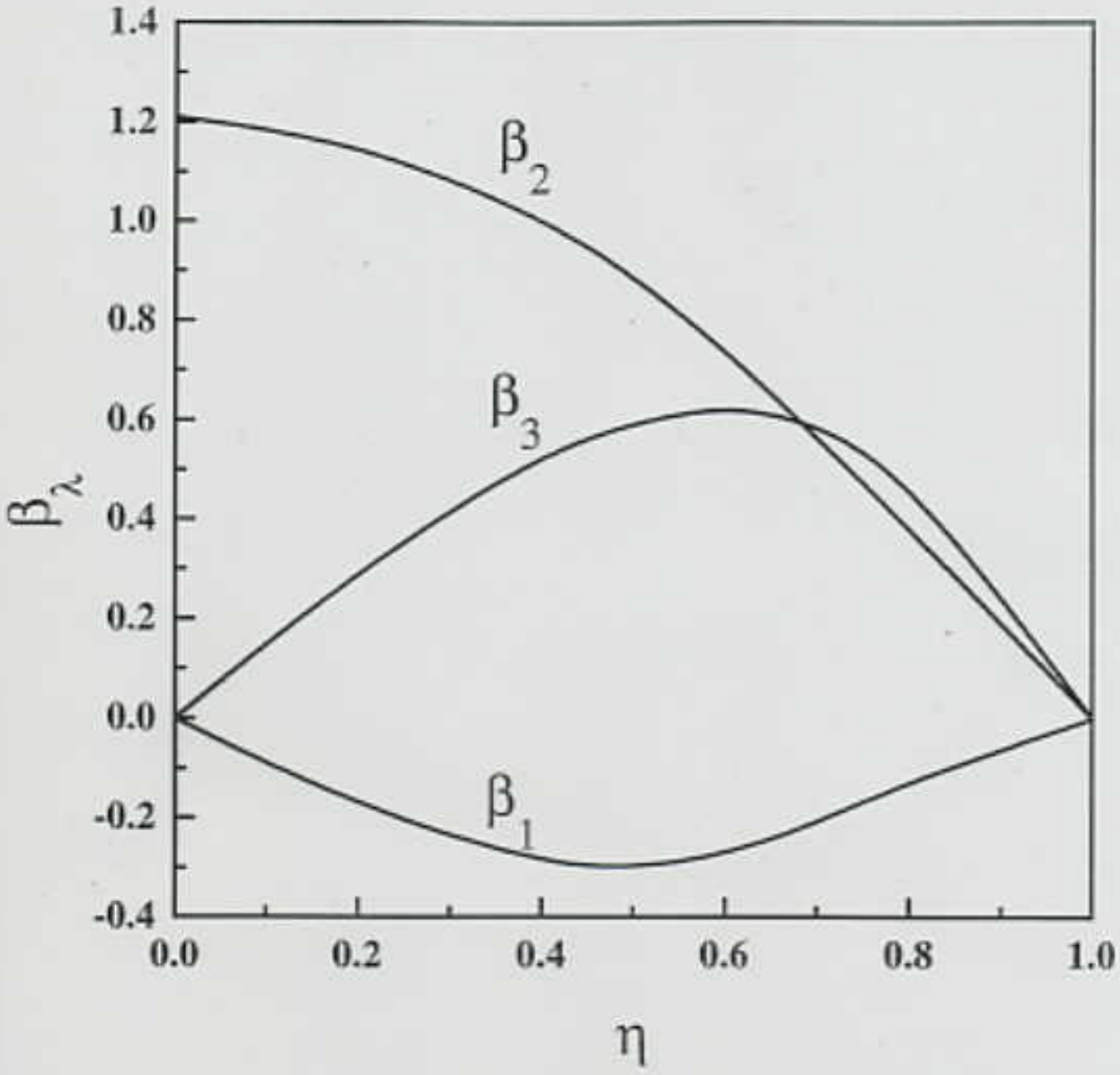
1.4
1.2
1.0
0.8
0.6
0.4
0.2
0.0
-0.2
-0.4
0.0
0.2
0.4
0.6
0.8
1.0
β_λ
η
β_2
β_3
β_1

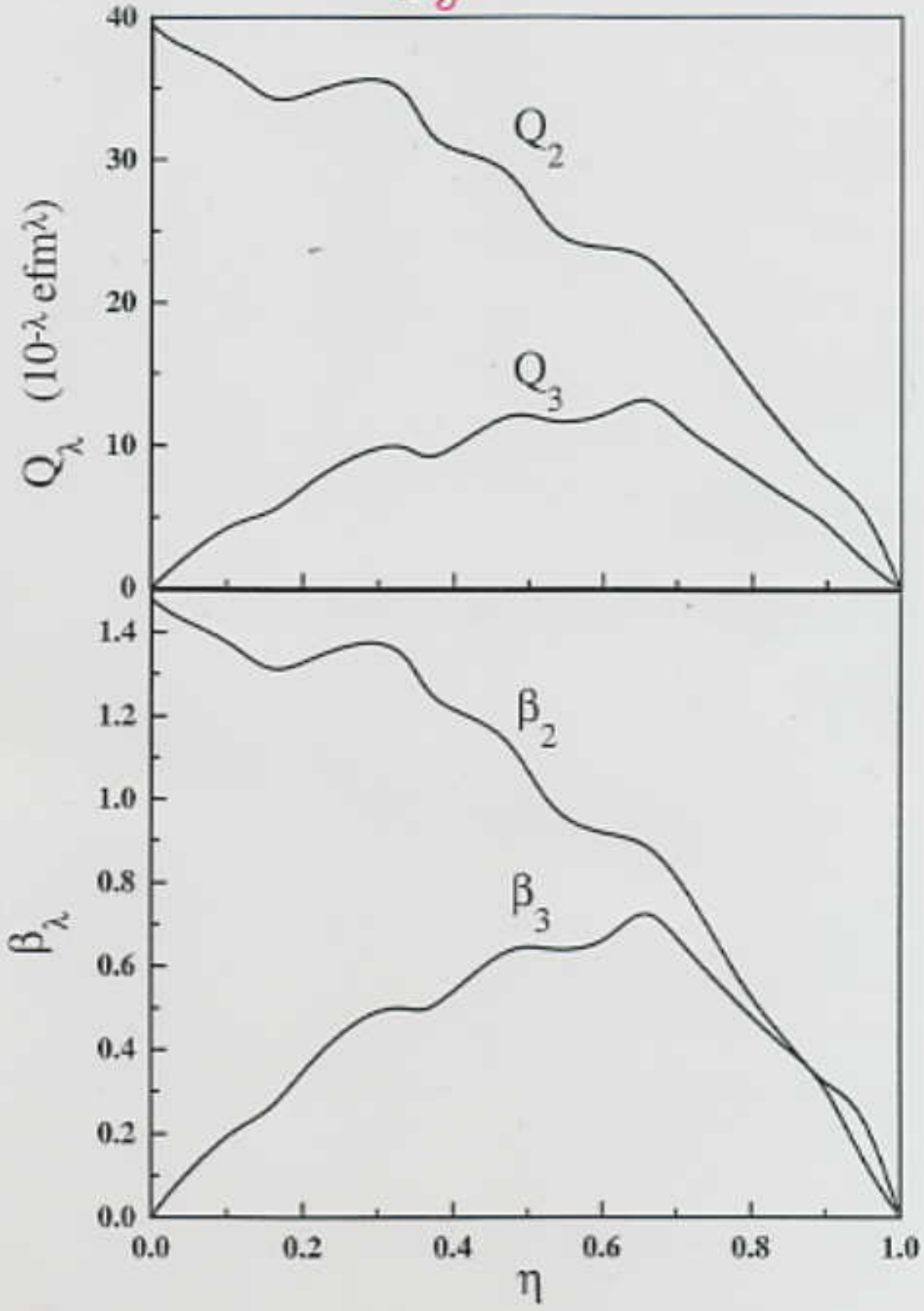
152 Dy
40
30
20
10
0
Q_λ ($10^{-\lambda}$ efm$^\lambda$)
Q_2
Q_3
1.4
1.2
1.0
0.8
0.6
0.4
0.2
0.0
β_λ
β_2
β_3
0.0
0.2
0.4
0.6
0.8
1.0
η

b) Potential energy of DNS

$$U(R,\eta,L) = B_1 + B_2 + V(R,\eta,L) - \left[B_0 + \frac{\hbar^2 L(L+1)}{2J_0}\right]$$

B_1, B_2, B_0 are negative binding energies of clusters 1 and 2 and of the united ($|\eta|=1$) nucleus.

$V(R,\eta,L)$ is nucleus-nucleus potential:

$$V(R,\eta,L) = V_{Coul}(R,\eta) + V_N(R,\eta) + \frac{\hbar^2 L(L+1)}{2J(R,\eta)},$$

also dependence on the deformations of clusters.

Assumption: pole-to-pole orientation

$$R = R_m = R_{01}\left(1+\sqrt{\frac{5}{4\pi}}\alpha_1\right) + R_{02}\left(1+\sqrt{\frac{5}{4\pi}}\alpha_2\right) + 0.5\,fm$$

Moment of inertia: $J = J_1 + J_2 + M\frac{A_1 A_2}{A}R_m^2$

J_1 and J_2 are moments of inertia of clusters.

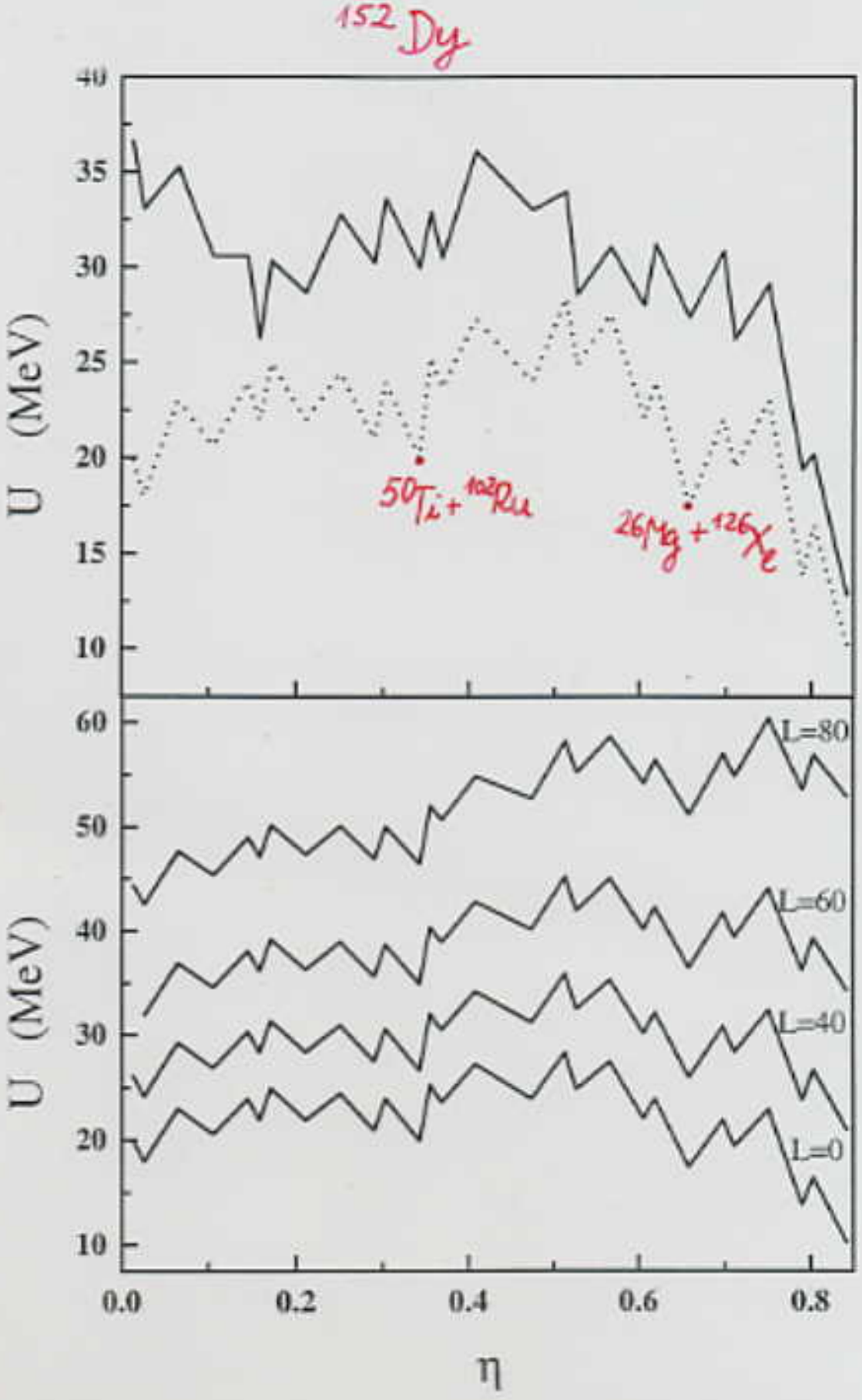
152 Dy
U (MeV)
50Ti + 102Ru
26Mg + 126Xe
L=80
L=60
L=40
L=0
U (MeV)
η

c) Example: ^{152}Dy

Clusterisation is most stable in minima of potential U as a function of η.
Minima by shell effects, e.g. magic clusters

$\eta = 0.34$: $^{50}Ti + ^{102}Ru$

$U = 20$ MeV above g.s., about estimated energy of $L=0$ HD-state of ^{152}Dy,

$\mathcal{J}^{calc.} = 131\,\hbar^2 MeV^{-1}$, $\mathcal{J}^{exp} = 130\,\hbar^2 MeV^{-1}$,

$\beta_2^{calc} = 1.3$, $\beta_2^{exp} \geq 0.9$

DNS at $^{50}Ti + ^{102}Ru$ is compatible with HD properties.

$\eta = 0.66$: $^{26}Mg + ^{126}Xe$

SD properties: $\mathcal{J}^{calc} = 104\,\hbar^2 MeV^{-1}$, $Q_2^{calc.} = 24\,eb$, $\beta_2^{calc.} = 0.9$

$\mathcal{J}^{exp} = (85 \pm 3)\,\hbar^2 MeV^{-1}$, $Q_2^{exp.} = (18 \pm 3)\,eb$

Similar $\eta = 0.71$: $^{22}Ne + ^{130}Ba$

$^{26}Mg + ^{126}Xe$ and $^{22}Ne + ^{130}Ba$ have SD properties.

3. Normal- and superdeformed bands

Application of dinuclear model to structure of ^{60}Zn

1. $^{60}Zn \rightarrow {}^{56}Ni + \alpha$, threshold 2.7 MeV above g.s.
   Assumption: g.s. band contains α-component

2. $^{60}Zn \rightarrow {}^{52}Fe + {}^{8}Be$, threshold 10.8 MeV above g.s.
   $\rightarrow {}^{48}Cr + {}^{12}C$, threshold 11.2 MeV above g.s.

extrapolated band head of superdeformed band: 7.5 MeV
moment of inertia: (692 - 795) M fm^2
moment of inertia of $^{52}Fe + {}^{8}Be$: 750 M fm^2

Assumption: superdeformed band contains ^{8}Be - component

Unified description of g.s. and sd bands by dynamics in mass asymmetry coordinate.

a) Potential $U(\eta, I)$

mononucleus ($\eta = \pm 1$)	$U =$ 0 MeV	$I = 0^-$
$^{56}Ni + \alpha$	$U = -4.5$ MeV	
$^{52}Fe + {}^{8}Be$	$U =$ 5.1 MeV	
$^{48}Cr + {}^{12}C$	$U =$ 9.0 MeV	

Stepwise potential because of large scale in η.
Barrier width determined by known 3^- state (3.504 MeV).

b) Solution of Schrödinger equation in mass asymmetry

$$\left(-\frac{\hbar^2}{2}\frac{d}{d\eta}\frac{1}{B(\eta)}\frac{d}{d\eta} + U(\eta, I)\right)\psi_I(\eta) = E_{n,I}\,\psi_I(\eta)$$

Wave function $\psi_I(\eta)$ contains different cluster configurations.

^{60}Zn

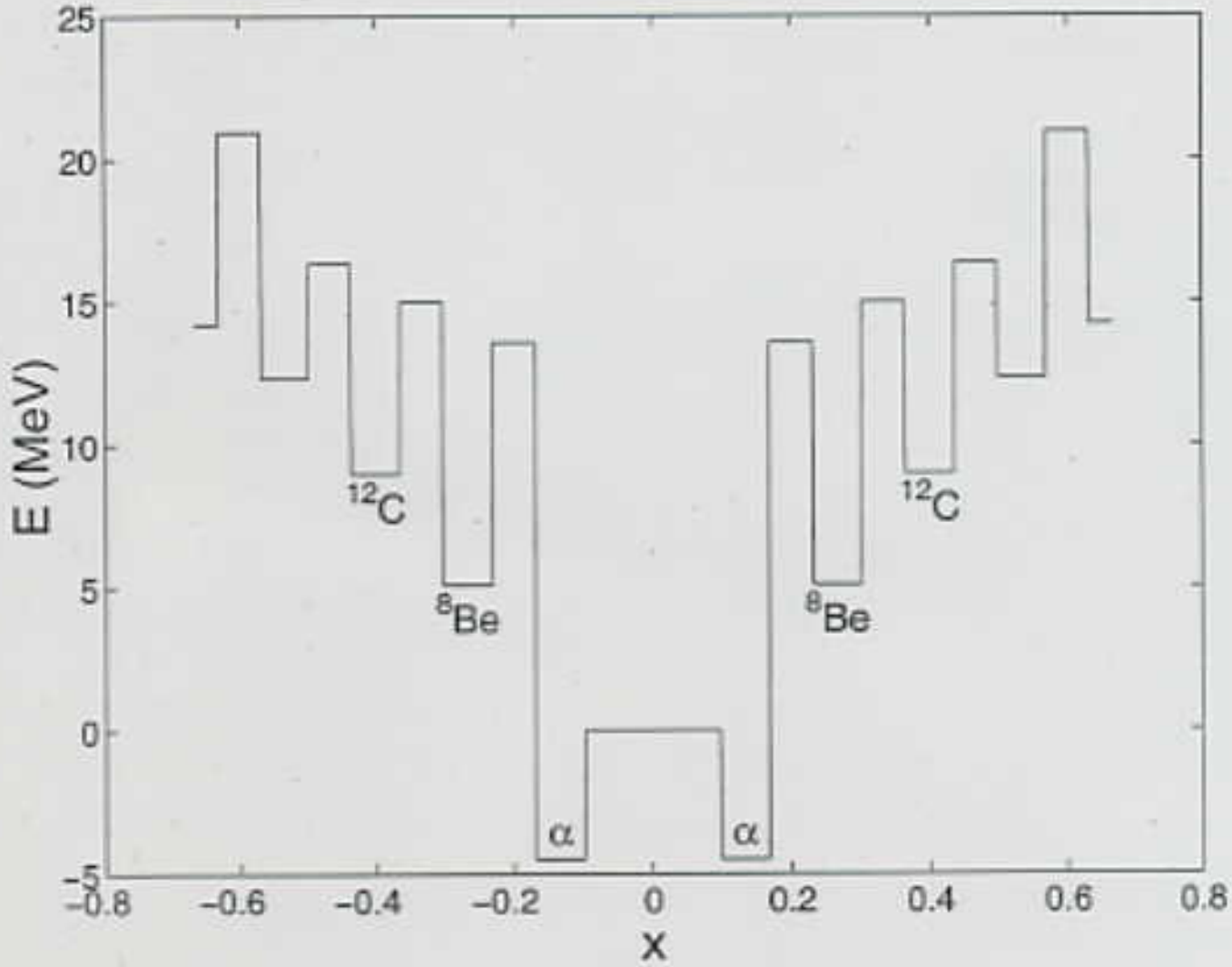

$X = \eta - 1$ for $\eta > 0$

$X = \eta + 1$ for $\eta < 0$

$^{60}_{Zn}$

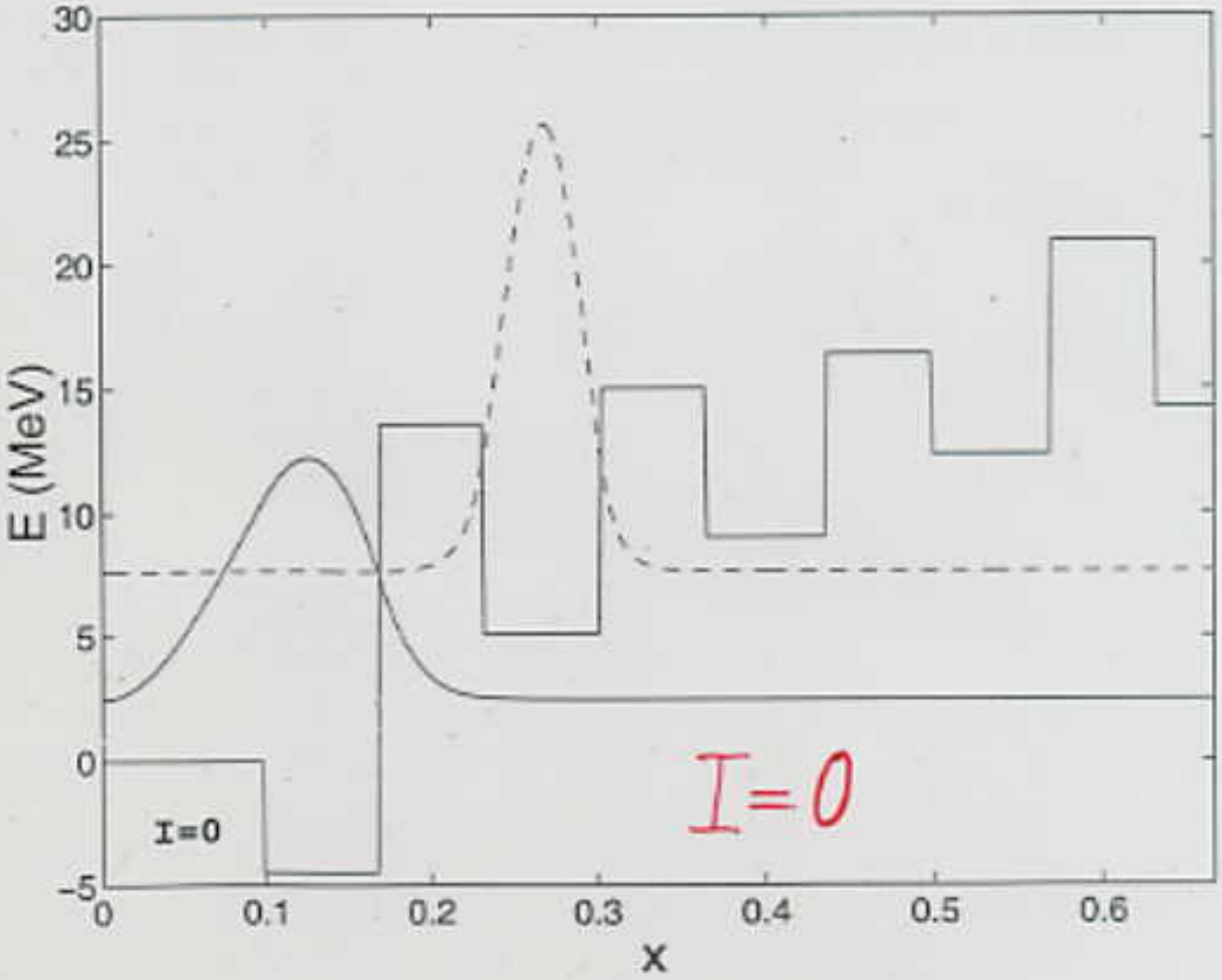

$^{60}_{30}Zn$

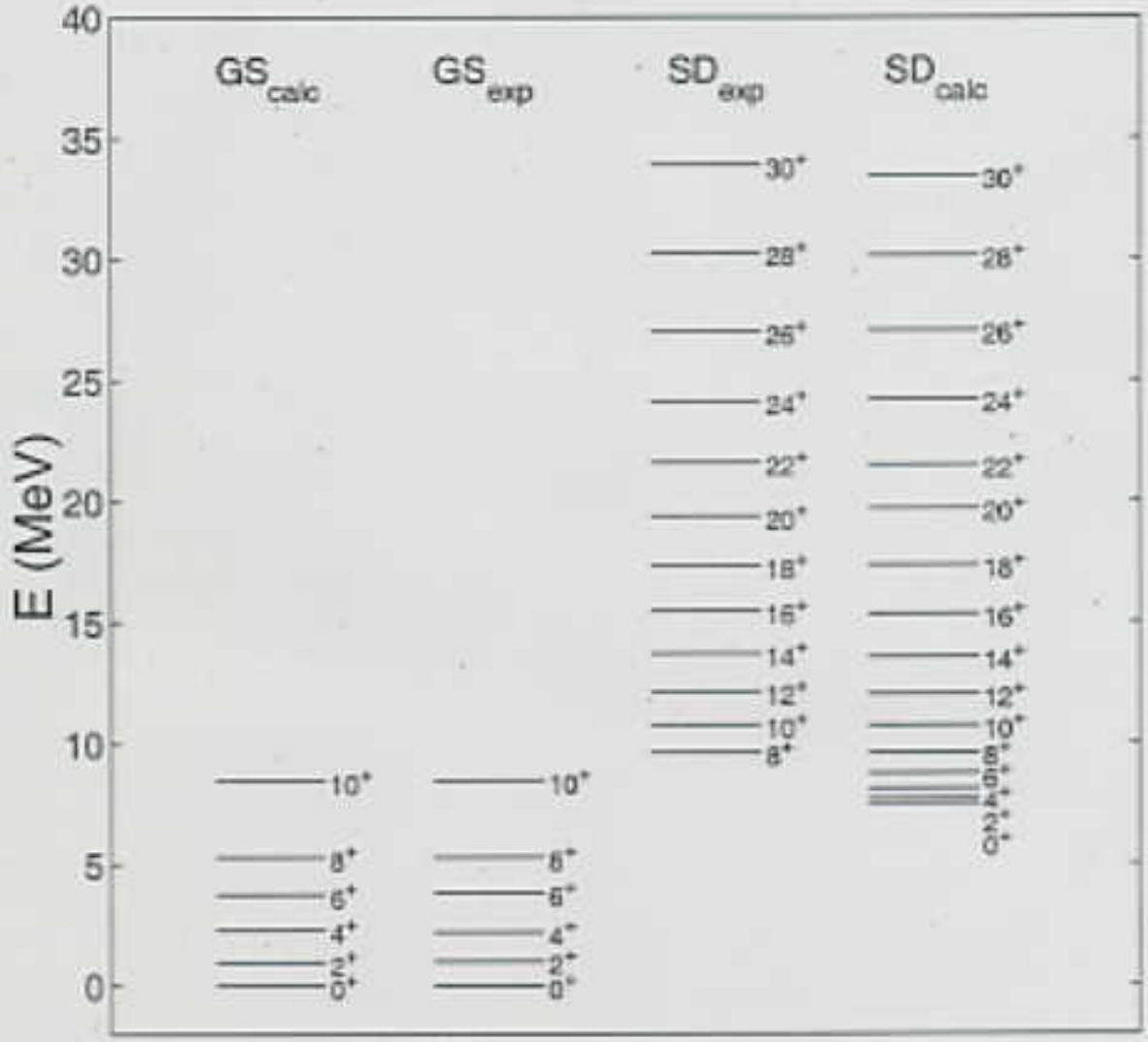
GS$_{calc}$
GS$_{exp}$
SD$_{exp}$
SD$_{calc}$
E (MeV)
40
35
30
25
20
15
10
5
0
10$^+$
8$^+$
6$^+$
4$^+$
2$^+$
0$^+$
30$^+$
28$^+$
26$^+$
24$^+$
22$^+$
20$^+$
18$^+$
16$^+$
14$^+$
12$^+$

^{60}Zn

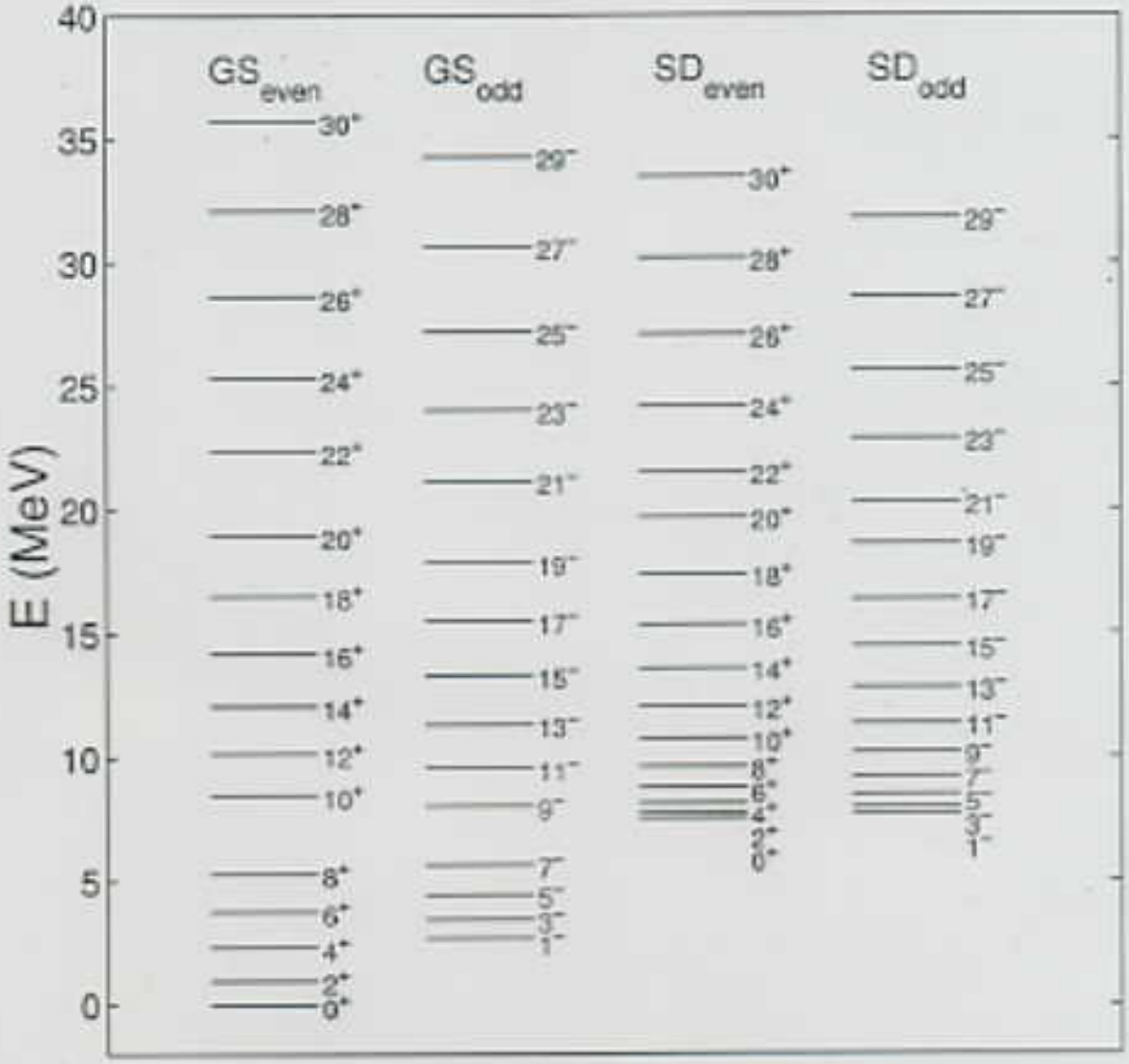
E (MeV)
40
35
30
25
20
15
10
5
0
GS even
30+
28+
26+
24+
22+
20+
18+
16+
14+
12+
10+
8+
6+
4+
2+
0+
GS odd
29-
27-
25-
23-
21-
19-
17-
15-
13-
11-
9-
7-
5-
3-
1-
SD even
30+
28+
26+
24+
22+
20+
18+
16+
14+
12+
10+
8+
6+
4+
2+
0+
SD odd
29-
27-
25-
23-
21-
19-
17-
15-
13-
11-
9-
7-
5-
3-
1-

C) Spectrum and E2 ($\Delta I=2$)-transitions

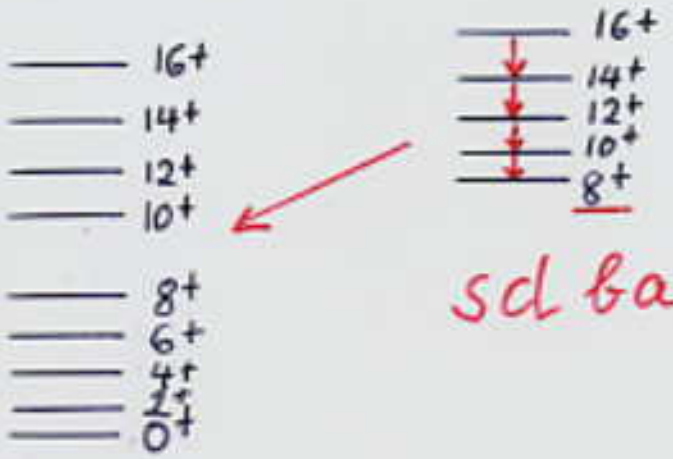

Experim. observed lowest level of sd band: 8^+

$$\frac{I(16^+_{sd} \to 14^+_{gs})}{I(16^+_{sd} \to 14^+_{sd})}\Big|_{calc} = 0.07, \qquad \frac{I(14^+_{sd} \to 12^+_{gs})}{I(14^+_{sd} \to 12^+_{sd})}\Big|_{calc} = 0.18,$$

$$\frac{I(12^+_{sd} \to 10^+_{gs})}{I(12^+_{sd} \to 10^+_{sd})} = \begin{cases} 0.42 \text{ calc.} \\ 0.54 \text{ exp.} \end{cases}, \qquad \frac{I(10^+_{sd} \to 8^+_{gs})}{I(10^+_{sd} \to 8^+_{sd})} = \begin{cases} 0.63 \text{ calc.} \\ 0.60 \text{ exp.} \end{cases}$$

4. Dinuclear dynamics in the fusion process

Heavy and superheavy nuclei can be produced by fusion reactions with heavy ions.

α) Pb- or Bi-based reactions

e.g. $^{64}Ni + {}^{208}Pb \longrightarrow {}^{272}110 \longrightarrow {}^{271}110 + n \quad \sigma = 15\,pb$

$^{70}Zn + {}^{208}Pb \longrightarrow {}^{278}112 \longrightarrow {}^{277}112 + n \quad \sigma = 1\,pb$

excitation energy of compound nucleus

$$E^*_{CN} \approx 12\,MeV \text{ for } Z \geq 108$$

β) Actinide-based reactions

e.g. $^{34}S + {}^{238}U \longrightarrow {}^{272}106 \longrightarrow {}^{267}106 + 5n$

$^{48}Ca + {}^{244}Pu \longrightarrow {}^{292}114 \longrightarrow {}^{289}114 + 3n \quad \sigma = 1\,pb$

Small cross sections: Competition between complete fusion and quasifission

4.1 Models for production of superheavy nuclei

Models for production of superheavy nuclei can be discriminated by the dynamics in the important collective degrees of freedom of the system.

1. Relative internuclear distance R

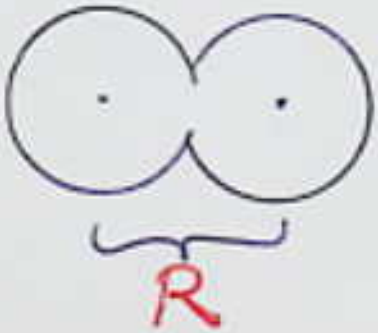

2. Mass (charge) asymmetry

$$\eta = \frac{A_1 - A_2}{A_1 + A_2}$$

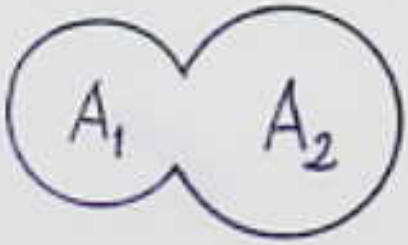

$\eta = 0$: symmetric system

$\eta = \pm 1$: fused system

Description of fusion process depends strongly whether an adiabatic or diabatic potential energy surface is assumed.

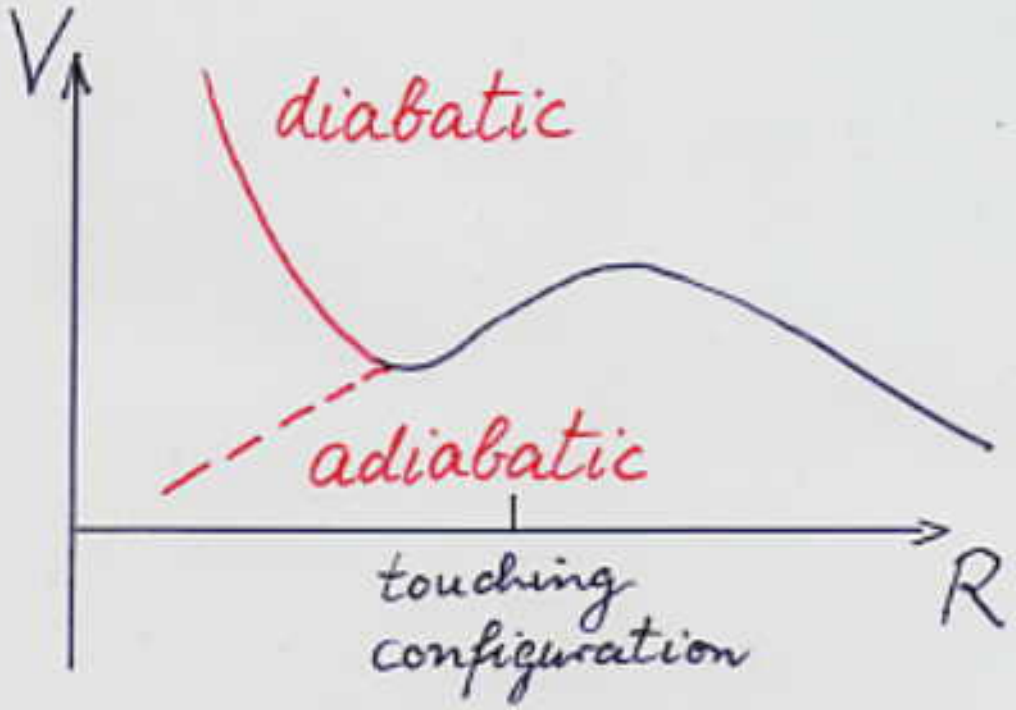

a) Models using adiabatic potentials

Minimalization of potential energy,
essentially adiabatic dynamics in the
internuclear distance,
nuclei melt together.

Large probabilities of fusion for producing
nuclei with similar projectile and
target nuclei.

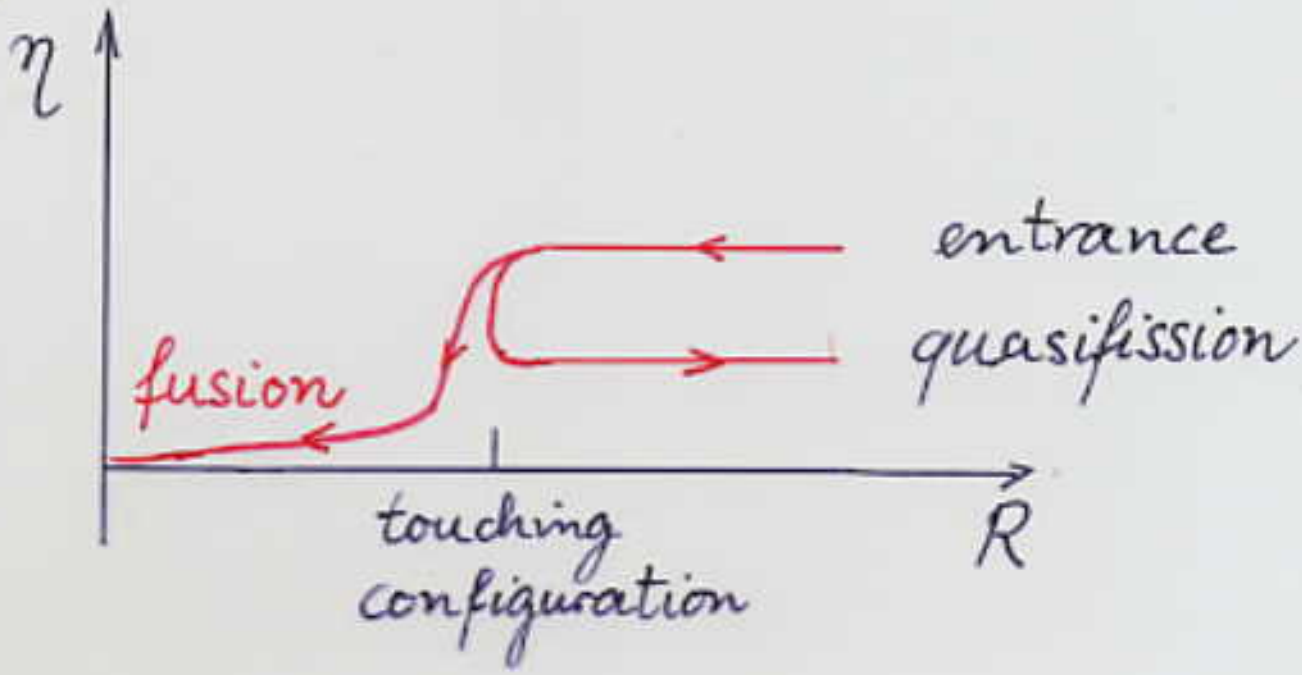

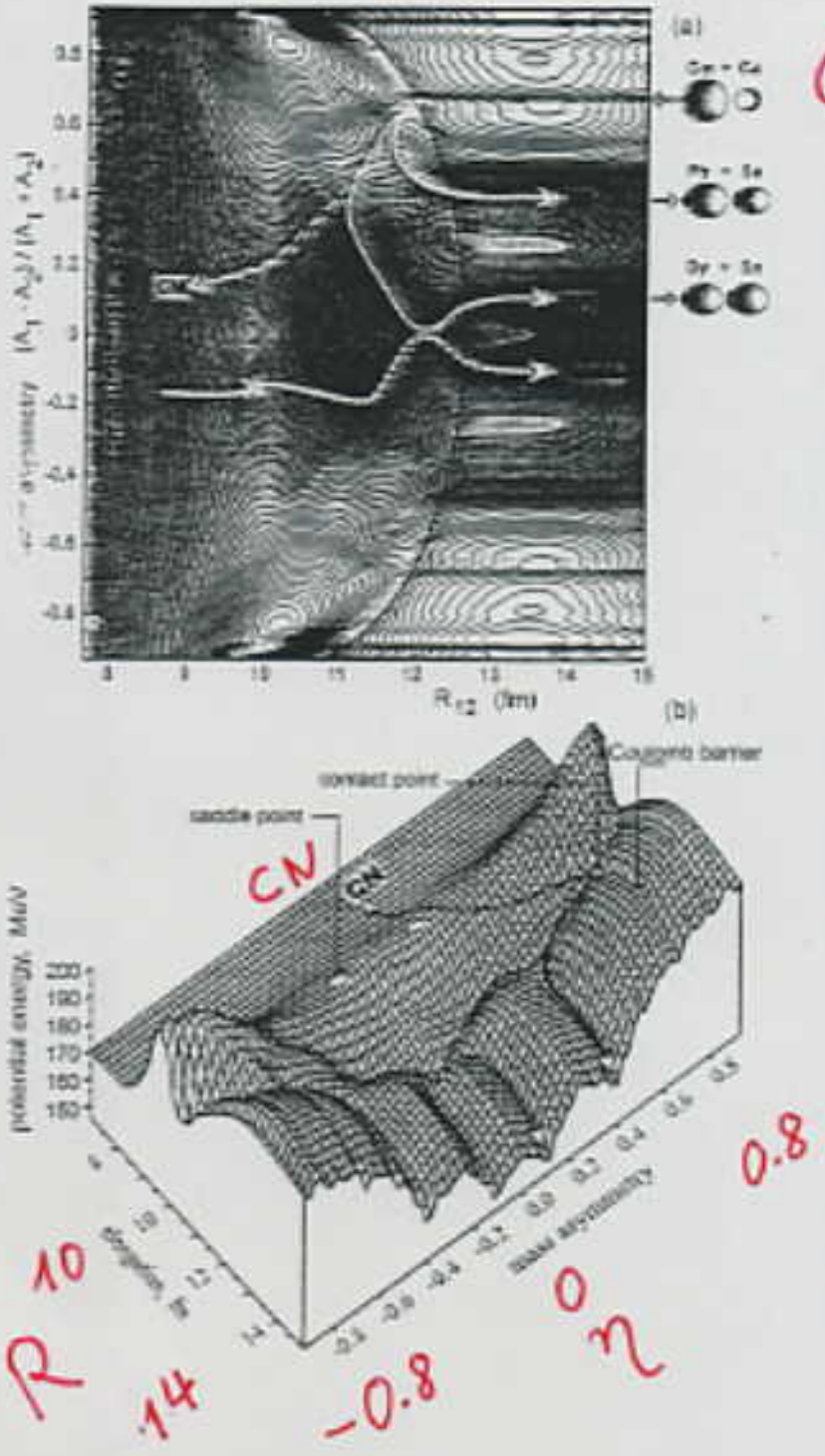
Ca+Cm
(a)
(b)
saddle point
contact point
Coulomb barrier
CN
CN
10
R
14
-0.8
0
η
0.8

b) Dinuclear system (DNS) concept

Fusion by transfer of nucleons between the nuclei (idea of V. Volkov), mainly dynamics in mass asymmetry degree of freedom, use of diabatic potentials, e.g. calculated with diabatic two-center shell model.

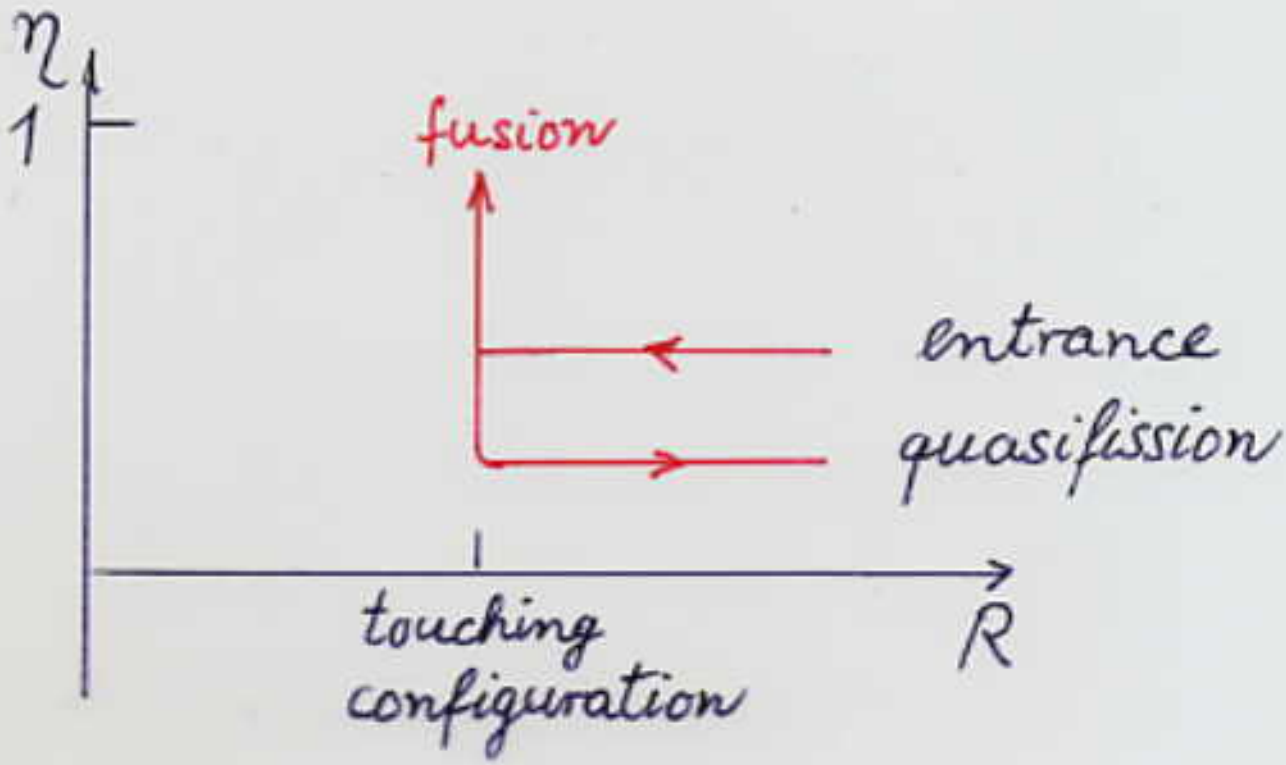

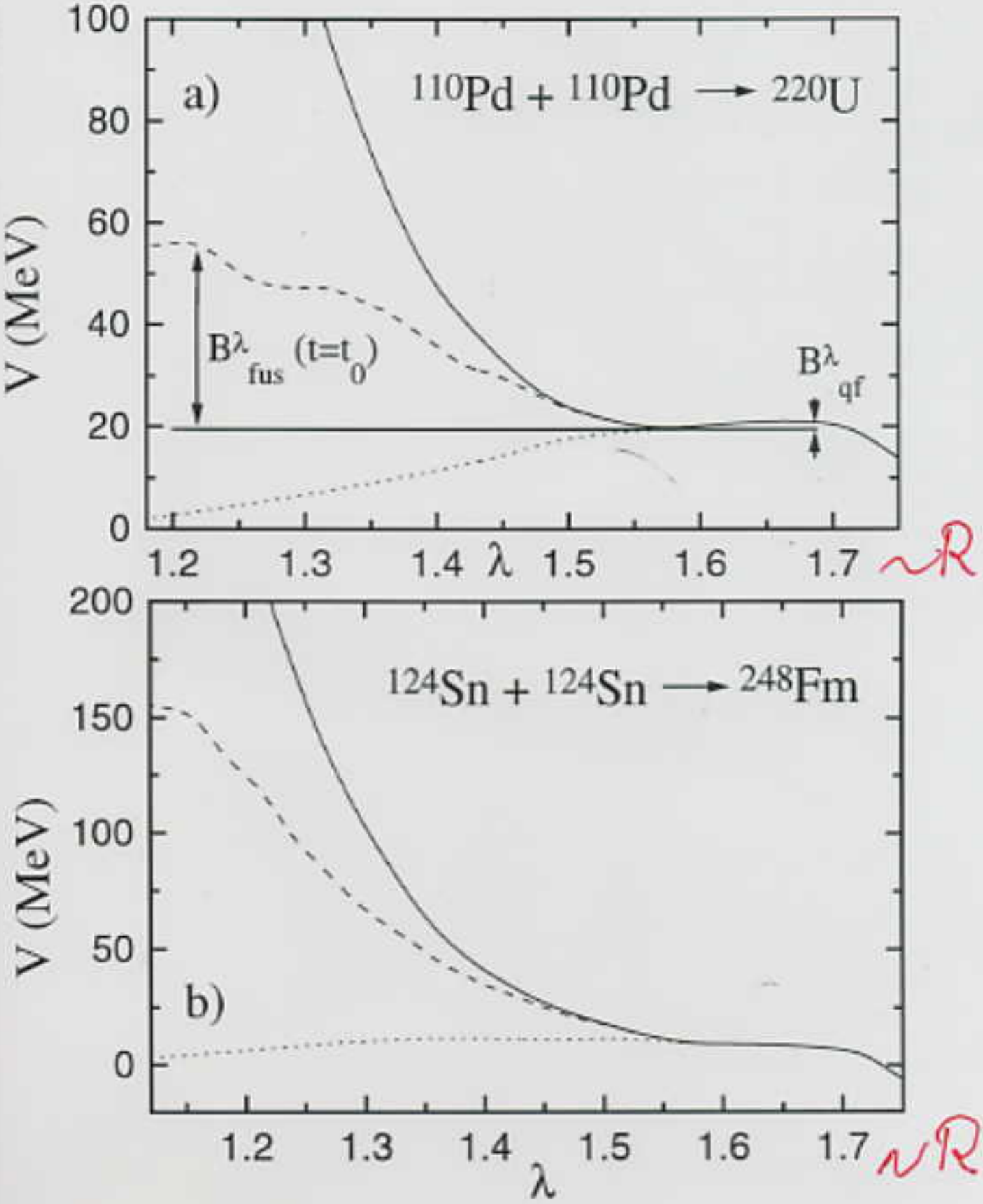

Fig 1. A. Diaz-Torres et al.

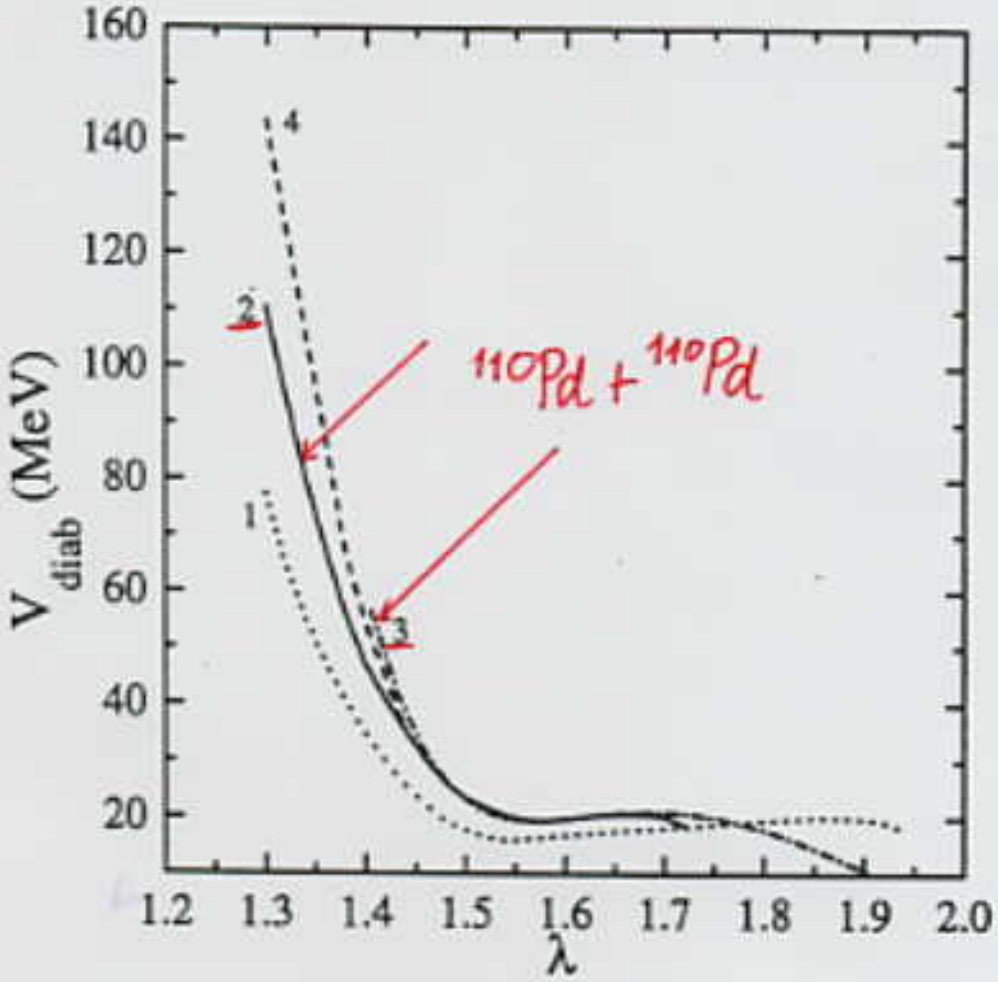

Fig.2. Diabatic potentials for the systems:

(1) $^{100}Mo + ^{100}Mo$ (TCSM)

(2) $^{110}Pd + ^{110}Pd$ (TCSM)

(3) $^{110}Pd + ^{110}Pd$ (double folding)

(4) Neck parameter ε is diminished with decreasing λ

$^{58}Fe + ^{244}Pu \rightarrow {}^{302}120$

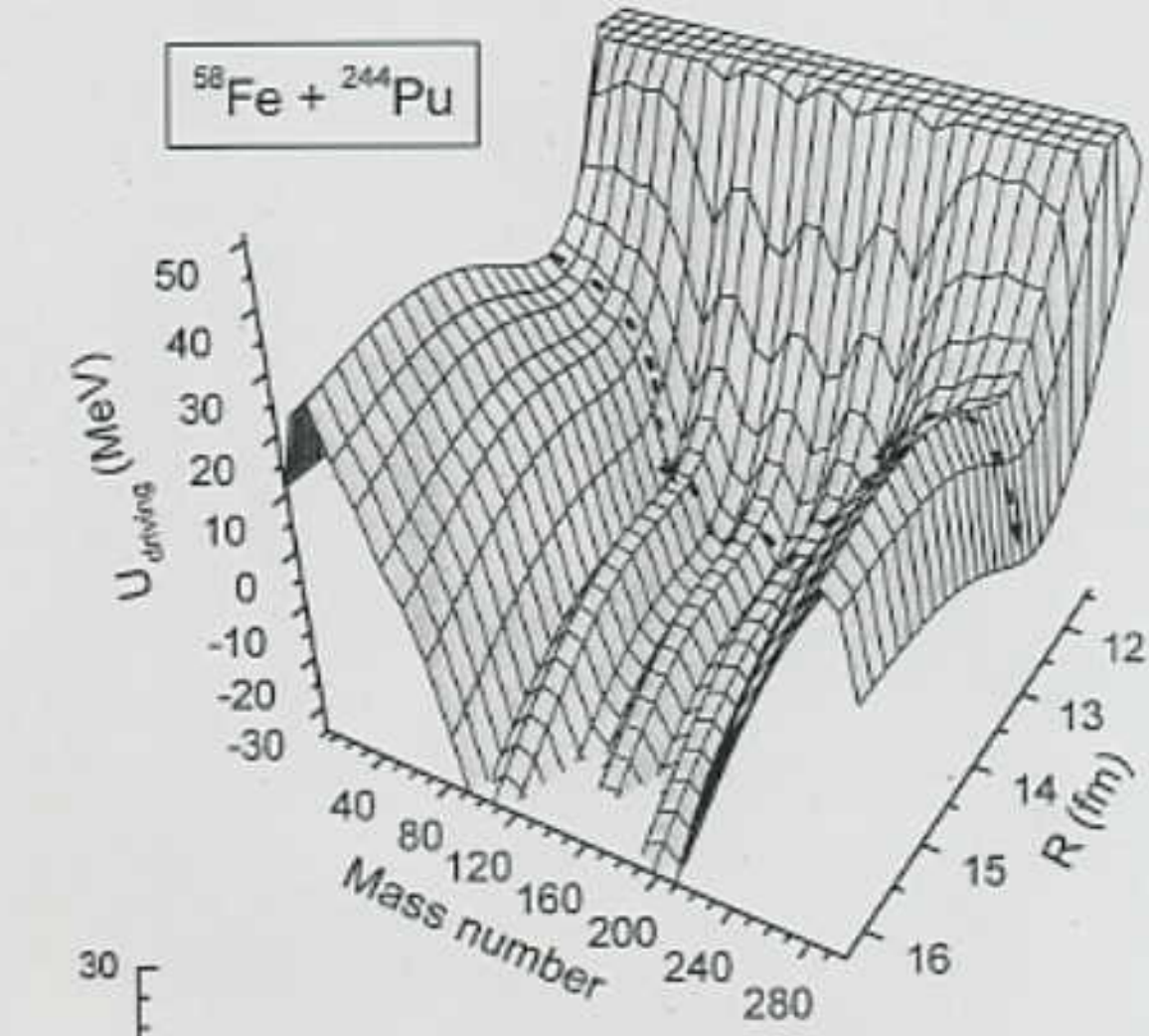

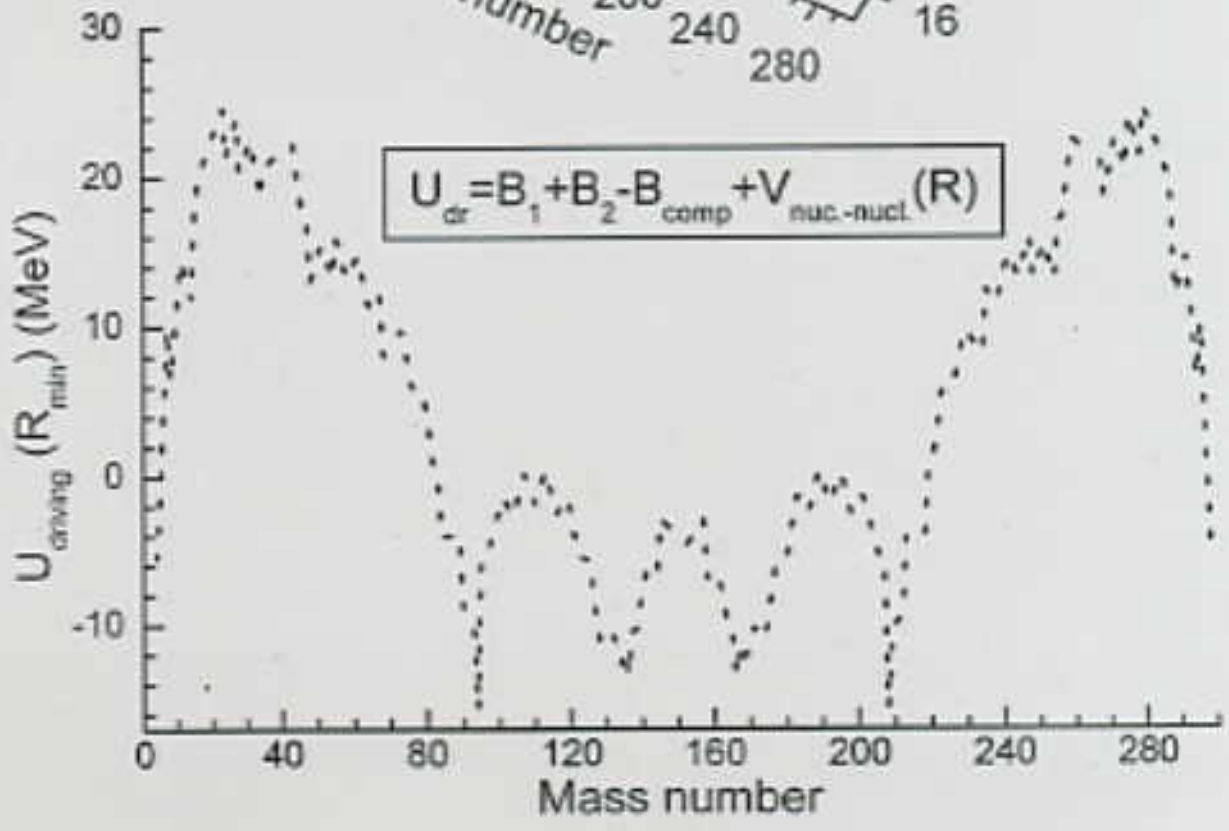

-1 η 1

c) Fusion probabilities for the compound system ^{246}Fm

1. Comparison of fusion probabilities in the coordinates λ (corresponding to R) and η

Adiabatic and dynamical diabatic potentials in λ ($\sim R$)
Potential in mass asymmetry η
Quasifission barrier is regarded.

Result: experimental fusion probabilities agree with fusion in η.

Strong support for dinuclear model.

2. Agreement between fusion probabilities calculated with Fokker-Planck equation and Kramers formula.

Two center shell model (TCSM)

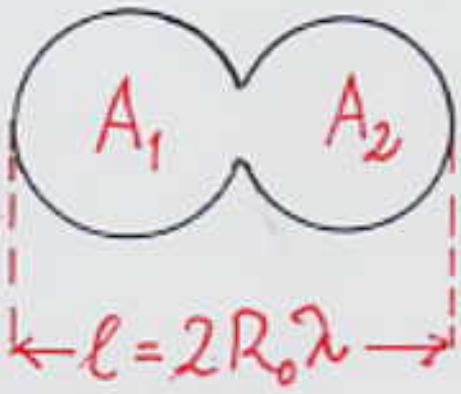

Parametrization:

1. Elongation $\lambda = \ell/(2R_0)$
   $2R_0$ = diameter of compound system
2. Mass asymmetry $\eta = (A_1 - A_2)/(A_1 + A_2)$

further coordinates:
charge asymmetry, neck parameter, deformations

246Fm

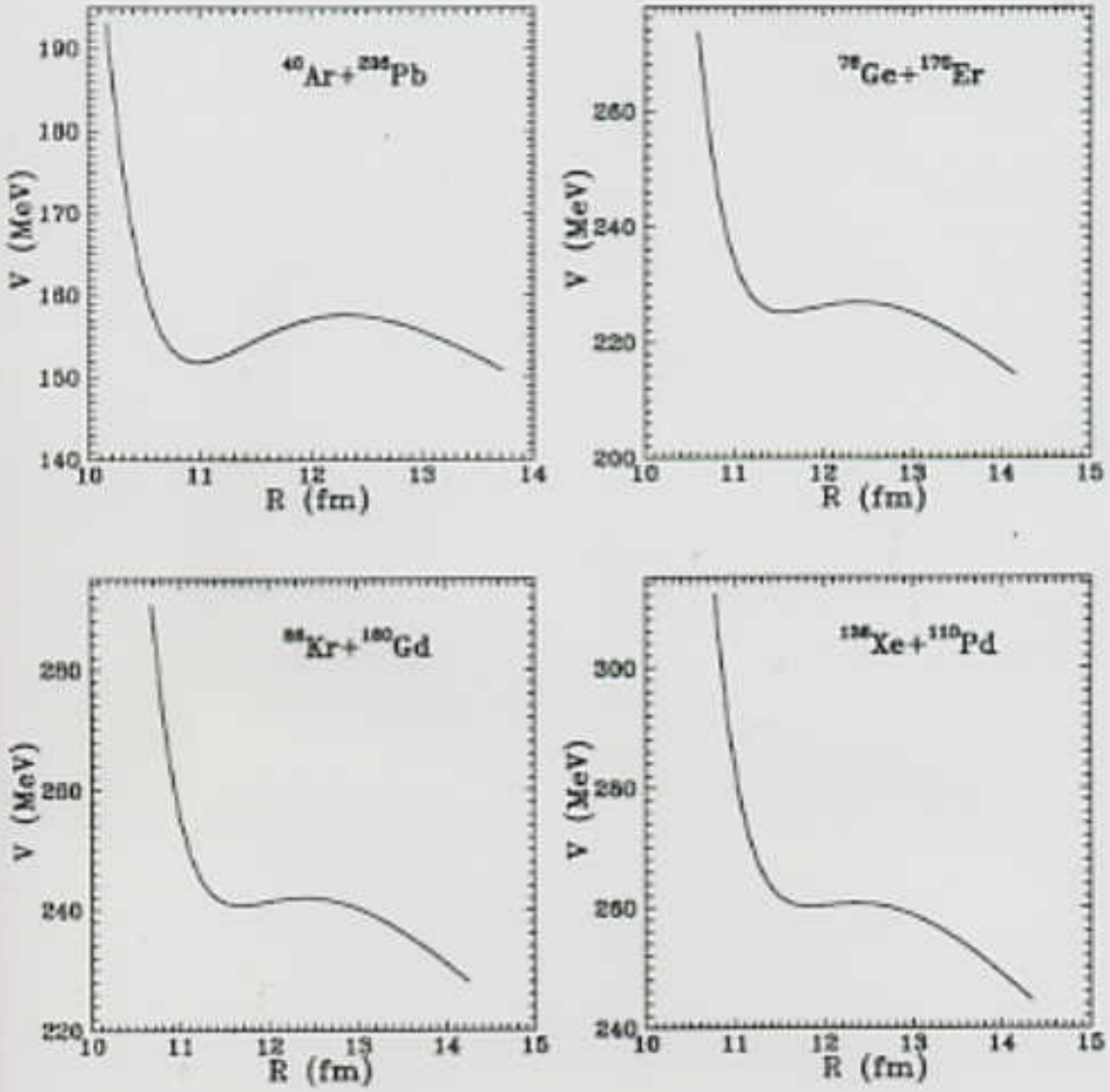

Fig. 2 G.G.Adamian et al.

Adiabatic potentials, ^{246}Fm

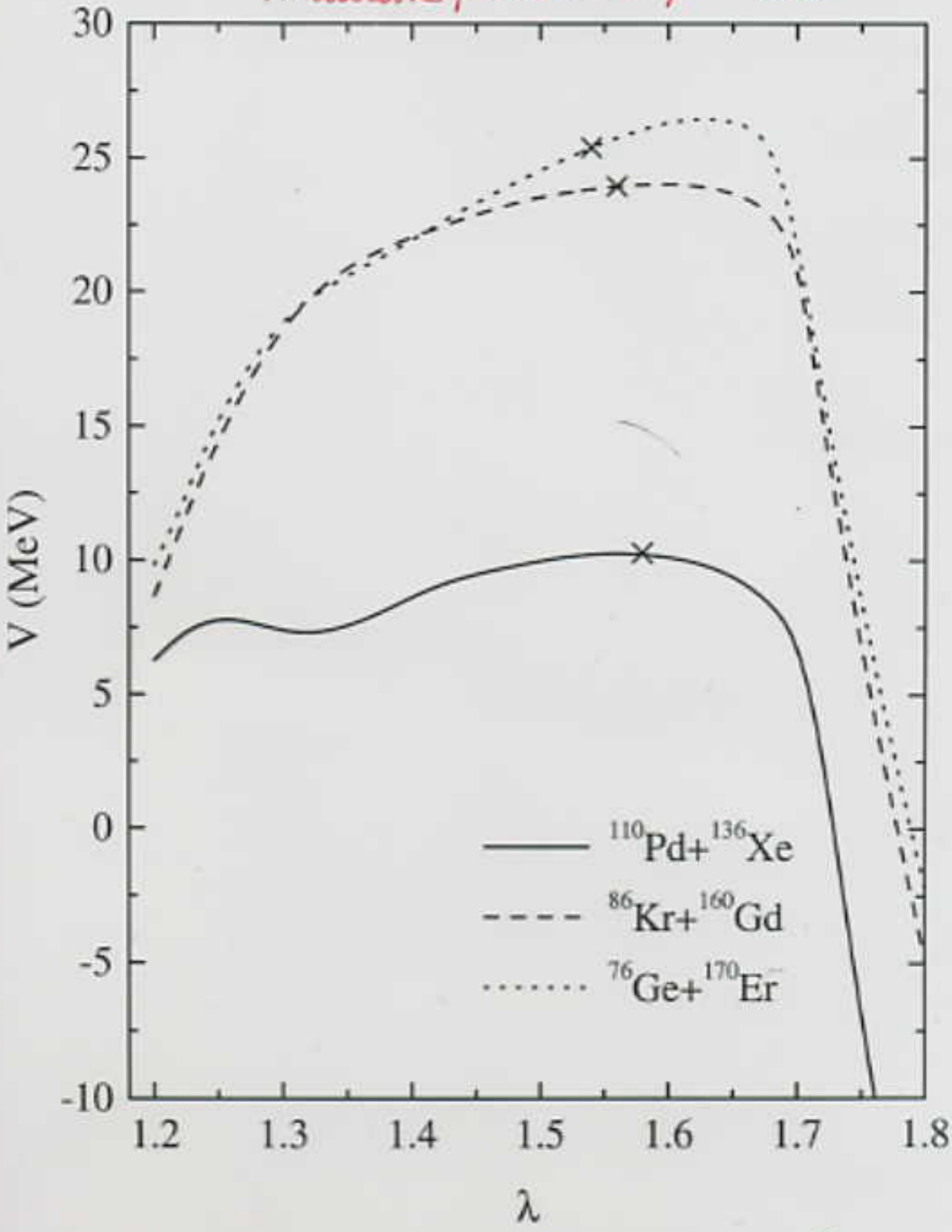

Fig.8.G.G.Adamian et al. ^{246}Fm

Dynamical diabatic potentials

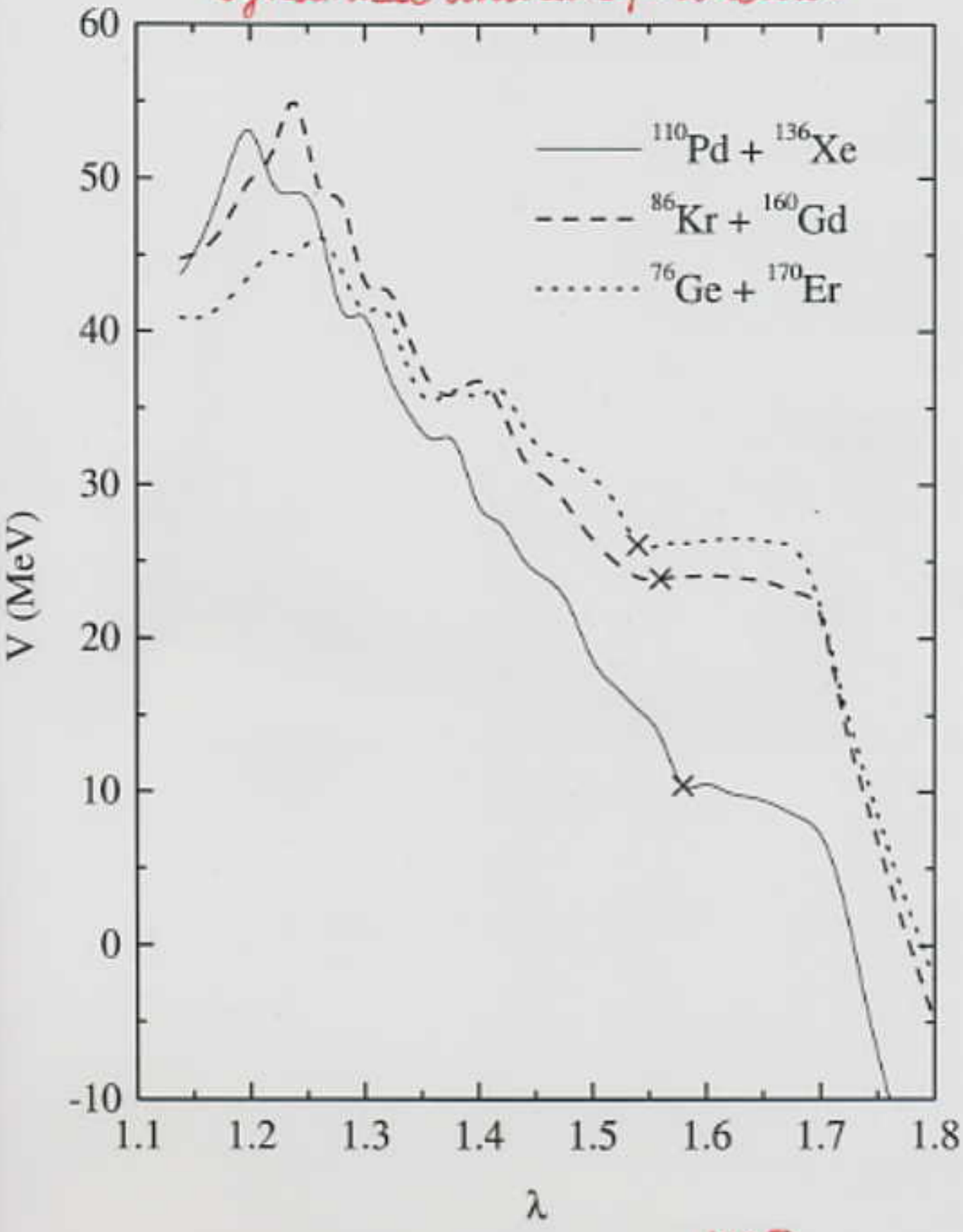

Fig.9. G.G.Adamian et al.

246 Fm

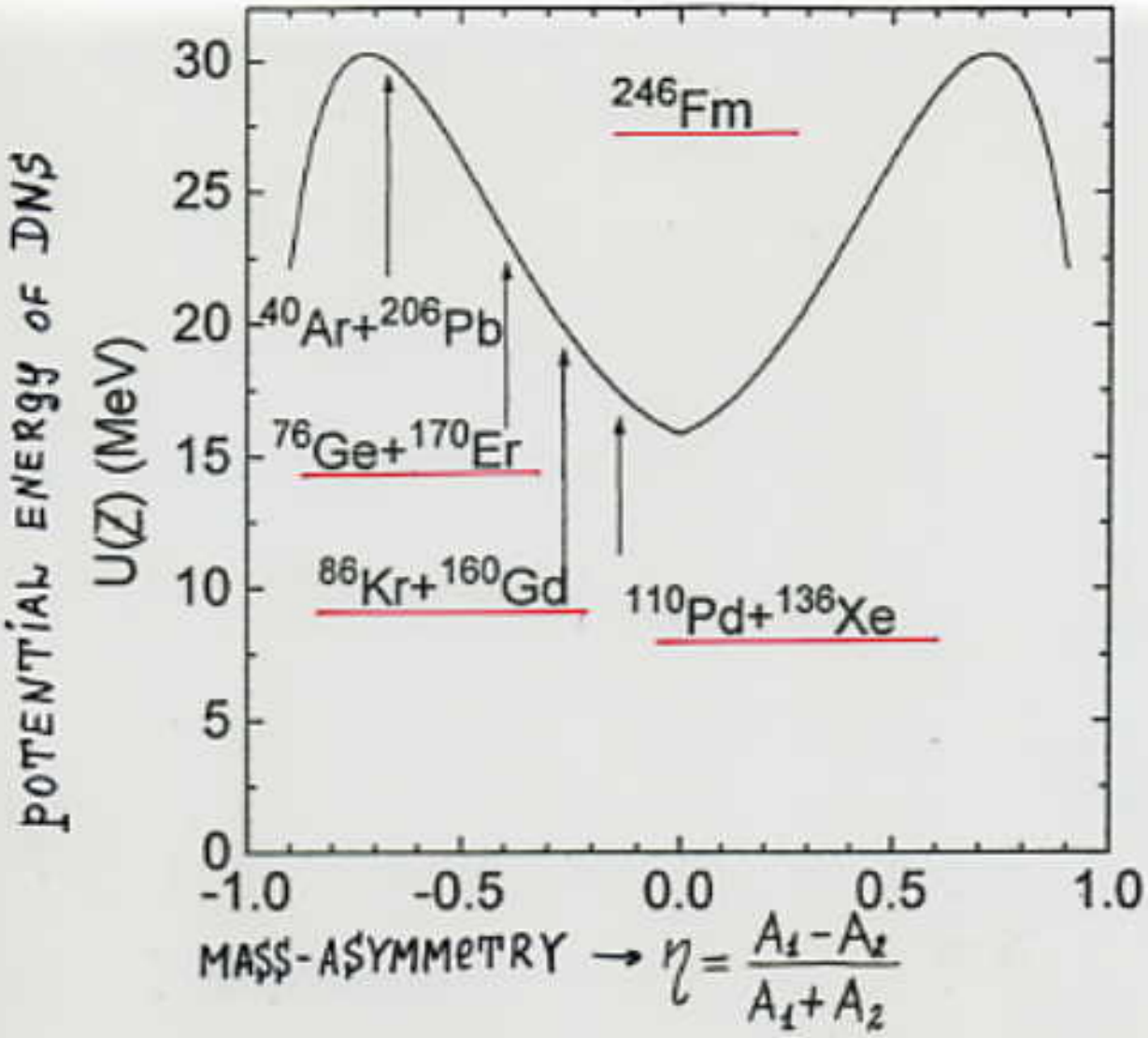

Fig. 2 G.G.Adamian et al. "Competition between ..."

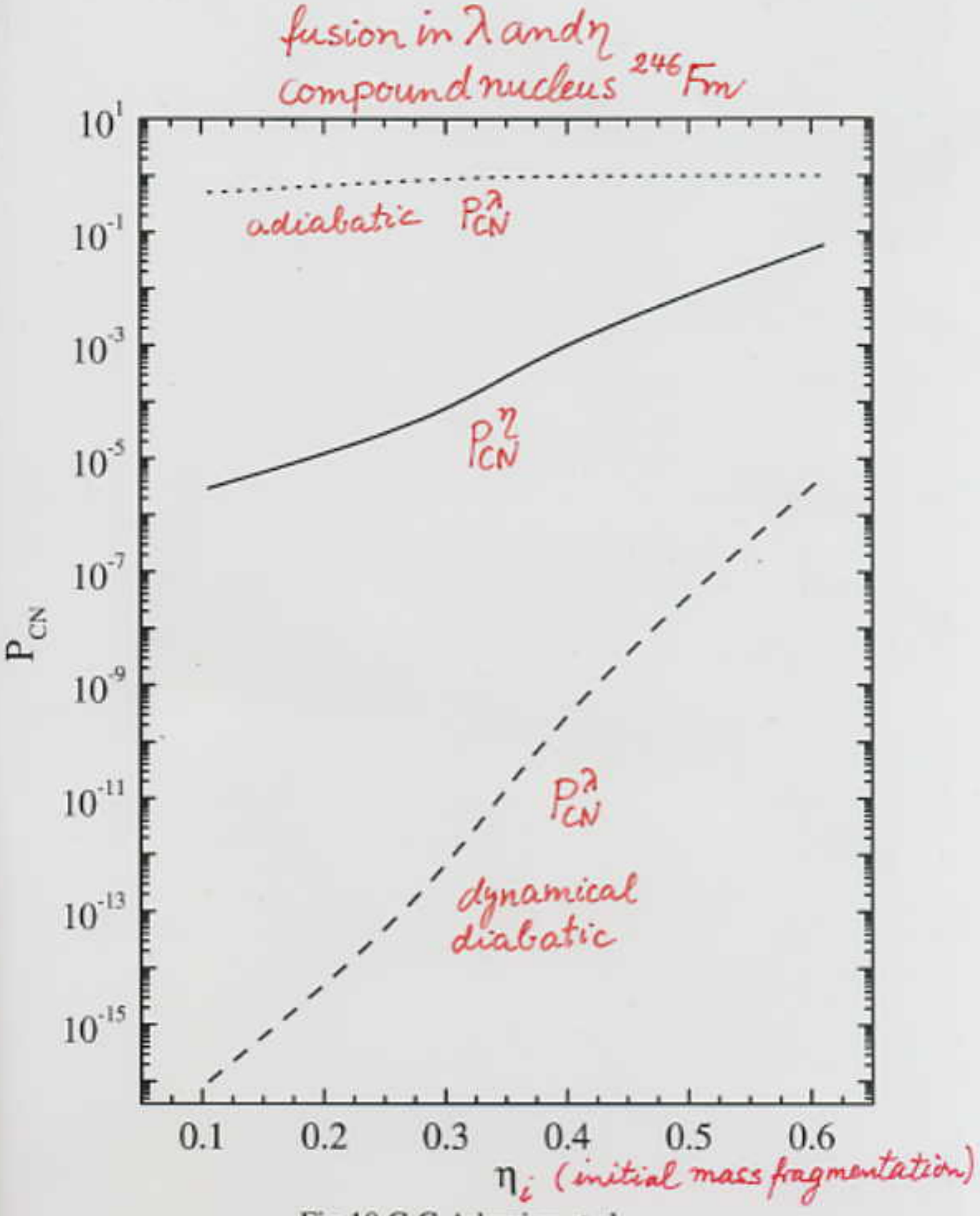

Fig.10.G.G.Adamian et al.

^{246}Fm , Fokker-Planck equ.

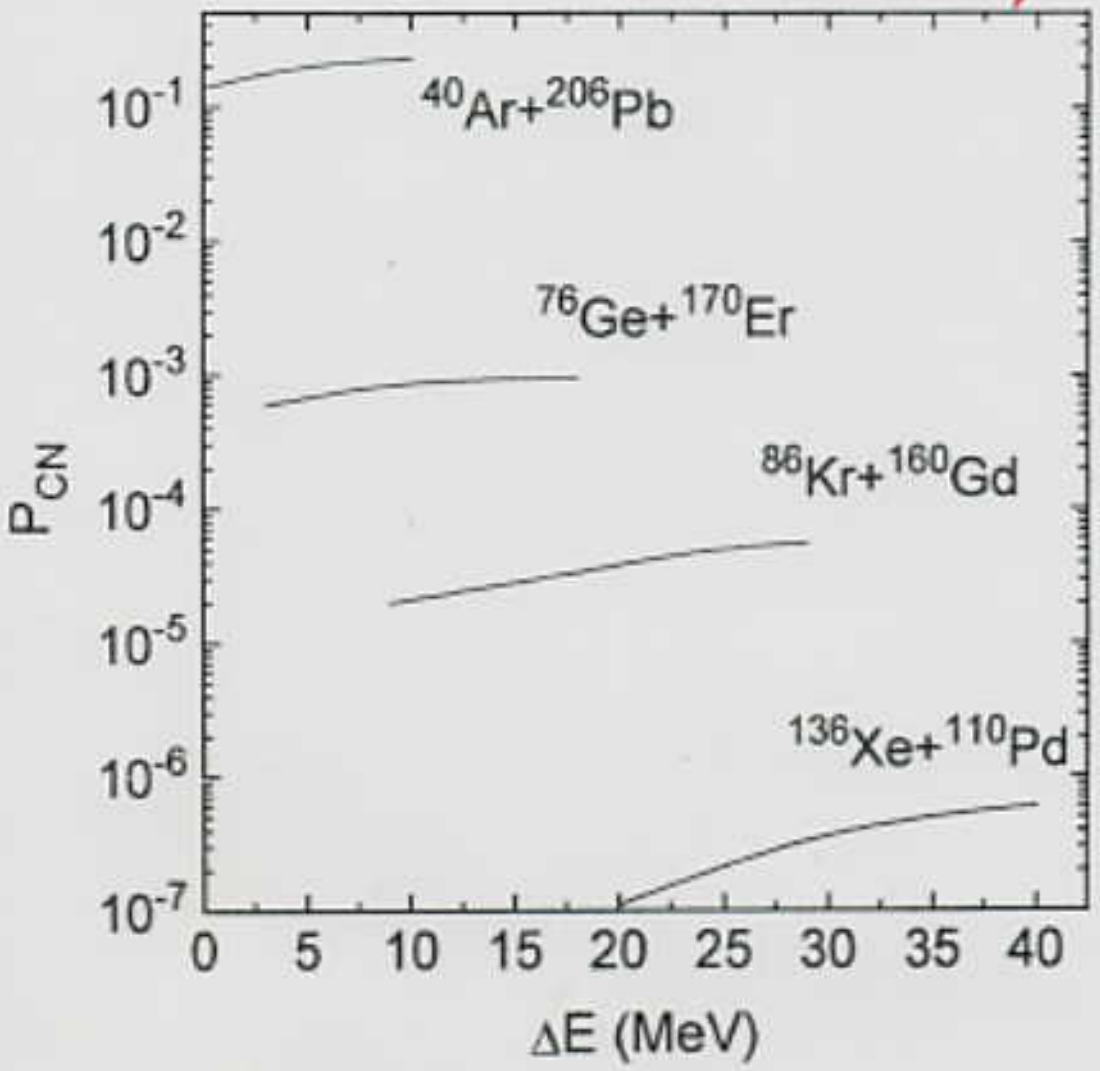

Fig. 6 G.G.Adamian et al. "Competition between..."

^{246}Fm , Kramers formula

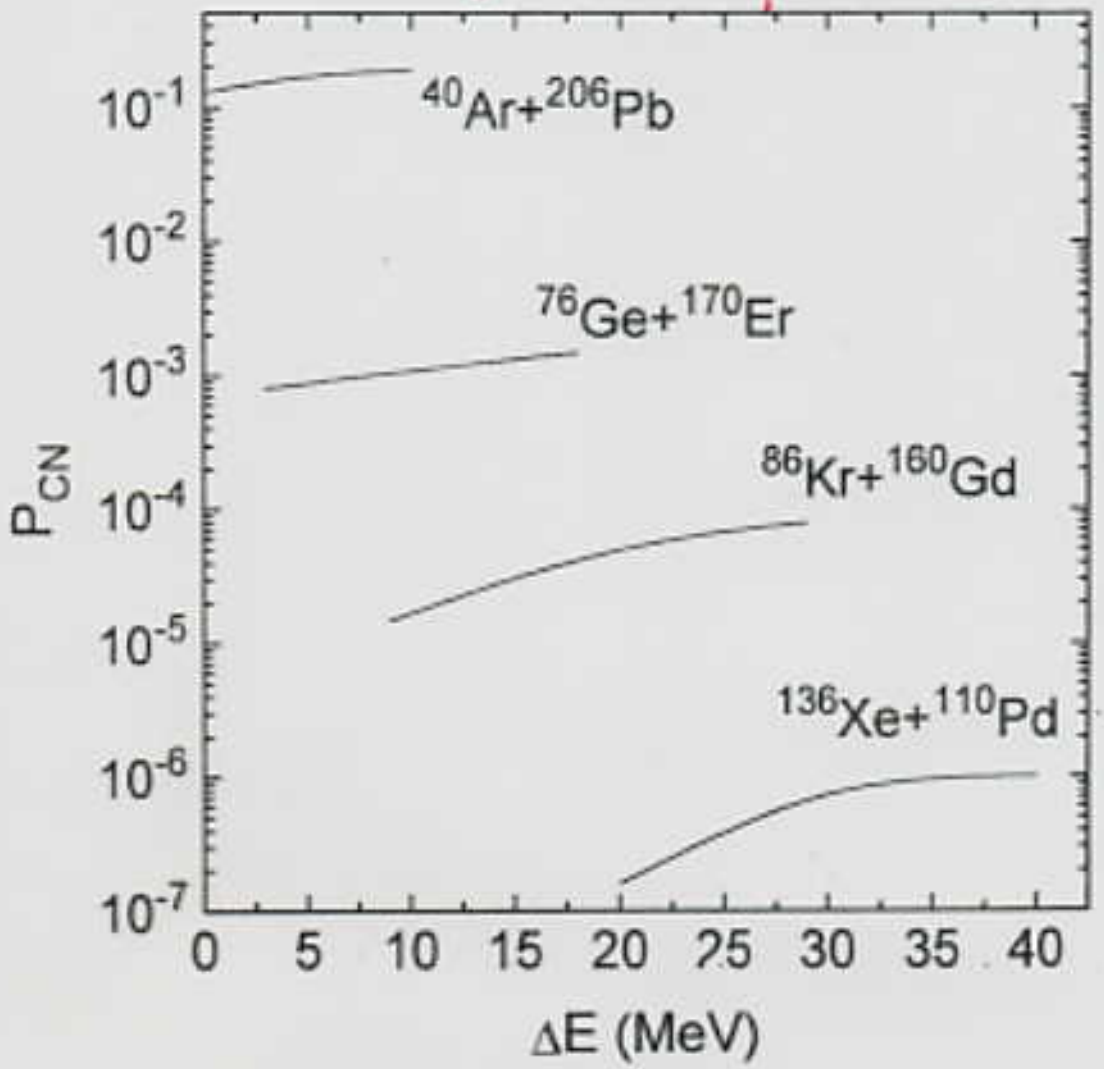

Fig. 7 G.G.Adamian et al. "Competition between

4.2 Evaporation residue cross section

$$\sigma_{ER}(E_{cm},J) = \sum_{J=0}^{J_{max}} \sigma_{cap}(E_{cm},J)\, P_{CN}(E_{cm},J)\, W_{sur}(E_{cm},J)$$

a) Partial capture cross section σ_{cap}

Dinuclear system is formed at the initial stage of the reaction,
kinetic energy is transferred into potential and excitation energy.

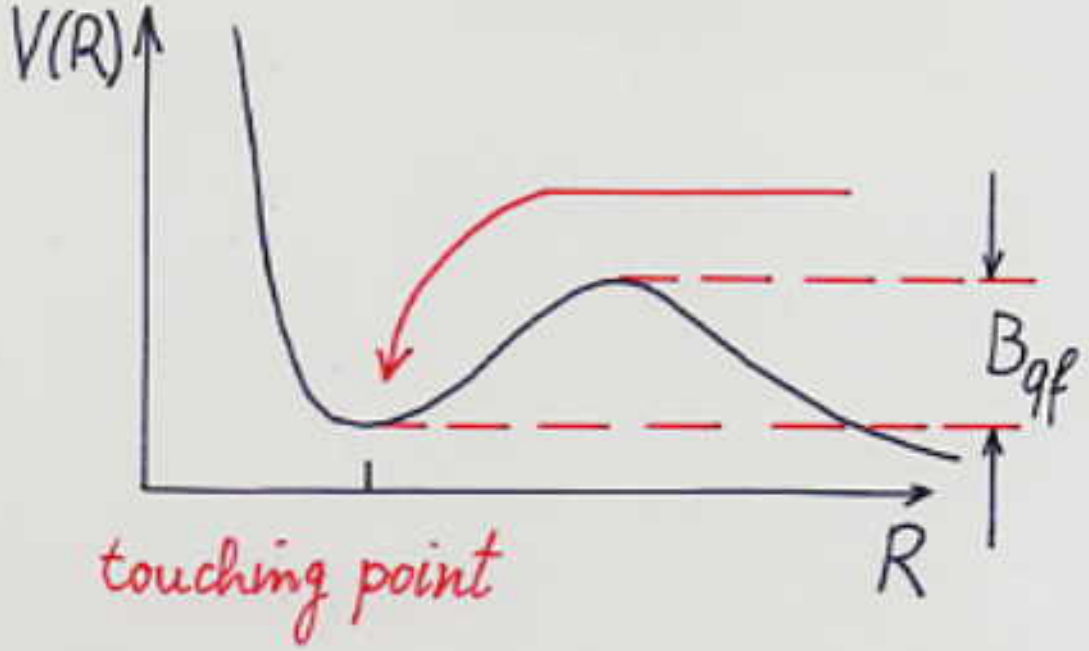

B_{qf} = barrier for quasifission

b) Probability for complete fusion P_{CN}

DNS evolves in mass asymmetry coordinate by diffusion processes toward fusion and in the relative coordinate toward the decay of the dinuclear system (quasifission).

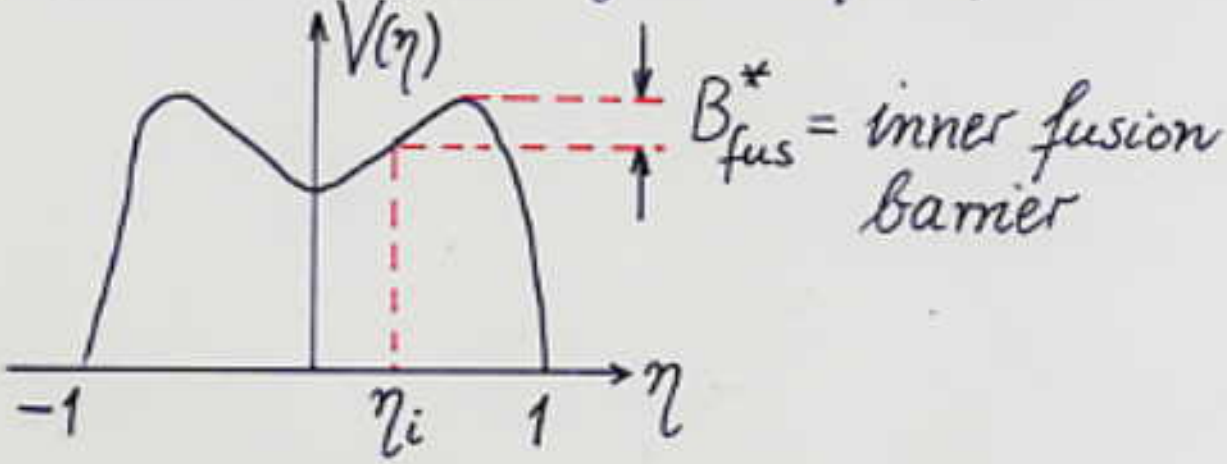

Competion between fusion and quasifission

Calculation of P_{CN} and quasifission distributions in η and R :

Fokker-Planck equation, master equations, Kramers formula

$$P_{CN} \sim \exp(-B^*_{fus}/kT)$$

c) Survival probability W_{sur}

Deexcitation of excited compound nucleus by neutron emission, other decays (γ-, α-decay) can be neglected.

For Pb-based reactions with emission of 1 neutron:

$$W_{sur}(E^*_{CN}, J) = P_{1n}(E^*_{CN}, J) \frac{\Gamma_n(E^*_{CN}, J)}{\Gamma_{tot}(E^*_{CN}, J)}$$

$\Gamma_{tot} \approx \Gamma_n + \Gamma_f$

Γ_n = width for neutron emission

Γ_f = fission width, $\Gamma_f \gg \Gamma_n$

P_{1n} = probability of realisation of 1n channel

$$P_{1n}(E^*_{CN}, J=0) = \exp(-(E^*_{CN} - B_n - 2T)^2 / 2\sigma^2)$$

$B_n + 2T$ is average energy needed for neutron emission.

222Th

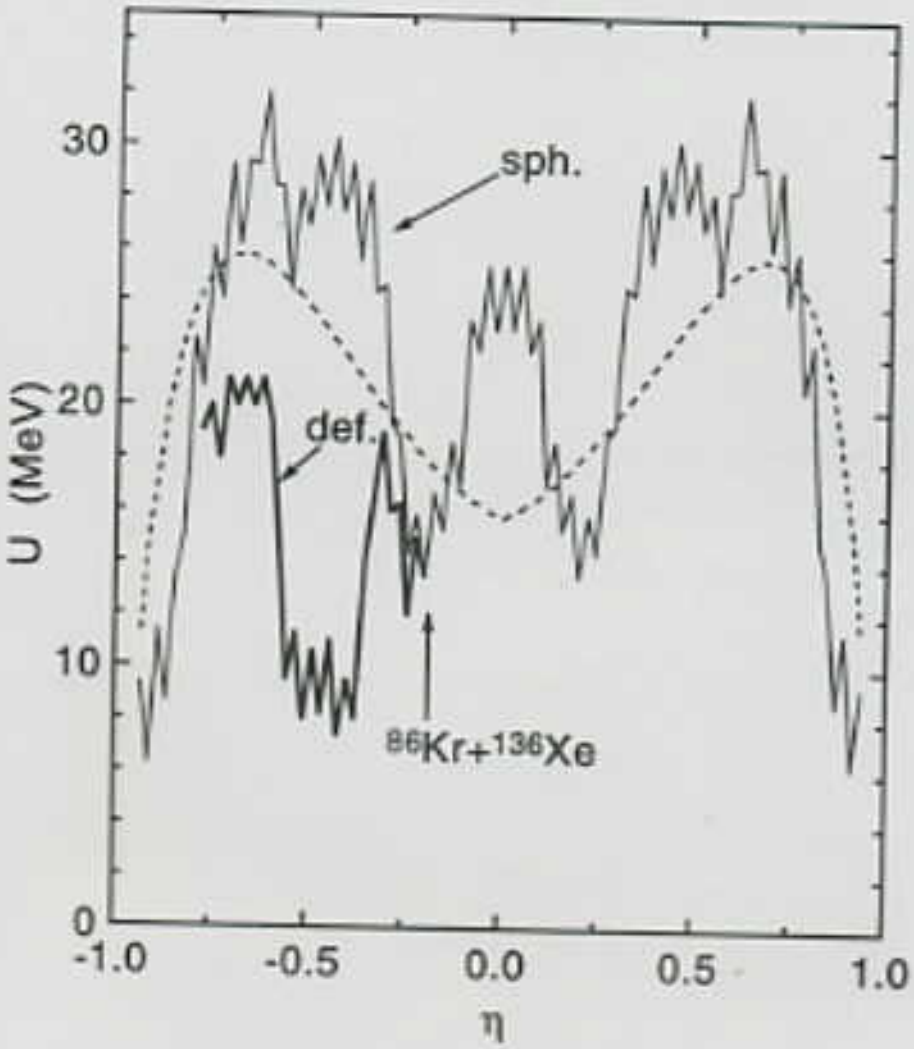

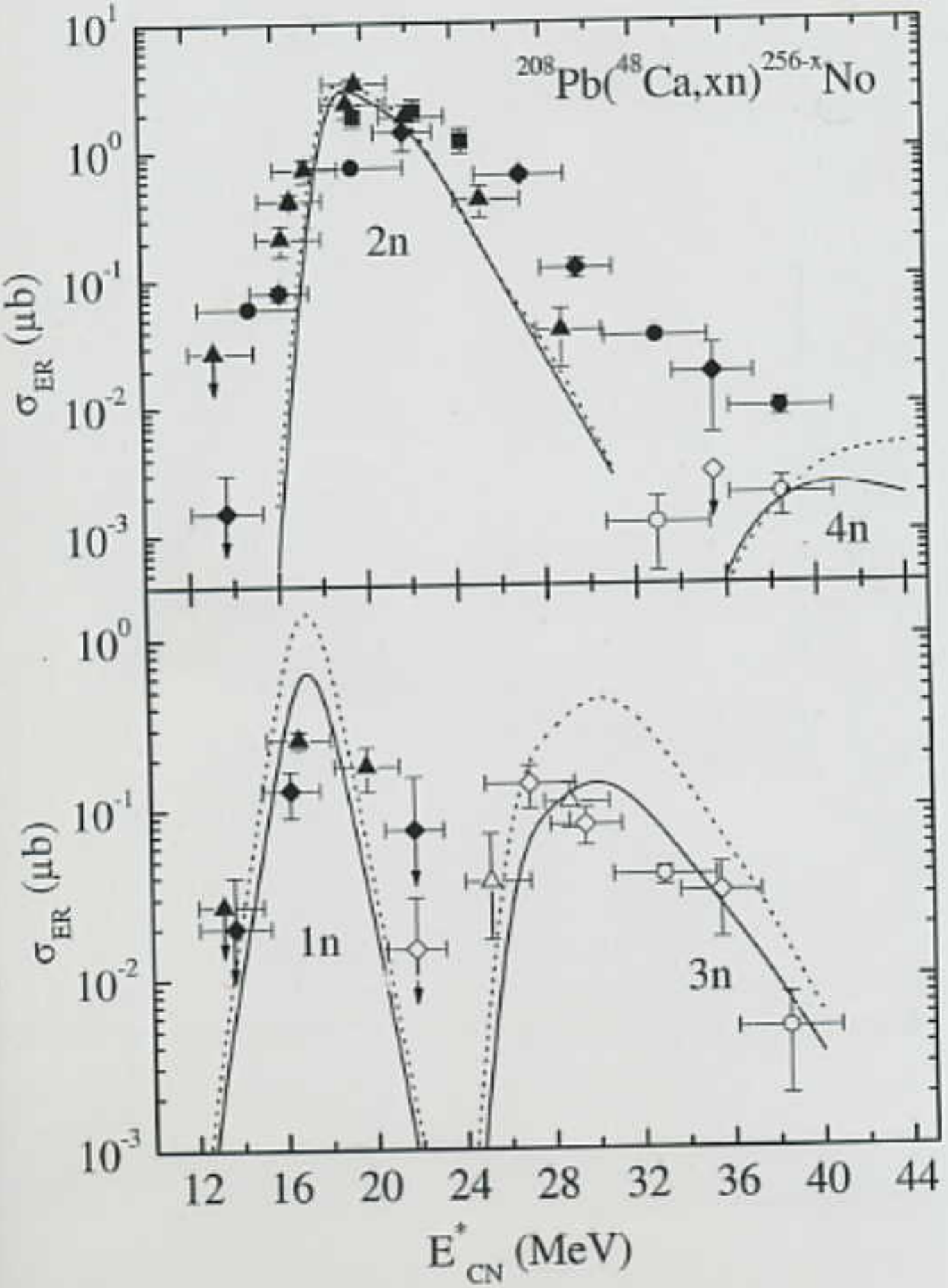
^{208}Pb(^{48}Ca,xn)$^{256-x}$No
2n
4n
1n
3n
σ_{ER} (μb)
E^*_{CN} (MeV)
10^1
10^0
10^{-1}
10^{-2}
10^{-3}
12
16
20
24
28
32
36
40
44

Fig.2

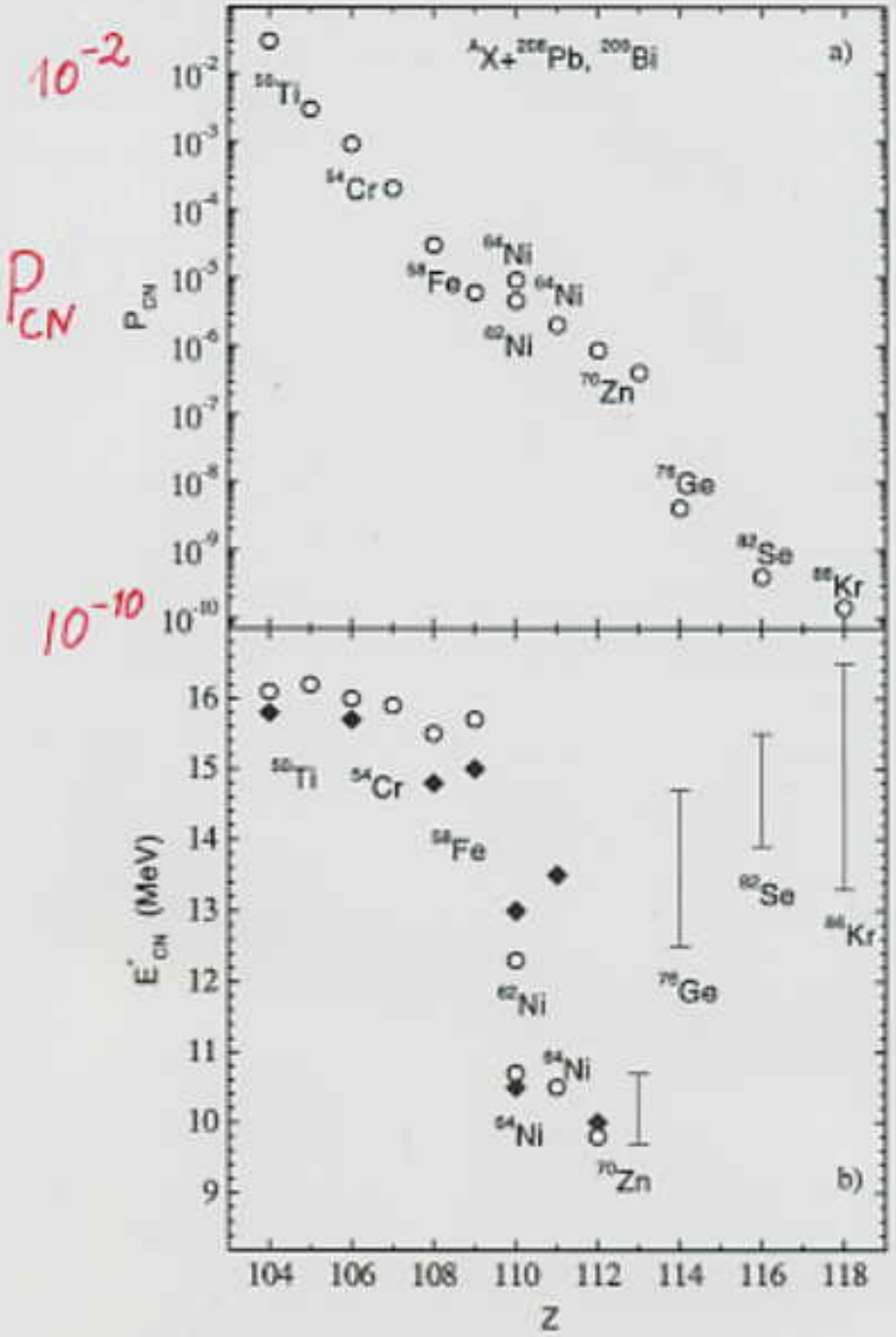

Fig.2 G.G.Adamian et al.

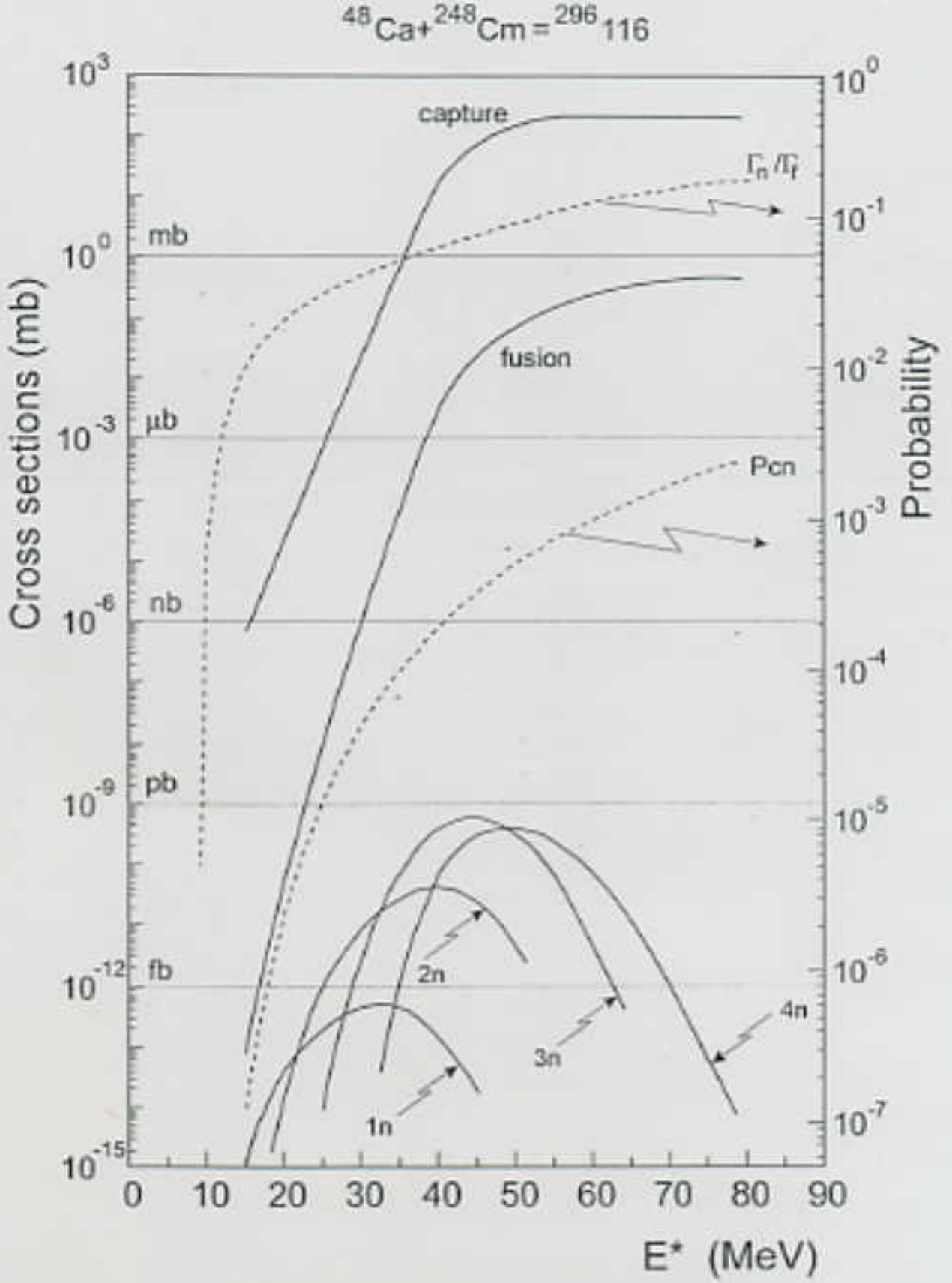

$$\sigma_{xn}(E) \approx \frac{\sigma_c}{\sigma_{tot}} \cdot P_{CN} \cdot W_{xn}(E^*) \approx \pi\lambda_0^2 \sum_{l=0}^{l_{tot}} (2l+1) T(l, E_{CM}) \cdot P_{CN} \cdot P_{xn}(E^*) \cdot \prod_{i=1}^{x} \left(\frac{\Gamma_n(E_i^*)}{\Gamma_f(E_i^*)} \right)_i$$

Chereparov

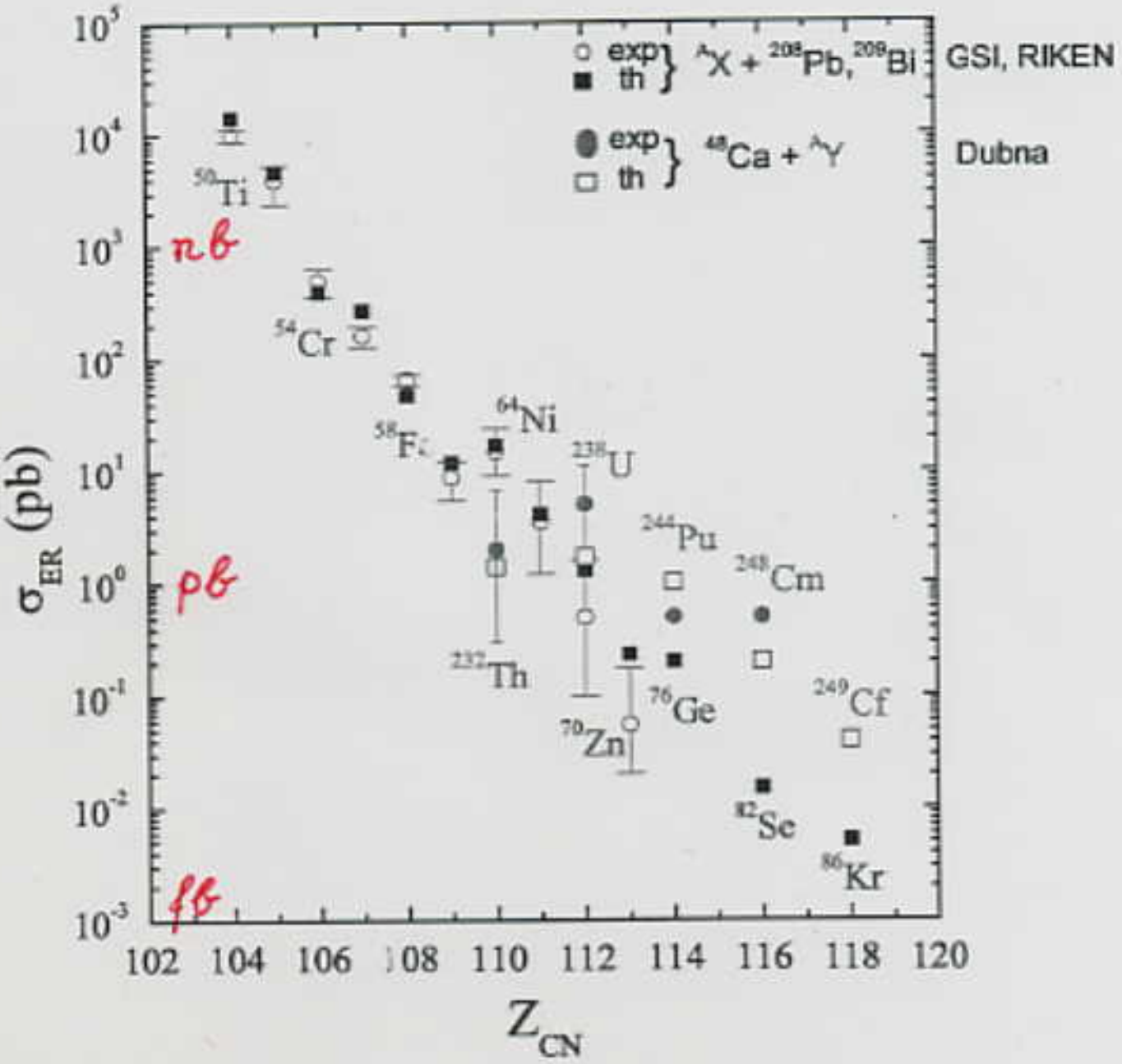
exp
th
$^{A}X + ^{208}Pb, ^{209}Bi$
GSI, RIKEN
exp
th
$^{48}Ca + ^{A}Y$
Dubna
^{50}Ti
^{54}Cr
^{64}Ni
^{238}U
^{244}Pu
^{248}Cm
^{232}Th
^{76}Ge
^{70}Zn
^{249}Cf
^{82}Se
^{86}Kr
nb
pb
fb
σ_{ER} (pb)
Z_{CN}
102 104 106 108 110 112 114 116 118 120

5. Quasifission as a signature for dinuclear systems

a) Master equations for dynamics of mass and charge transfer

New notation: $A_1 + A_2 = A_{tot}$

Fragmentation: $Z_1 = \underline{Z}$, $N_1 = \underline{N}$, $A_1 = \underline{A}$

$Z_2 = Z_{tot} - Z_1$, $N_2 = N_{tot} - N_1$

Starting point: shell model Hamiltonian

$$H = \sum_{i=1}^{A_{tot}} \left(-\frac{\hbar^2}{2m} \Delta_i + U_{A_1}(\vec{r}_i - \vec{R}) + U_{A_2}(\vec{r}_i) \right)$$

in second quantization: $H = \underline{H_0 + V_{int}}$

$$H_0 = \sum_{\mu} \epsilon_{A_1 \mu} a^+_{A_1 \mu} a_{A_1 \mu} + \sum_{\nu} \epsilon_{A_2 \nu} a^+_{A_2 \nu} a_{A_2 \nu}$$

$$V_{int} = \sum_{\mu,\nu} \left(g_{A_1 \mu, A_2 \nu}(R)\, a^+_{A_1 \mu} a_{A_2 \nu} + h.c. \right)$$

$$g_{A_1 \mu, A_2 \nu}(R) = \frac{1}{2} \langle A_1 \mu | U_{A_1} + U_{A_2} | A_2 \nu \rangle$$

R is distance of nuclei in the minimum of internuclear potential.

Master equation for probability $P_{ZN}(t)$ to find the system in fragmentation

$$Z_1 = Z,\ N_1 = N,\ Z_2 = Z_{tot} - Z,\ N_2 = N_{tot} - N$$

$$\begin{aligned}\frac{d}{dt}P_{ZN}(t) = {} & \Delta^{(-,0)}_{Z+1,N} P_{Z+1,N}(t) + \Delta^{(+,0)}_{Z-1,N} P_{Z-1,N}(t) \\ & + \Delta^{(0,-)}_{Z,N+1} P_{Z,N+1}(t) + \Delta^{(0,+)}_{Z,N-1} P_{Z,N-1}(t) \\ & - \left(\Delta^{(-,0)}_{Z,N} + \Delta^{(+,0)}_{Z,N} + \Delta^{(0,-)}_{Z,N} + \Delta^{(0,+)}_{Z,N}\right) P_{Z,N}(t) \\ & - \left(\Lambda^{qf}_{Z,N} + \Lambda^{fis}_{Z,N}\right) P_{Z,N}(t)\end{aligned}$$

Rates $\Delta^{(\,,\,)}$ depend on single-particle energies and temperature related to excitation energy.
Only transitions $Z \rightleftarrows Z \pm 1$ and $N \rightleftarrows N \pm 1$.

$\Lambda^{qf}_{Z,N}$: rate for quasifission in R

$\Lambda^{fis}_{Z,N}$: rate for fission of heavy nucleus

Transfer rates:

$$\Delta^{(\pm,0)}_{Z,N} = \frac{1}{\Delta t}\sum_{\mu,\nu}^{Z} |g_{A_1\mu,A_2\nu}|^2 \, n_{\substack{A_2\nu \\ A_1\mu}}(T)\left(1 - n_{\substack{A_1\mu \\ A_2\nu}}(T)\right) \times \frac{\sin^2(\Delta t\,(\epsilon_{A_1\mu} - \epsilon_{A_2\nu})/2\hbar)}{(\epsilon_{A_1\mu} - \epsilon_{A_2\nu})^2/4}$$

$$\Delta^{(0,\pm)}_{Z,N} = \frac{1}{\Delta t}\sum_{\mu,\nu}^{N} |g_{A_1\mu,A_2\nu}|^2 \, n_{\substack{A_2\nu \\ A_1\mu}}(T)\left(1 - n_{\substack{A_1\mu \\ A_2\nu}}(T)\right) \times \frac{\sin^2(\Delta t\,(\epsilon_{A_1\mu} - \epsilon_{A_2\nu})/2\hbar)}{(\epsilon_{A_1\mu} - \epsilon_{A_2\nu})^2/4}$$

temperature $T(Z,N)$

$n(T)$ Fermi occupation numbers

$\epsilon_{A_1\mu}, \epsilon_{A_2\nu}$ Single particle energies

b) Fusion probability and mass and charge yields

Fusion probability:

$$P_{CN} = \sum_{\substack{Z<Z_{BG} \\ N<N_{BG}}} P_{Z,N}(t_0)$$

} inner fusion barrier

t_0 = reaction time $\approx (3-5) \times 10^{-20}$ s

Yield of quasifission:

$$Y_{Z,N}(t_0) = \Lambda^{qf}_{Z,N} \int_0^{t_0} P_{Z,N}(t)\,dt$$

Reaction time determined by

$$1 - P_{CN} = \sum_{Z,N} \left(\Lambda^{qf}_{Z,N} + \Lambda^{fis}_{Z,N} \right) \int_0^{t_0} P_{Z,N}(t)\,dt$$

mass yield: $Y(A) = \sum_Z Y_{Z,A-Z}(t_0)$

charge yield: $Y(Z) = \sum_N Y_{Z,N}(t_0)$

c) Hot fusion reactions with ^{48}Ca beam

Quasifission measurements by Itkis et al.

e.g. $^{48}Ca + ^{248}Cm \longrightarrow ^{296}116$

In our calculations only quasifission is shown.
Calculated primary fragment distributions.

Maxima in yields arise from minima of driving potential $U(\eta)$.

Minima in σ^2_{TKE} related to stiff nuclei: Zr, Sn, Pb.
Importance of fluctuations of deformations for σ^2_{TKE}.

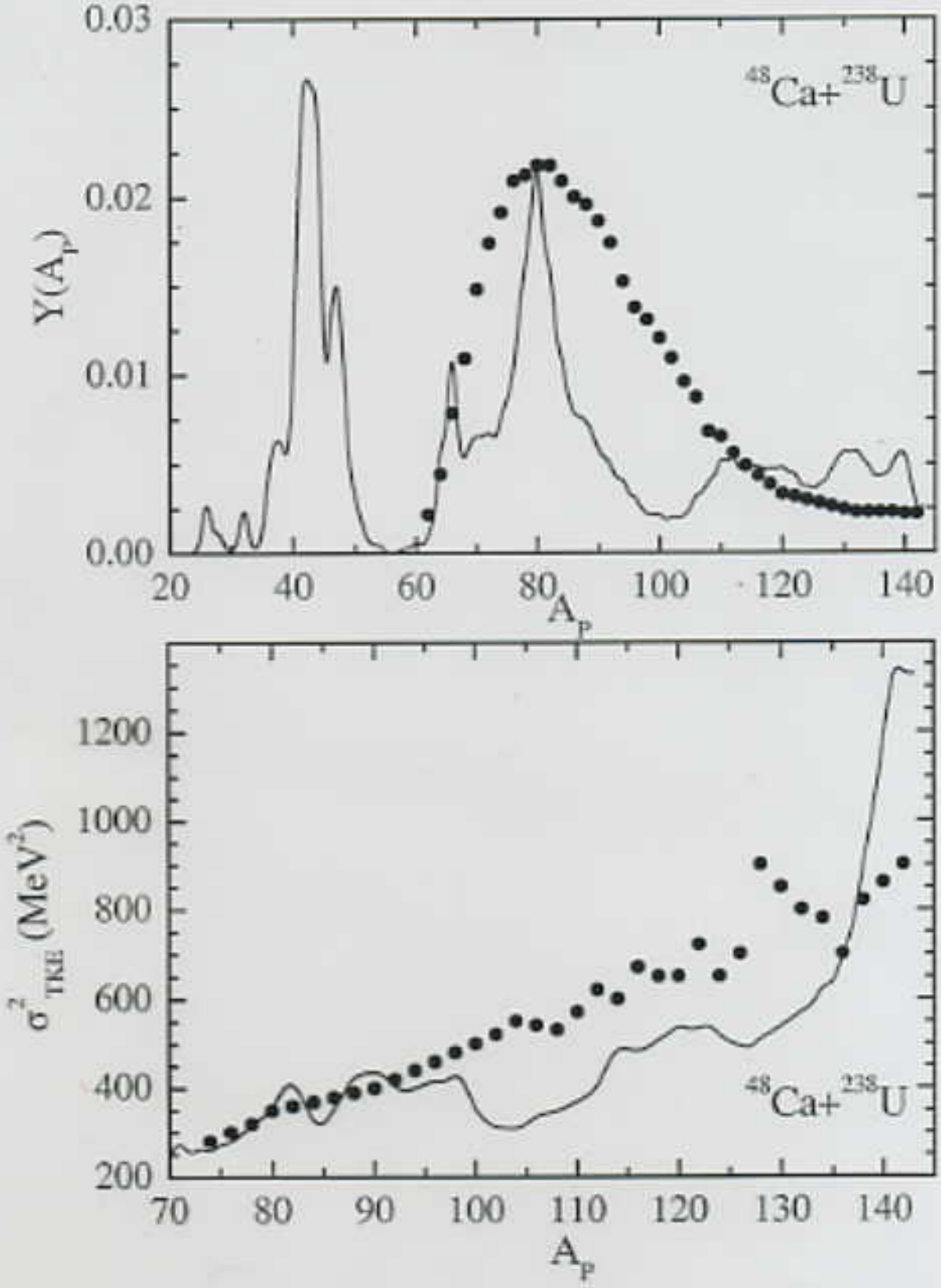

Fig. 2

E^*_{CN}=33.4MeV

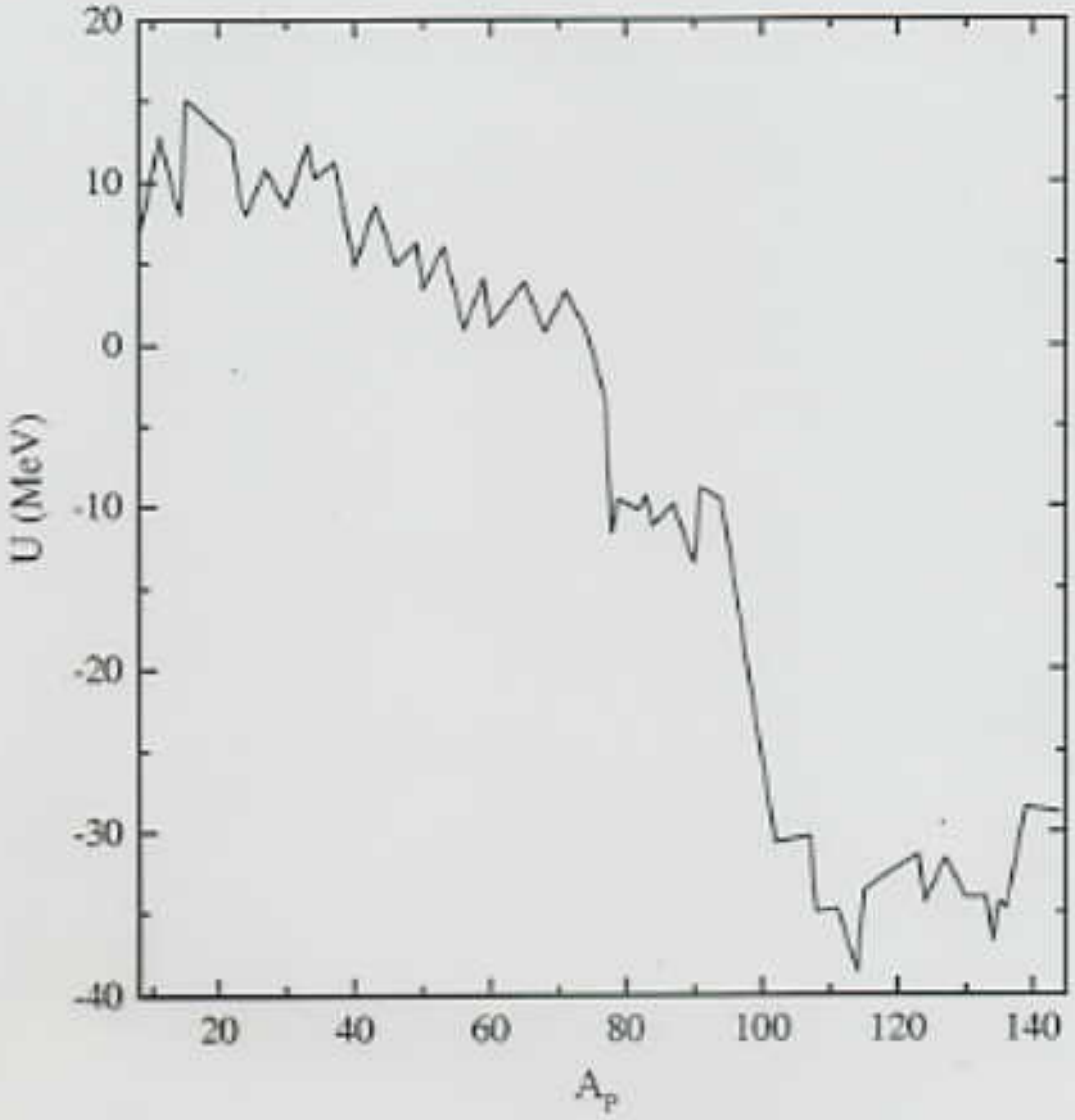

$^{286}112$, $J=0$

Fig. 3

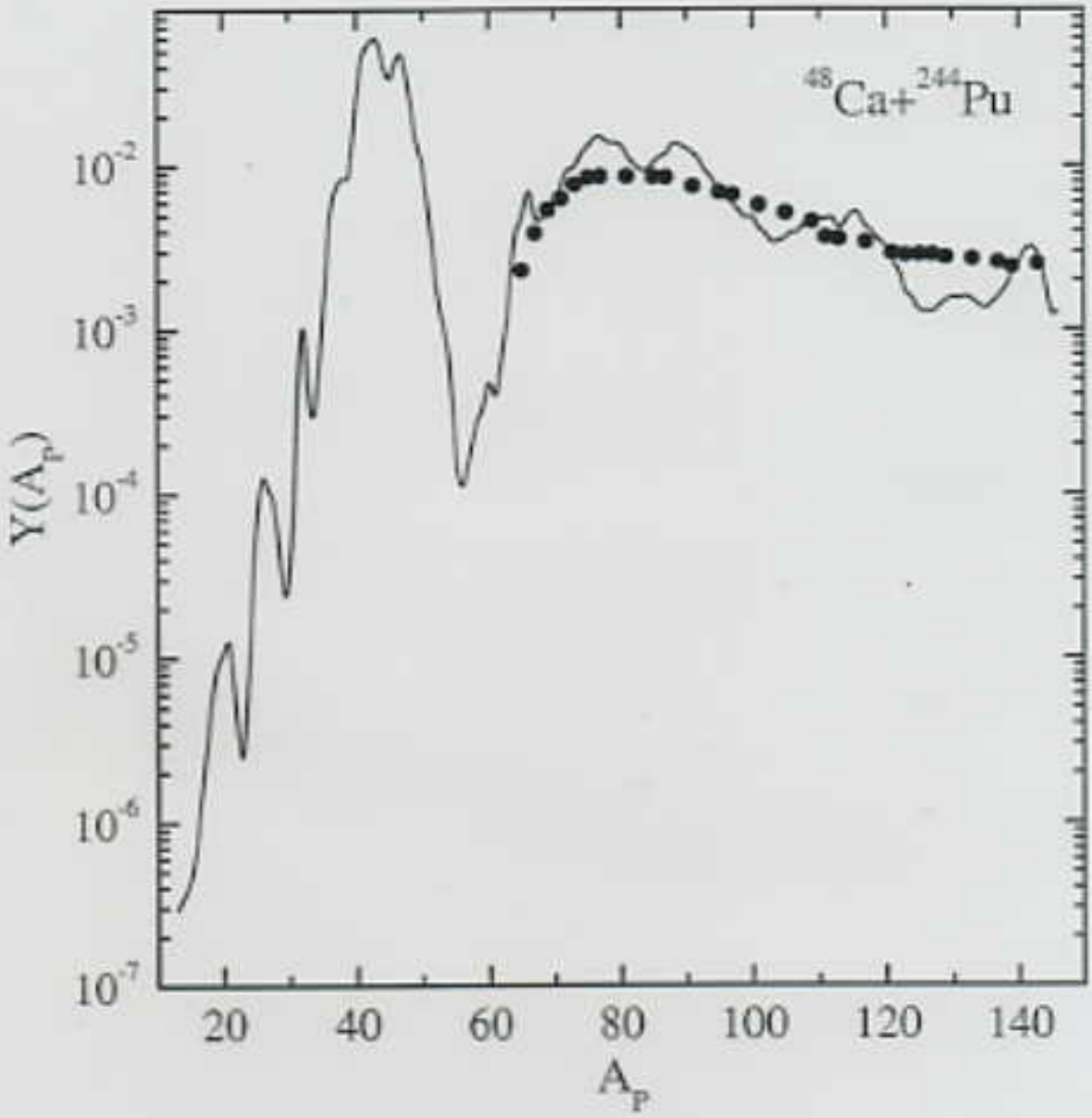

$E^*_{CN} = 42$ MeV

Fig. 1

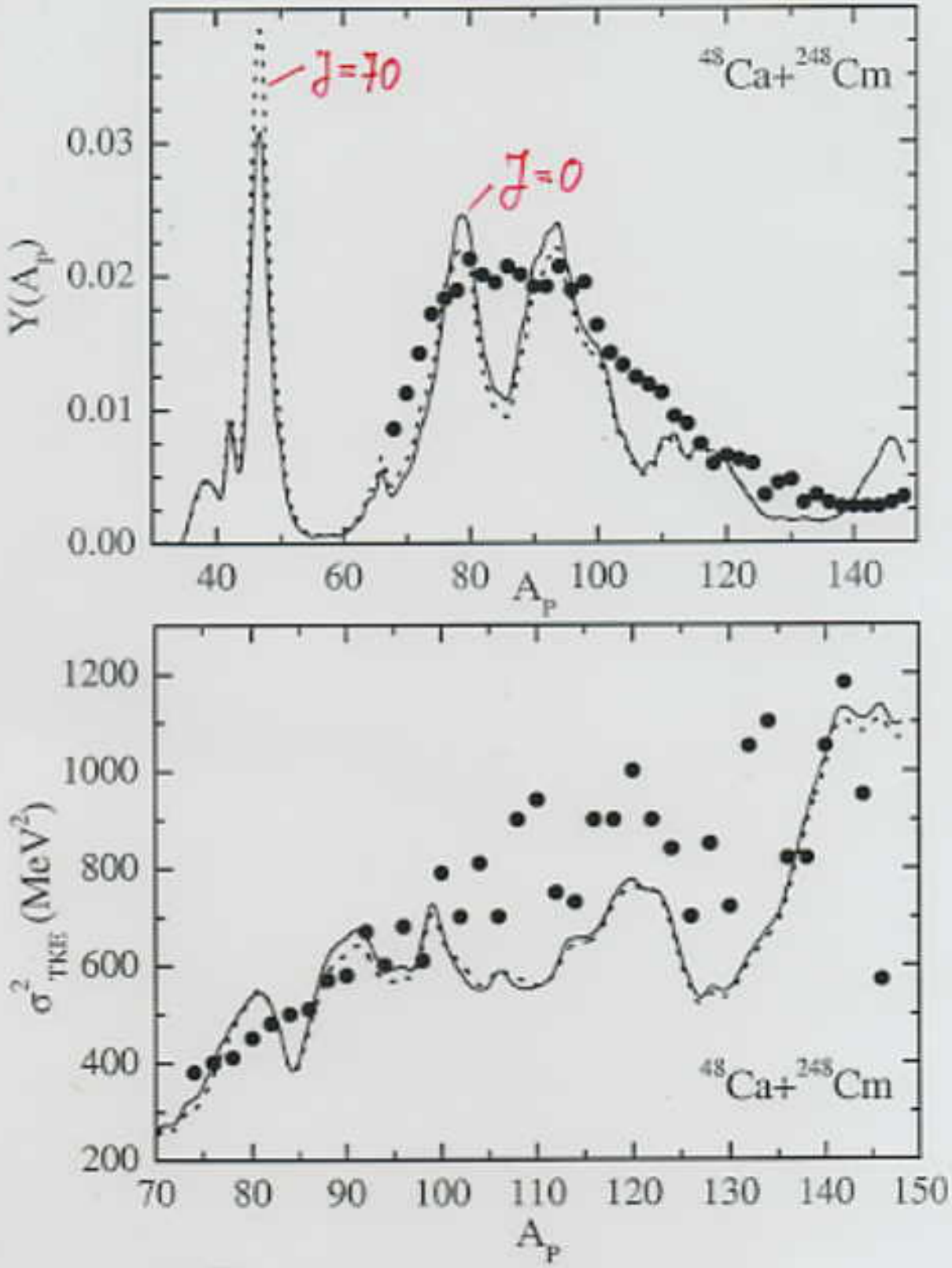

Fig. 4

$E^*_{CN} = 37$ MeV

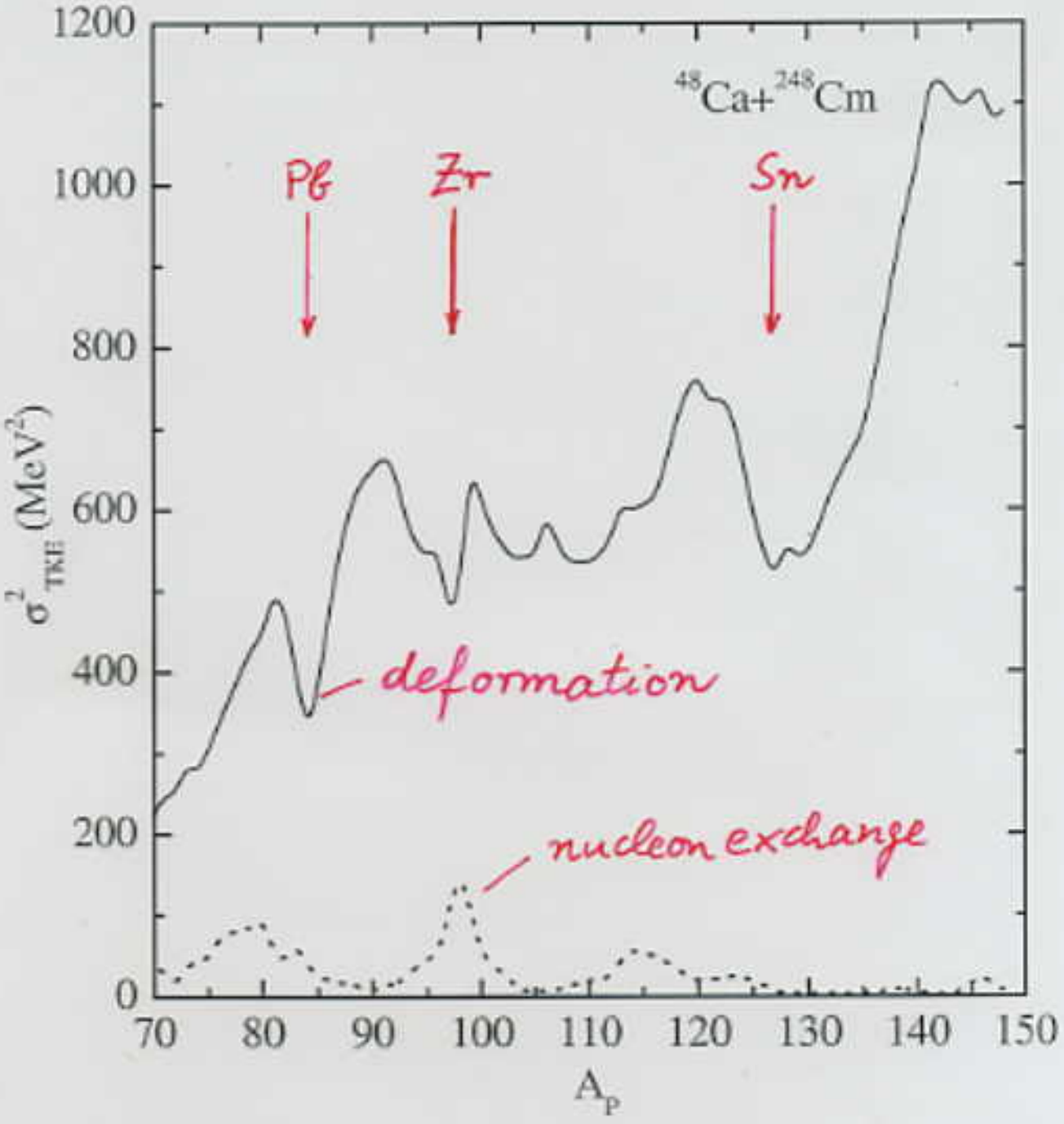
1200
1000
800
600
400
200
0
70
80
90
100
110
120
130
140
150
A_P
σ^2_{TKE} (MeV^2)
^{48}Ca+^{248}Cm
Pb
Zr
Sn
deformation
nucleon exchange

Fig. 5

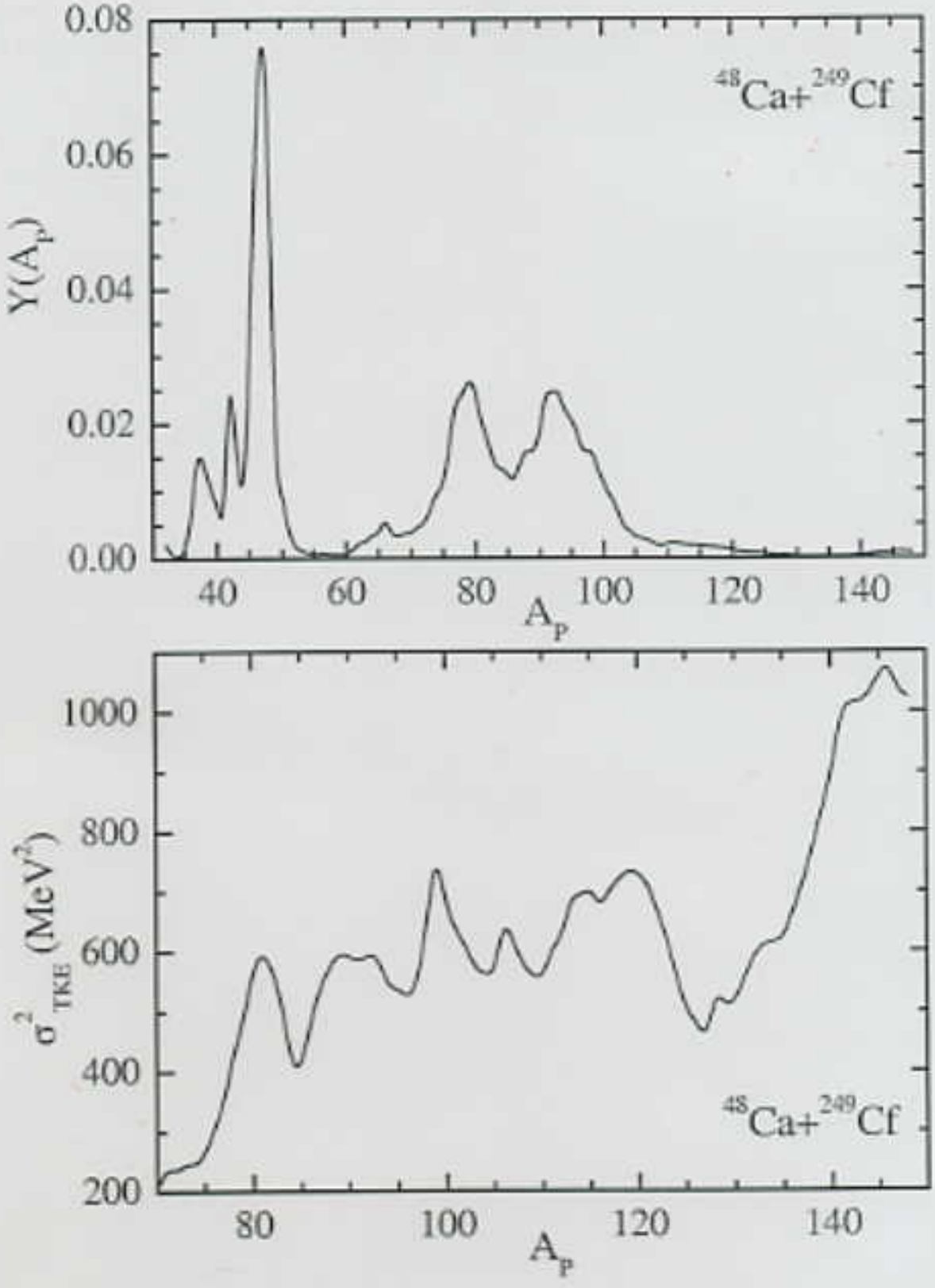
0.08
0.06
0.04
0.02
0.00
Y(A_P)
48Ca+249Cf
40
60
80
100
120
140
A_P
1000
800
600
400
200
σ²_TKE (MeV²)
48Ca+249Cf
80
100
120
140
A_P

Fig. 7

d) Ratio of fusion-fission to quasifission

$$r = P_{CN} / \sum_{A=A_{tot}/2-20}^{A_{tot}/2} Y(A)$$

	E^*_{CN} (MeV)	r
$^{40}Ar + ^{165}Ho$	89	1.1
	120	0.7
$^{48}Ca + ^{244}Pu$	34.8	$1.4 \cdot 10^{-2}$
	50	$1.1 \cdot 10^{-1}$
$^{86}Kr + ^{208}Pb$	17	$2.1 \cdot 10^{-7}$
	30	$2.0 \cdot 10^{-5}$

e) Transfer cross sections to more asymmetric systems

here: $^{76}Ge + ^{208}Pb$

Measurement would prove dinuclear model.

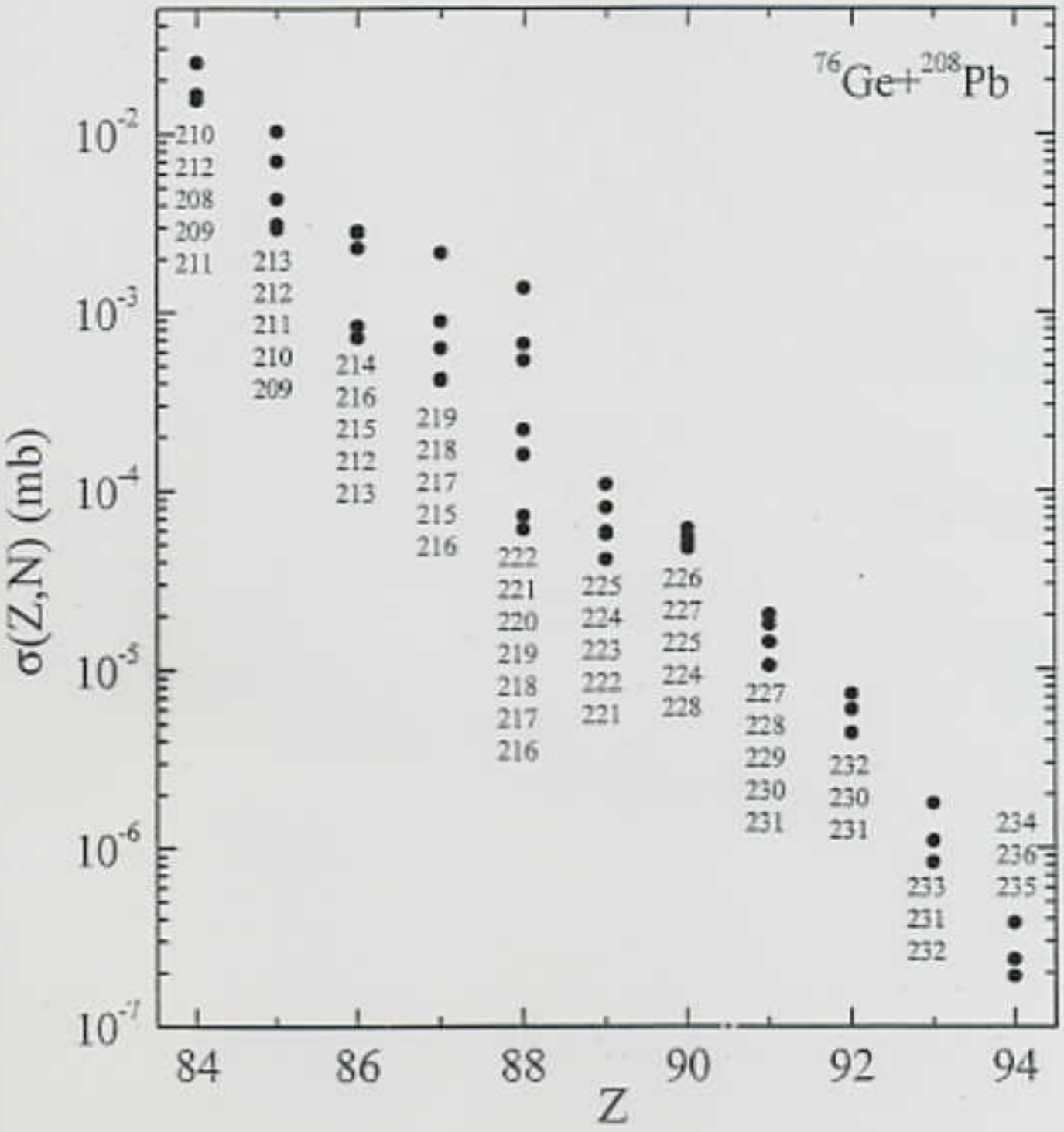
$^{76}Ge+^{208}Pb$
σ(Z,N) (mb)
10^{-2}
10^{-3}
10^{-4}
10^{-5}
10^{-6}
10^{-7}
210
212
208
209
211
213
212
211
210
209
214
216
215
212
213
219
218
217
215
216
222
221
220
219
218
217
216
225
224
223
222
221
226
227
225
224
228
227
228
229
230
231
232
230
231
233
231
232
234
236
235
84
86
88
90
92
94
Z

6. Summary

The dinuclear system concept assumes two touching nuclei which can exchange nucleons by transfer.

In this concept one describes nuclear structure phenomena, the fusion of heavy nuclei to superheavy nuclei and the competing quasifission.

The dynamics of the dinuclear system has two degrees of freedom: the mass asymmetry degree of freedom and the relative motion of the nuclei to larger internuclear distances.

Normal- and superdeformed bands of ^{60}Zn can be interpreted with cluster structures by using the dinuclear model.

Superheavy nuclei are produced in three stages:

1. Capture of the nuclei in a touching configuration and forming a dinuclear system.
2. Fusion to the compound nucleus by nucleon transfer between the touching nuclei. The mass asymmetry changes up to the point when an excited compound nucleus is formed.
3. De-excitation of the compound nucleus by neutron emission into the ground-state of the superheavy nucleus.

The dinuclear system can decay which is called quasifission since no compound nucleus is formed. Fusion and quasifission are simultaneously treated in this theory.

The transfer of nucleons and quasifission are statistical diffusion processes in the excited dinuclear system. They are described by the Fokker - Planck equation, with master equations or simply by the Kramers approximation.

The available experimental data for fusion and quasifission can be well reproduced within the dinuclear system concept and support the correctness of the dinuclear system idea.

The ideas and results, presented in the second lecture, originated from Prof. V. Volkov, Dr. G. Adamian, Dr. N. Antonenko, Prof. S. Ivanova, Prof. R. Jolos, Dr. A. Nasirov, Dr. Yu. Palchikov, Dr. T. Shneidman, A. Zubov all JINR, Dubna, and Prof. Yu. Tchuvil'sky (Moscow).

D. G.